THE EFFECT OF FREQUENCY, TEMPERATURE AND MATERIALS STRUCTURE ON FATIGUE CRACK PROPAGATION IN POLYMERS.

SKIBO MICHAEL DAVID

DEGREE DATE: 1977

Page 1 Document Name: untitled

DTIC DOES NOT HAVE THIS ITEM

-- 1 - AD NUMBER: D428356
-- 6 - UNCLASSIFIED TITLE: THE EFFECT OF FREQUENCY, TEMPERATURE AND
--   MATERIALS STRUCTURE ON FATIGUE CRACK PROPAGATION IN POLYMERS
--10 - PERSONAL AUTHORS: SKIBO, M. D.
--11 - REPORT DATE: 1977
--12 - PAGINATION: 81P
--20 - REPORT CLASSIFICATION: UNCLASSIFIED
--21 - SUPPLEMENTARY NOTE: PH.D. THESIS PRESENTED TO LEHIGH UNIVERSITY.
--22 - LIMITATIONS (ALPHA)   APPROVED FOR PUBLIC RELEASE. DISTRIBUTION
--   UNLIMITED. AVAILABILITY: UNIVERSITY MICROFILMS INTERNATIONAL 300 N
--   ZEEB RD. ANN ARBOR, MI 48106. NO. 77-20726.
--33 - LIMITATION CODES: 1 24

DISCLAIMER NOTICE

UNCLASSIFIED

Technical Report
distributed by

**DEFENSE
TECHNICAL
INFORMATION
CENTER**

DTIC Acquiring Information
Imparting Knowledge

Cameron Station
Alexandria, Virginia 22304-6145

UNCLASSIFIED
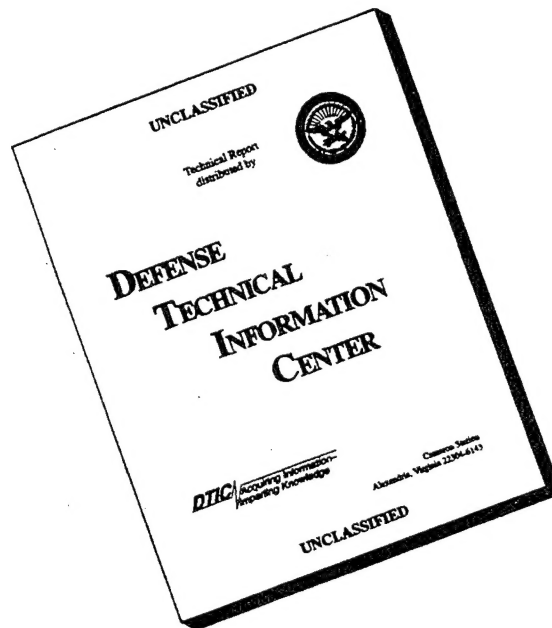
THIS DOCUMENT IS BEST QUALITY AVAILABLE. THE COPY FURNISHED TO DTIC CONTAINED A SIGNIFICANT NUMBER OF PAGES WHICH DO NOT REPRODUCE LEGIBLY.

INFORMATION TO USERS

77-20,726

SKIBO, Michael David, 1952-
THE EFFECT OF FREQUENCY, TEMPERATURE AND
MATERIALS STRUCTURE ON FATIGUE CRACK PROPAGATION
IN POLYMERS.

Lehigh University, Ph.D., 1977
Engineering, materials science

THE EFFECT OF FREQUENCY, TEMPERATURE AND MATERIALS STRUCTURE

ON FATIGUE CRACK PROPAGATION IN POLYMERS

by

Michael D. Skibo

A Dissertation

Presented to the Graduate Faculty

of Lehigh University

in candidacy for the Degree of

Doctor of Philosophy

in

Metallurgy and Materials Science

Lehigh University

1977

Approved and recommended for acceptance as a dissertation in partial fulfillment of the requirements for the degree of Doctor of Philosophy.

May 13, 1977
  (date)

Richard W. Heffer
Professor in Charge

Accepted, _May 13, 1977_
           (date)

Special Committee directing the doctoral work of Mr. Michael D. Skibo.

Richard W. Heffer
Chairman

David A. Thomas

John A. Thomas

A. Robinson

ii

ACKNOWLEDGEMENTS

The author gratefully acknowledges the instruction and guidance of his advisor, Professor R. W. Hertzberg and Professor J. A. Manson. Sincere appreciation is also expressed to the other members of the author's doctoral committee, Professor D. A. Thomas and Dr. C. N. Robinson for their cooperation and support of this research effort. The author wishes to thank the machine shop, secretarial and technical personnel for their assistance with the current research.

The author acknowledges Dr. Soojaa Kim, Subodh Misra and Carol Vasoldt for the preparation and characterization of the poly(methyl methacrylate) and epoxy specimens studied in this dissertation. The donation of carefully characterized samples of poly(vinyl chloride) by Dr. Collins of B. F. Goodrich is also appreciated.

Finally, the author wishes to acknowledge the financial support of the Army Research Office-Durham Grant DAHCO4 7460010.

iii

TABLE OF CONTENTS

List of Figures

xi

List of Tables

ABSTRACT

The effect of cyclic frequency, temperature and internal structure on the fatigue crack propagation (FCP) response of polymers of varied structure and properties was evaluated comprehensively.

Crack propagation data in poly(methyl methacrylate) (PMMA), poly(vinyl chloride) (PVC), polystyrene (PS), polycarbonate (PC), and polysulfone (PSF) were obtained as a function of frequency. These results determined over a maximum frequency range of 0.1 to 100 Hz show frequency sensitivity to be a function of several, sometimes competitive, factors. The importance of two of these factors, strain rate and creep crack growth on fatigue crack propagation are isolated through waveform studies. Another parameter, the β transition, seems to play a dominant role with the FCP frequency sensitivity being a maximum for polymers where the β transition at room temperature occurs in the range of the experimental test frequency. This correlation was further examined by evaluating the FCP frequency sensitivity of PMMA, PSF, and PC as a function of temperature. The results are rationalized in terms of crack tip heating and associated blunting.

The observed fatigue response of polymers was seen to be a strong function of internal structure. The recognized superior fatigue resistance of crystalline polymers was confirmed by additional results which revealed the FCP response of highly crystalline

1

polyacetal (PA) to be superior to all previously examined polymeric materials at 10 and 100 Hz. To determine the effect of molecular weight (M) (g/mole) on FCP, 100 Hz fatigue tests were performed on carefully characterized specimens of PMMA and PVC ranging in M from $1-8 \times 10^5$ and $6-23 \times 10^4$, respectively. While toughness increased by a maximum factor of 3 (in PVC) with M in this range, crack growth rates decreased by 10^3. At all molecular weights in PVC, the effects of the external plasticizer (dioctyl phthalate) at contents of 0 - 13% were minimal although significant embrittlement was noted at 6% DOP. Conversely, the internal plasticizer butyl acrylate in PMMA (BA-MMA copolymer) produced a complex effect on both fatigue crack growth rates and toughness. An examination of the cyclic behavior of of epoxies with M_c (distance between crosslinks) ranging from 326 to > 2000 showed FCP to be sensitive to M_c. Over the test range of M_c, crack growth rates decreased by $>10^3$ with increasing M_c.

A careful study of the fatigue fracture surface morphology of selected polymers was perfoemed to determine the mechanisms of fatigue crack propagation. In those uncrosslinked amorphous poly-mers with viscosity-average molecular weight $\leq 2 \times 10^5$ and crystal-line PA, the microscopic appearance of the fracture surface at low values of the stress intensity range and high cyclic test frequency (100 Hz) revealed many parallel bands, oriented perpendicular to the direction of crack growth. The bands were seen to increase in size with ΔK. In all instances, the crack front advanced discontinuously in increments equal to the band width after remaining stationary for

2

hundreds and even thousands, of fatigue cycles. By equating the band size to the Dugdale plastic zone ahead of the crack, a relatively constant yield strength was inferred which agreed well with reported craze stress values for each material. At higher stress intensity levels in most polymers, another series of parallel bands were observed. These were also oriented perpendicular to the direction of crack growth and likewise increased in size with the range in stress intensity factor, ΔK. Each band corresponded to the incremental advance of the crack during one load cycle, indicating these markings to be classical fatigue striations.

I. Introduction

As an important class of engineering materials, polymers have been finding increased application in load bearing structures. While many plastic structural members will be subjected to only static stresses, complex cyclic loading conditions are also possible. The static failure characteristics of most polymers has been thoroughly catalogued by many independent researchers. However, few in-depth studies of the fatigue behavior of polymers have been reported. Also, much of this research has been carried out on uncharacterized commercial materials under limited test conditions. Clearly, further knowledge of the dynamic response of engineering plastics is needed.

It is generally accepted that fatigue failure in polymers can occur by two distinct mechanisms.[1] Investigators have found that fatigue failure of an unnotched specimen may develop as a result of the constant input of hysteretic energy during each load cycle.[2-11] This energy is, in part, dissipated as heat within the test sample which causes a monotonic temperature rise. The accumulation of thermal energy culminates either with the melting of the entire gage section as T_g or T_m is surpassed or as a result of excessive sample compliance. In the latter instance, the specimen is no longer capable of supporting the load and may be considered to have failed, although no physical fracture need have occurred. The hysteretic energy input per cycle as presented by Ferry[11] is given

4

by

$$\dot{E} = \pi f J'' (f,T) \sigma^2 \qquad\qquad (1.1)$$

where f = test frequency

J'' = loss modulus

σ = maximum stress

$\dot{E}$ = dissipated energy/cycle

From equation 1.1, the heating rate is related directly to the cyclic frequency and J''. Consequently, increasing the frequency should decrease the cyclic life under a given set of experimental conditions. The loss compliance J'' is a rather complex term. A given polymer may exhibit one or more J'' peaks. In these regions of maximum damping, the fatigue life will be curtailed. Since the location of maxima   in J'' are sensitive to both temperature and frequency, the relative temperature rise will be a strong function of testing conditions.

If the build up of hysteretic energy is balanced by the conduction and convection of heat to the cooler environment, cyclic induced thermal softening will not occur. However, this does not eliminate the accumulation of fatigue damage by the initiation and stable propagation of a crack. Since most polymeric materials contain flaws, either introduced through some fabrication process or as a result of a poor structural design, fatigue crack propagation (FCP) probably represents the dominant mechanism of cyclic failure. It is this mechanism which will be studied exclusively in this dissertation.

5

Of the many parameters which have been introduced in an attempt to characterize the FCP response of polymers, the stress intensity factor seems to be the most promising. Derived from principles of fracture mechanics, the stress intensity factor describes the stress conditions at the tip of the advancing crack and is defined by

$$K = Y \sigma \sqrt{a} \qquad (1.2)$$

where K is the stress intensity factor, Y the correction for specimen geometry, σ the applied stress, and a the crack length.

Fatigue crack propagation data are generated by cycling notched samples such as the two shown in Figure 1.1 within a constant stress range ($\Delta\sigma$) and recording the crack growth increment over a corresponding number of fatigue cycles. Under fatigue conditions, K must also vary over a range defined by ΔK. As the crack length increases for the specimens shown in Figure 1.1, ΔK will also increase. Consequently, it is possible to measure in one sample the rate of crack growth per cycle, da/dN, over a large range of ΔK. The strong relationship between ΔK and da/dN, is demonstrated clearly in Figure 1.2. Note the strong ΔK-crack growth rate correlation for several polymers having different molecular structures and mechanical properties.[1] It has been shown that such a relationship between da/dN and ΔK could be best represented by a simple equation of the form:[14]

$$da/dN = A \, \Delta K^m \qquad (1.3)$$

where A and m are material variables for a given polymer.

6
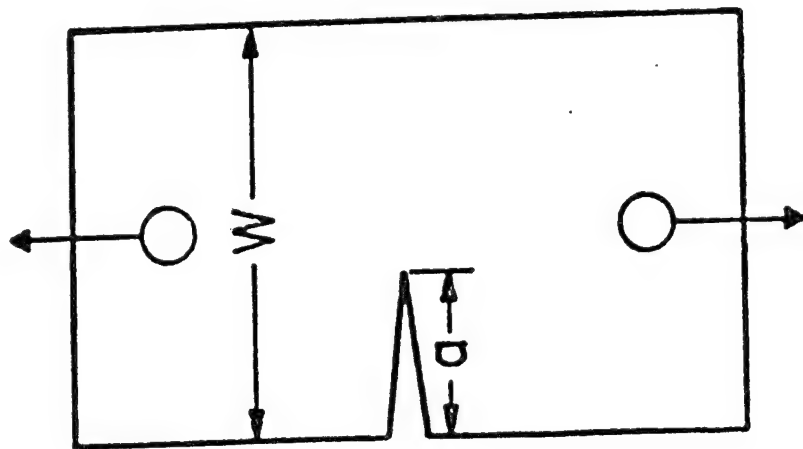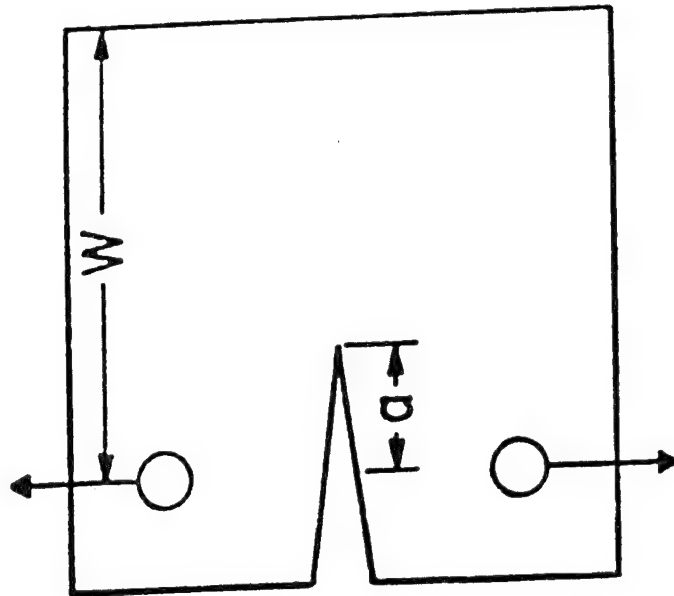
Figure 1.1 Specimen configurations used to generate fatigue crack propagation data in this study: (a) single edge notched specimen (SEN); (b) compact tension specimen (CT).

7
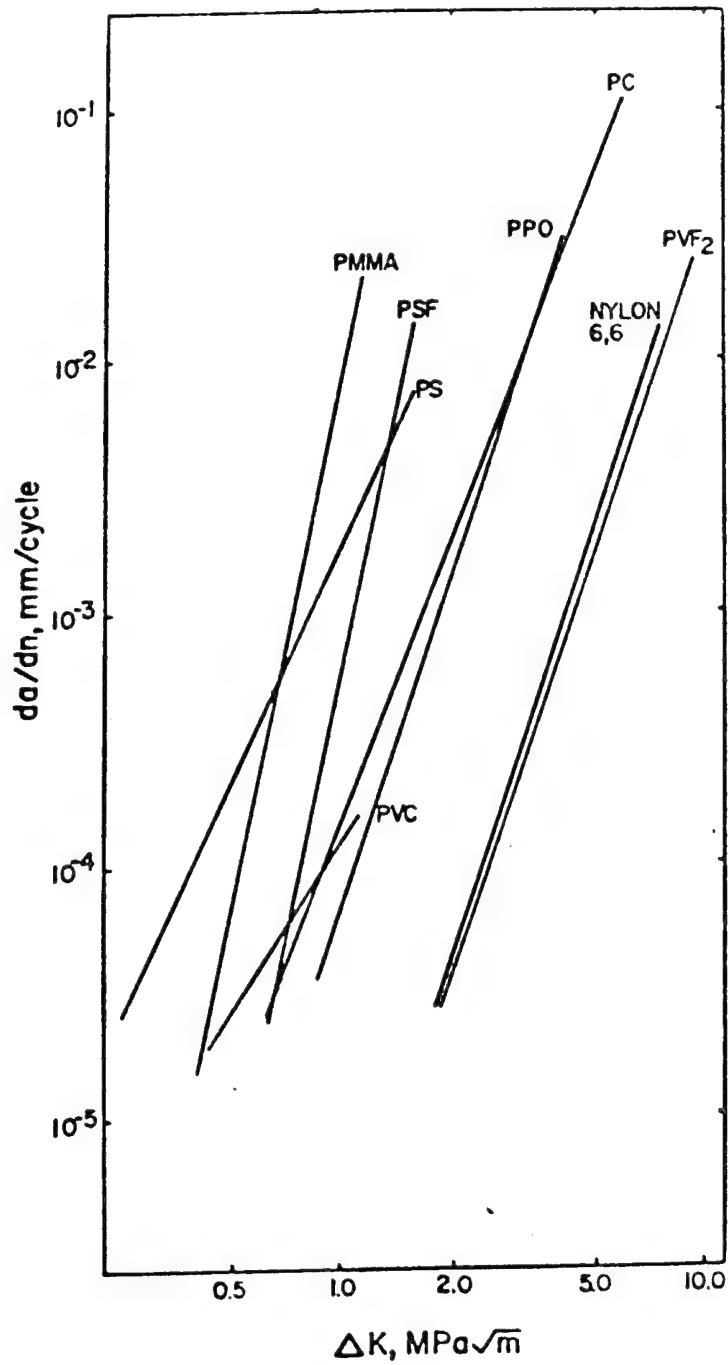
Figure 1.2 Relationship between crack growth rate per cycle in several polymers as a function of stress intensity factor range ΔK.[1,13,Al*]

*Refers to special reference list in Appendix IV

8

With equation 1.3, it is possible to analyze the FCP response of a polymer as a function of various external as well as internal structural parameters. For example, investigators have reported the FCP behavior of plastics to be highly sensitive to testing conditions.[1,13-28] As is typical of the mechanical response of most viscoelastic polymers, FCP is affected by strain rate and test temperature. In some polymers an increase in strain rate induced by an increase in cyclic frequency leads to a diminition of da/dN [1,13-22] while the complex effect of temperature on crack growth rates has been related directly to the loss spectrum.[26-28] Note that the effect of frequency on FCP is directly opposite to the results predicted by equation 1.1. This apparent anomaly will be discussed in detail in Chapter III. The least understood of all parameters affecting FCP is the internal structure. The importance of structure is evident when crack growth rates in amorphous PMMA are compared with results from semicrystalline nylon at the same ΔK; a 1000 fold difference in crack growth rates is found (Figure 1.2). The FCP response of certain crystalline polymers such as PA and PTFE have never been reported, but are expected to be comparable to reported results for nylon. Preliminary fatigue studies have implied that other structural parameters such as molecular weight [29-32] and plasticizer content[1,33] may also affect the cyclic behavior of certain polymers.

In addition to a study of the fatigue behavior of polymers, much insight may be gained by an analysis of the micro-mechanisms

9

of crack growth. This can best be accomplished by a study of the fatigue fracture surface micromorphology. Many detailed fractographic reports of static fracture have been published;[34-37] however, few studies of fatigue fracture mechanisms have been performed.

Since the cyclic behavior of polymers is not completely understood, it is the purpose of this research to evaluate comprehensively the fatigue response of a variety of characterized polymers under a wide range of test conditions.

The objectives of this dissertation will be:

1) To determine the effect of frequency, waveform, and temperature on the FCP response of a group of polymers with diversified properties and structure and to develop rational models which can account for the observed behavior.

2) To ascertain the effect of structural parameters on fatigue crack growth rates in selected polymers.

   a) The cyclic behavior of the fatigue resistant crystalline polyacetal will be evaluated.

   b) The role of molecular weight, distribution, and plasticizer content on FCP in PMMA and PVC will be examined.

   c) Fatigue testing of epoxy specimens will be performed to assess the importance of chain crosslink density.

10

3) To develop models to describe the micro-mechanisms

of fatigue fracture in engineering polymers.

II. Experimental Procedures

2.1 Materials

The polymeric materials used in this dissertation were obtained from several different sources (Table 2.1). Since the purpose of this research was to evaluate the FCP response of a wide variety of polymers, much synthesis time was saved by preparing specimens from sheets of readily available commercial grades of polycarbonate (PC), poly(vinyl chloride) (PVC), polystyrene (PS), crosslinked polystyrene (CLPS), Noryl, nylon, polysulfone (PSF) and poly(methyl methacrylate) (PMMA). In addition to these materials, carefully characterized specimens of PMMA and PVC were prepared at different molecular weights (M) and plasticizer contents. The PMMA supplies were synthesized in our laboratory by both emulsion and bulk polymerization techniques over a $\overline{M}_v$ range of 1×10^5 to 8×10^6. A third series of PMMA samples copolymerized with butyl acrylate (BA) were prepared at 6 different MMA-BA ratios where MMA/BA ranged from 100/0 to 50/50. (Polymerization performed by Dr. Soojaa L. Kim. Details of procedure presented in Appendix I.) A series of carefully synthesized PVC specimens with $\overline{M}_w$=60,500 to 225,000 were donated by Dr. E. A. Collins of the B. F. Goodrich Rubber Co. A second batch of variable M PVC plates was plasticized with 0-20% dioctyl phthalate (DOP).

The epoxy resins tested in this study were diglycidal ethers of Bisphenol-A oligomers: Epon series 825, 828, 1001, and 10004.

12

The curing agent used in most syntheses was methyl dianyline (MDA). By varying the stoichiometry of the epoxy prepolymer, the MDA mixture and the temperature, molecular weights between cross-links (M_c) from 320 to 2000 were produced. (See Appendix II)

2.2 Characterization

Molecular weights of all materials tested were determined by either viscosity measurements or through the use of Gel Permeation Chromatography. The glass transition and β transition temperatures were determined by either dynamic absorption spectroscopy or differential scanning calorimetry. All M and transition temperatures are tabulated in Tables 2.1 - 2.5. (Details of the characterization procedure are presented in Appendix III.)

2.3 FCP Specimen Preparation

All specimens of commercial plastic sheet used in the generation of FCP data were oriented in the same direction in the sheet. Cast samples were assumed to be completely isotropic and therefore, constant orientation was not maintained. Little difficulty was encountered in machining most materials to the proper configuration; however, the epoxies and low M PMMA required care in machining due to their low inherent toughness. All test specimens were either of the single edge notch (SEN) (Figure 1.1a) or compact tension (CT) (Figure 1.1b) geometry where the stress intensity range is given by[39]

13

TABLE 2.1   MATERIALS

Polymer (fabrication)	$\bar{M}_v$	Thickness (mm)
PC (extruded)	4.9×10^4	6.3
PVC (extruded)	8.8×10^4	3.2
(suspension-polymerized molded)	$\bar{M}_w = 0.97 - 2.3 \times 10^5$	6.4
PS (extruded)	2.7×10^5	6.5
PSF (extruded)	5×10^4	4.4
PMMA (commercial cast)	1.25×10^6	6.4
(bulk-polymerized cast)	$0.19 - 3.6 \times 10^6$	4 - 6.4
(bulk-polymerized cast)	1.1×10^5	6.2
(emulsion-polymerized)	1.0×10^5	6.4
(molded commercial resins)	$1 - 2 \times 10^5$	5.5 - 6.4
DELRIN (extruded)	-	6.4
Celcon (extruded)	-	6.4

TABLE 2.2   CHARACTERIZATION OF PMMA

Specimen	$[\eta]$, dl/g	$\bar{M}_v$, x 10^{-5}	T_g, °C	T_β, °C
0	4.4	36	110	56
1	3.5	23	108	56
2	2.5	15	110	56
3	0.9	3.5	108	56
4	0.57	1.9	104	56
5	0.35	1.0	96	54
6	0.28	0.72	92	54
7	0.22	0.55	a	a
8	0.15	0.33	a	a

[a] too brittle to test

15

TABLE 2.3   MOLECULAR WEIGHTS OF EMULSION-POLYMERIZED
AND COMMERCIAL PMMA

Specimen	Description		$\overline{M}_v \times 10^{-5}$
1E	Emulsion Polymerized at 40°C		81
2E	Emulsion Polymerized at 40°C		6.0
3E	Emulsion Polymerized at 60°C		3.7
4E	Emulsion Polymerized at 40°C		2.6
5E	Emulsion Polymerized at 40°C		1.9
6E	Emulsion Polymerized at 60°C		1.5
7E	Emulsion Polymerized at 40°C		1.0
8E	Emulsion Polymerized at 40°C		0.76
VS	Plexiglas VS		1.4
V9	Plexiglas V-920	molded	1.3
V8	Plexiglas V-811	commercial	1.2
LF	Lucite 4F	PMMA	2.0
L4	Lucite 40	resins	2.0
L1	Lucite 140		2.0

16

TABLE 2.4   CHARACTERIZATION OF MMA-nBA COPOLYMERS

Mole Ratio MMA/nBA	T_g,[a] °C	T_β,[a] °C	$[\eta]$, ml/g	$\overline{M}_v \times 10^{-6}$
100/0	110	56	4.8	3.6
90/10	86	54	9.0	3.7
85/15	68	40	14.9	7.1
80/20	65	40	15.0	7.2
75/25	57	-	14.5	7.1
70/30	53	-	14.5	6.2
60/40	23	-	10.5	5.0
50/50	7	-	12.5	6.5

[a]From maximum in E"; the β peak is increasingly overlapped by the glass transition peak as T_g decreases.

17

TABLE 2.5   COMPOSITION AND M^a OF PVC SPECIMENS

Code	% DOP	$\bar{M}_n \times 10^{-5}$	$\bar{M}_v \times 10^{-5}$	$\bar{M}_w \times 10^{-5}$	$\bar{M}_z \times 10^{-5}$	$\bar{M}_w/\bar{M}_n$
M-1-P-0	0	1.04	2.04	2.25	4.10	2.16
M-1-P-13	13	"	"	"	"	"
M-2-P-0	0	0.673	1.28	1.41	2.45	2.09
M-2-P-6	6	"	"	"	"	"
M-3-P-0	0	0.465	0.882	0.965	1.67	2.07
M-3-P-13	13	"	"	"	"	"
M-4-P-0	0	0.279	0.553	0.605	1.02	2.17
M-4-P-13	13	"	"	"	"	"

[a]By gel permeation chromatography, $\bar{M}_n$, $\bar{M}_v$, $\bar{M}_w$, and $\bar{M}_z$ being the number-, viscosity-, weight-, and z-average molecular weight, respectively. All values are for unplasticized polymer.

Data supplied by Dr. E. A. Collins

$$\Delta K = \frac{Y \, \Delta P \, \sqrt{a}}{BW}$$

where ΔP is the load range, B the specimen thickness, W the specimen width, a the crack length and the correction factors

$$Y = 29.6 - 185.5(a/w) + 655.7(a/w)^2 - 1017.(a/w)^3$$
$$+ 638.9(a/w)^4 \text{ for CT}$$

$$Y = 1.99 - 0.41(a/w) + 18.70(a/w)^2 - 38.48(a/w)^3$$
$$+ 53.85(a/w)^4 \text{ for SEN.}$$

2.4 Fatigue Testing

Fatigue tests were performed on a MTS electrohydraulic closed loop testing machine spanning a test frequency range of 1 to 100 Hz. The ratio of minimum to maximum load (R) was maintained at 0.1. Unless specified otherwise, all fatigue tests were run in air under sinusoidal waveform. When isolating the effect of strain rate, the triangle $\wedge$, negative $\wedge$ and positive sawtooths $\wedge$, and the square $\sqcap$ waveforms were utilized at 1 and 10 Hz. Crack growth was monitored in increments of approximately 0.25mm with the aid of a Gaertner travelling microscope.

2.5 Precracking

Precracking refers to the initiation and growth of a crack from the tip of the machined notch to a certain length where measurement of the crack propagation process could be monitored. Although initiation is an important fatigue process, it is of secondary concern in studies of FCP; consequently, techniques were

19

developed to minimize this step. In the tougher materials, in-itiation is hastened by cutting a chevron at the crack tip and sharpening with a scalpel. The specimen is then cycled at high frequency (100 Hz) at loads approximately 30% higher than cal-culated for obtaining the desired initial da/dN level. The crack usually initiates after 50-100,000 cycles by this method. At this point, the load is reduce in 5% steps every 10,000 cycles until the loads calculated for the assumption of the data-taking procedure are reached. The crack is then grown 5 mm before the first data point is taken to insure against overload interactions.

For those materials which are exceedingly brittle (all epox-ies and low-M PMMA) a type of "dynamic crack sharpening technique" was developed which dramatically aided crack initiation. With this method, the sample is cycled at high frequency at the de-sired testing loads. At the same time a sharp razor is drawn across the crack tip chevron. Initiation of FCP is usually in-stantaneous.

2.6 Low Temperature Testing

Low temperature fatigue testing was carried out in a small well insulated environmental test chamber. The desired tempera-ture was obtained by carefully controlling the flow of cooled nitrogen vapor through the chamber. The temperature control was believed to be within ±2 K, measured adjacent to the crack. A double glass window separated by dry nitrogen enabled crack meas-

20

urements to be made readily without fear of frost forming on the external glass pane.

2.7 Fracture Surface Analysis

Fracture studies were conducted with an optical metallograph, a Philips EM 300 transmission electron microscope (TEM) and an ETEC scanning electron microscope (SEM). Specimens prepared for use in the SEM were carbon and gold coated. Two stage replicas for TEM observation were made by first applying a thin layer of 10% poly(acrylic acid) in water to the fracture surface. After allowing sufficient time for drying, the plastic replica was stripped from the fracture surface, chromium shadowed and carbon coated. Finally, the poly(acrylic acid) was dissolved in water leaving the shadowed carbon film read to be mounted for viewing in the TEM.

III. The Effect of Frequency, Waveform and
Temperature on FCP in Polymers

3.1 Introduction

It is generally accepted that the mechanical response of viscoelastic solids, such as polymers, is highly sensitive to the rate of deformation. Therefore, it is not unexpected that under fatigue loading, crack growth rates in certain polymers are strongly affected by the cyclic rate or frequency. However, unlike fatigue induced thermal softening, discussed earlier, no melting has ever been reported during FCP at frequencies ranging from 0.01 to 100 Hz. Presumably, the entire cross section must be highly stressed to incur melting. When FCP is dominant, the zone of highly stressed material is localized at the tip of the advancing crack. Apparently, the cooler, less stressed material surrounding this zone of deformation is capable of absorbing any excess hysteretic energy, thus preventing an unstable temperature rise. Consequently, although some crack tip heating does occur,[39] melting is precluded and crack growth always occurs by a mechanical process. It is therefore surprising that investigators have reported a considerable decrease in crack growth rates in PMMA,[15-19] and PVC[20,22,23] with increasing frequency while PC, PSF, nylon 66 and PVDF were insensitive to frequency changes.[1] Using an expanded data base, an attempt will be made to thoroughly evaluate these hypotheses.

22

Closely related to cyclic frequency is the form of the re-
peating wave. By evaluating fatigue crack growth rates as a
function of various waveforms having different loading rates,
the basic importance of strain rate may be isolated from fre-
quency. From an enginnering standpoint it is unlikely that
cyclically loaded structures will be subjected to a perfect
sinusoidal waveform. At present only two investigations have
been reported which discuss waveform effects on polymers.
Harris and Ward[40] examined the FCP response of a complex vinyl
urethane under square and triangular waveforms. The triangu-
lar wave was reported to have produced crack growth rates 6
times faster than were observed uner the square wave. They
rationalized that the rapid load ramping or ascending strain
rate associated with the square wave produced a stiffening and
strengthening of the material consistent with the predicted
response of a viscoelastic material. Conversely, FCP waveform
studies of PC[1] showed no significant differences in da/dN be-
tween sinusoidal and square waves at 1 and 10 Hz. Clearly,
further investigation is required to adequately understand poly-
mer fatigue response to cyclic waveform.

If a similarity existed between the effect of temperature
on FCP and the static tensile properties of polymers, one might
expect an improvement in cyclic behavior (decrease in da/dN)
with decreasing temperature. This is consistent with the in-
crease in modulus and strength which accompanies a drop in test

23

temperature. However, such a simplistic explanation cannot account for the temperature dependence of the many complex mechanisms which control fatigue crack growth rates. In fact, Kurobe and Wakashima noted a decrease in the fatigue life of PMMA and PC when test temperature was decreased from 323 K to 263 K.[24,25] This was in agreement with their fractographic evidence which also indicated an increase in crack growth rates with decreasing temperature. Recent papers by Gerberich and Martin have in part confirmed the deleterious effect of lower temperatures on FCP in PC[26] and have found a similar response in PSF.[27] In FCP tests at temperatures ranging from 125 K to 380 K, they reported a minimum in toughness and a maximum in da/dN at 223 K. After a thorough analysis, they concluded that the minimum in properties corresponded to a minimum in the loss modulus when integrated over a 100 K temperature interval. A 100 K increase in crack tip temperature was hypothesized to occur by cyclic induced heating at 1 Hz. While a considerable temperature rise might be incurred during rapid fracture or high frequency fatigue test conditions, this writer believes that the hysteretic heat build-up at 1 Hz should be negligible.

Due to the limited amount of FCP data as a function of temperature and questionable interpretation of previously reported results, more extensive experimentation is in order. An attempt will be made to evaluate further the importance of test temperature on crack growth rates at 1 and 100 Hz in PC, PSF, and PMMA.

24

3.2 Results and Discussion

3.2.1 The Effect of Cyclic Frequency in Polymers

The effect of cyclic test frequency on fatigue crack growth
rates in a variety of polymers is shown in Figures 3.1-3.6. Of
these curves, the data base for PS (Figure 3.5a) spanning a four
decade change in da/dN obtained over a 3 decade change in frequency
may represent the most extensive FCP data base available for any one
polymer. It is evident that all polymers evaluated in this study
may be placed in one of two categories with regard to their respec-
tive frequency sensitivity. As previously reported, crack growth
rates in PC and PSF (Figures 3.1 and 3.2) were found to be insensi-
tive to test frequency. Conversely, PVC, PMMA, PS, and Noryl all
showed some decrease in da/dN with increasing frequency (Figures
3.3, 3.4, 3.5a, and 3.6). While the absolute effect of frequency
was not the same in all polymers tested, it is important to note
that da/dN never increased with increasing frequency. Therefore,
the frequency response of FCP and cyclic induced softening are anti-
podal. Confirming the occurrence of heating in both mechanisms of
fatigue, Attermo and Östberg[39] reported a 30 K crack tip temperature
rise in PVC at 11 Hz; however, this condition appears to be bene-
ficial to FCP. Consistent with this observation are the results
obtained in a test of an internally plasticized PMMA (to be dis-
cussed in greater detail in Chapter IV). Having a very high value
of J", this polymer, when tested at high frequency, became hot to

25
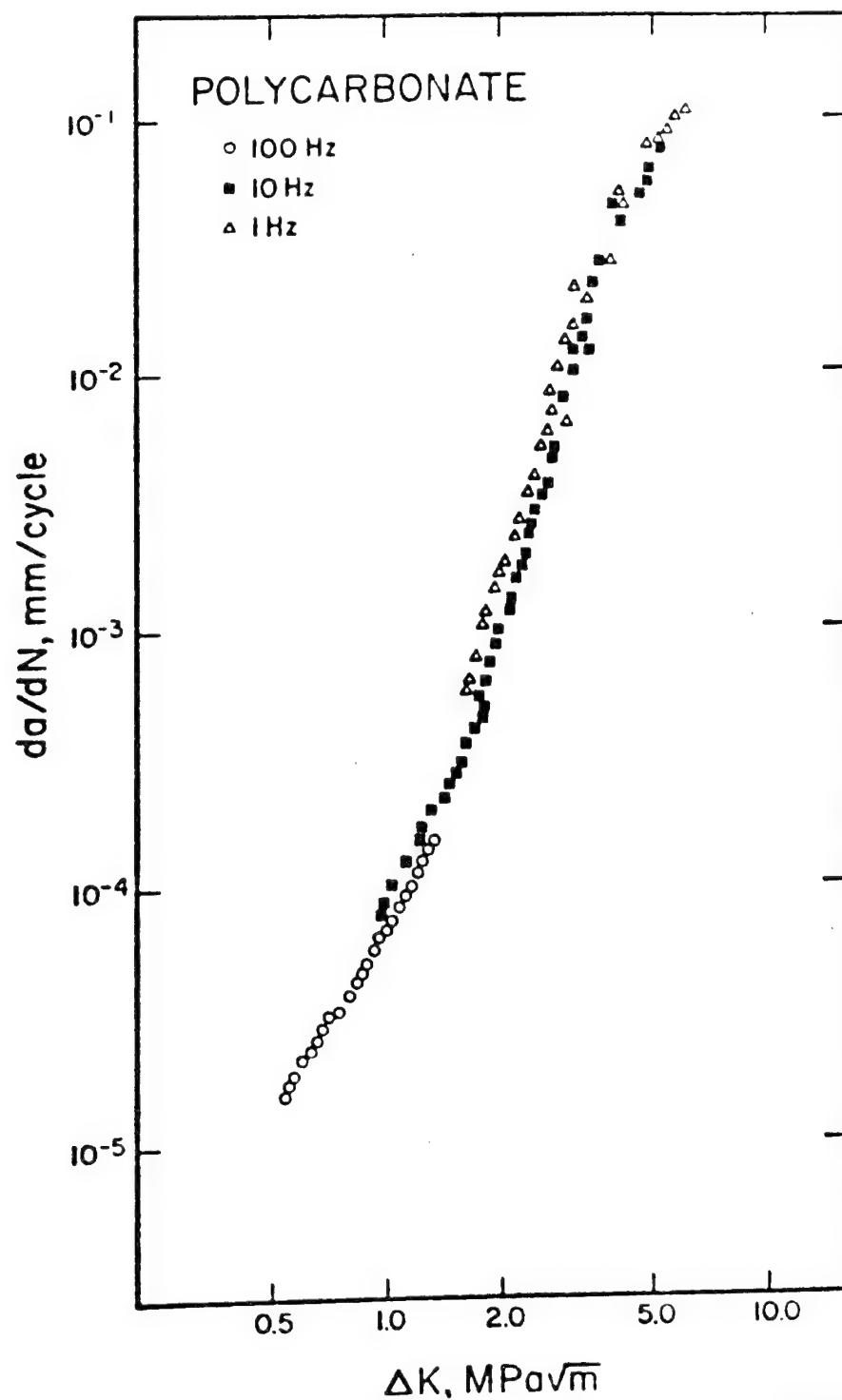
Figure 3.1 Effect of cyclic frequency on fatigue crack propagation in polycarbonate.[A1]

26
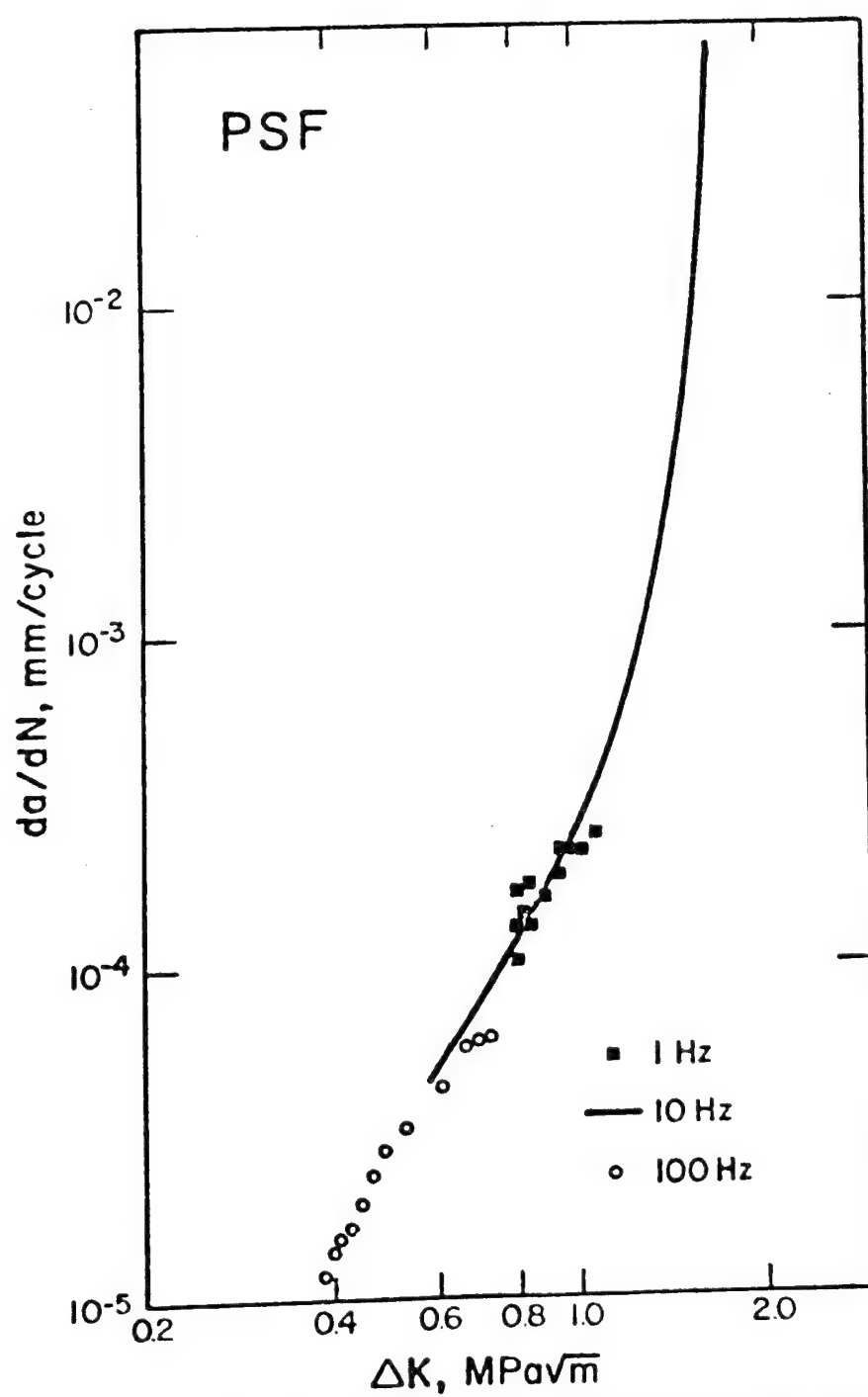
Figure 3.2 Effect of test frequency on crack growth rates as a function of ΔK in polysulfone.

27
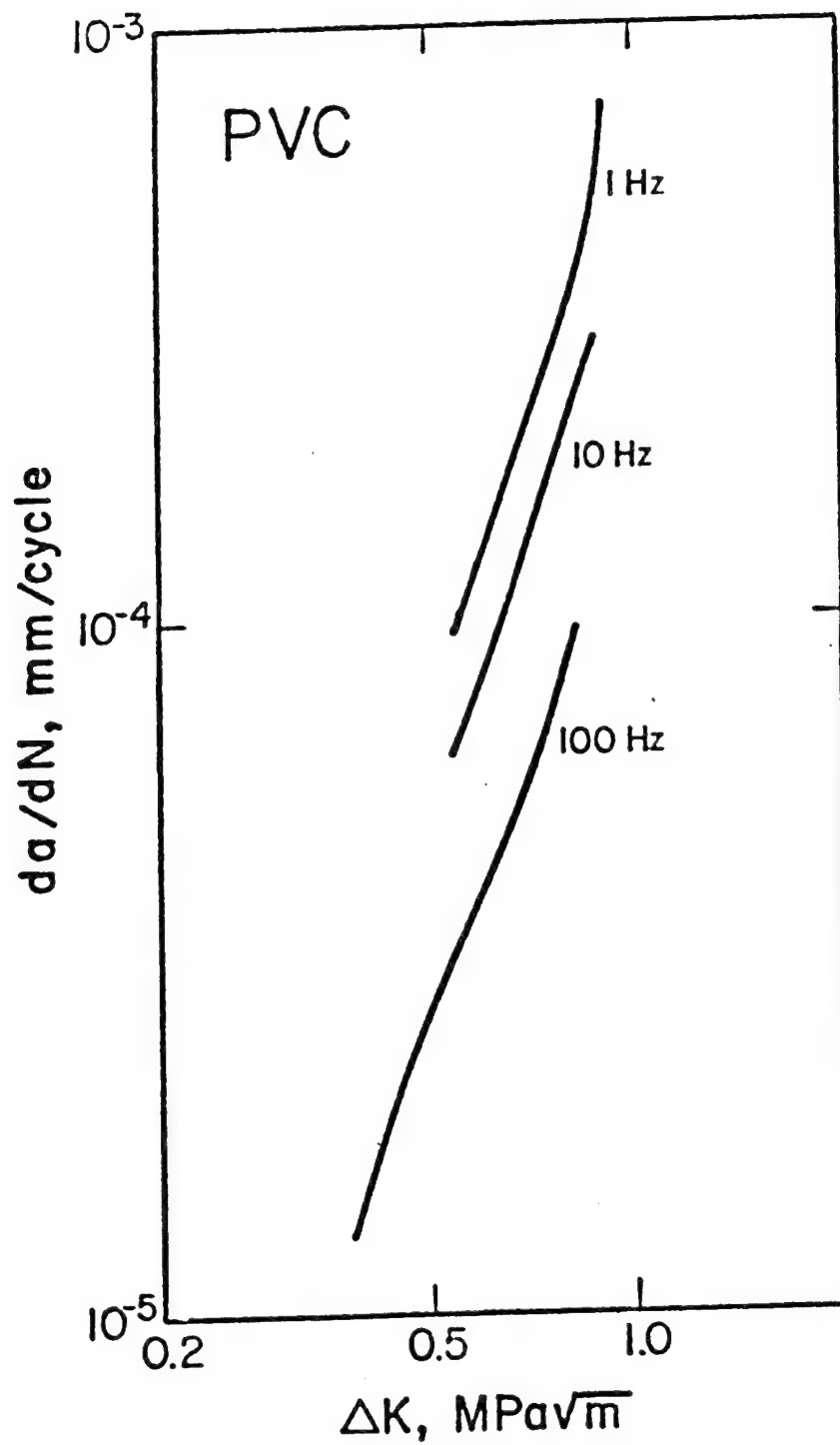
Figure 3.3 Effect of cyclic frequency on da/dN in PVC.

28
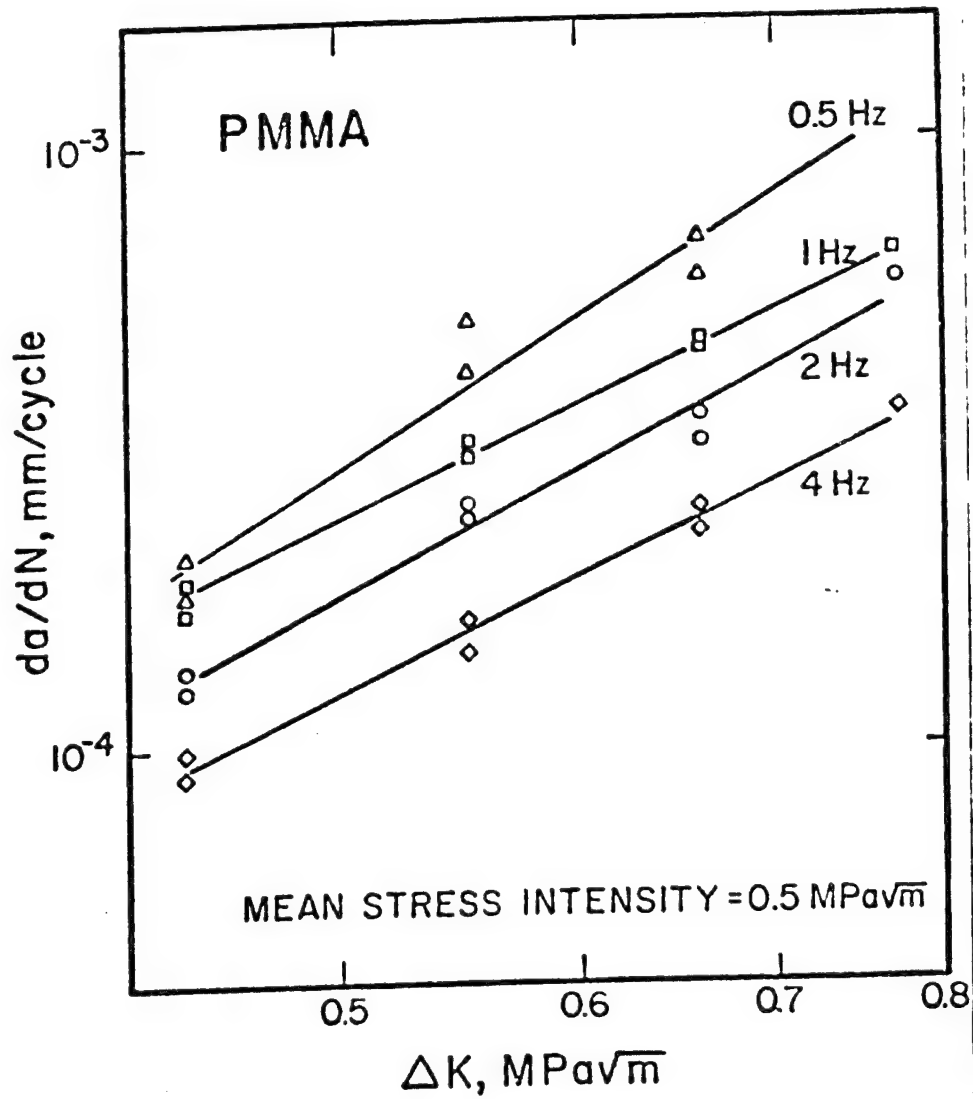
Figure 3.4 Effect of cyclic frequency on fatigue crack propagation in PMMA.[18]

29
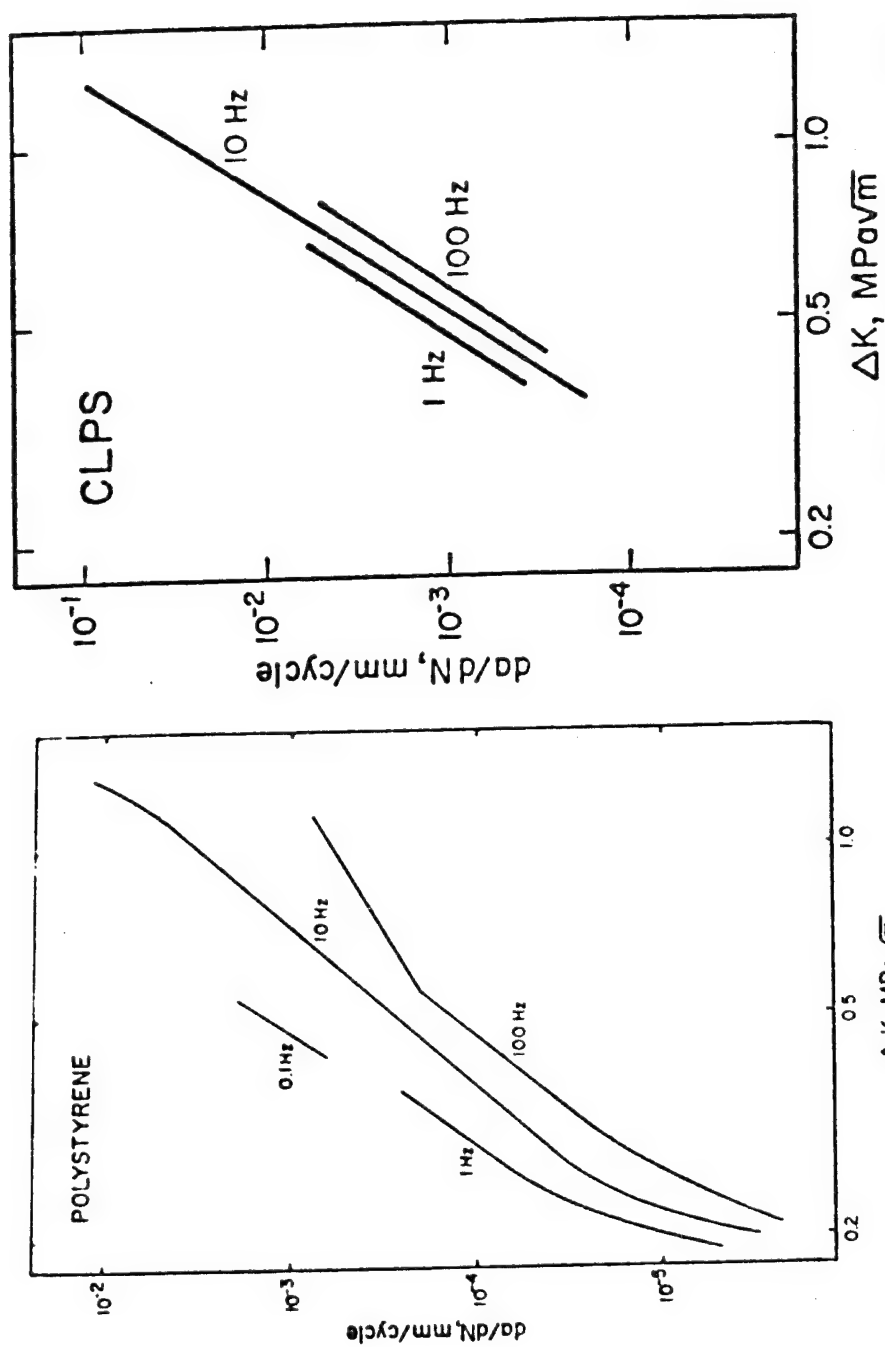
Figure 3.5 Fatigue crack propagation data in a) polystyrene and b) crosslinked polystyrene showing the effect of cyclic frequency and crosslinking. A1,A2

30
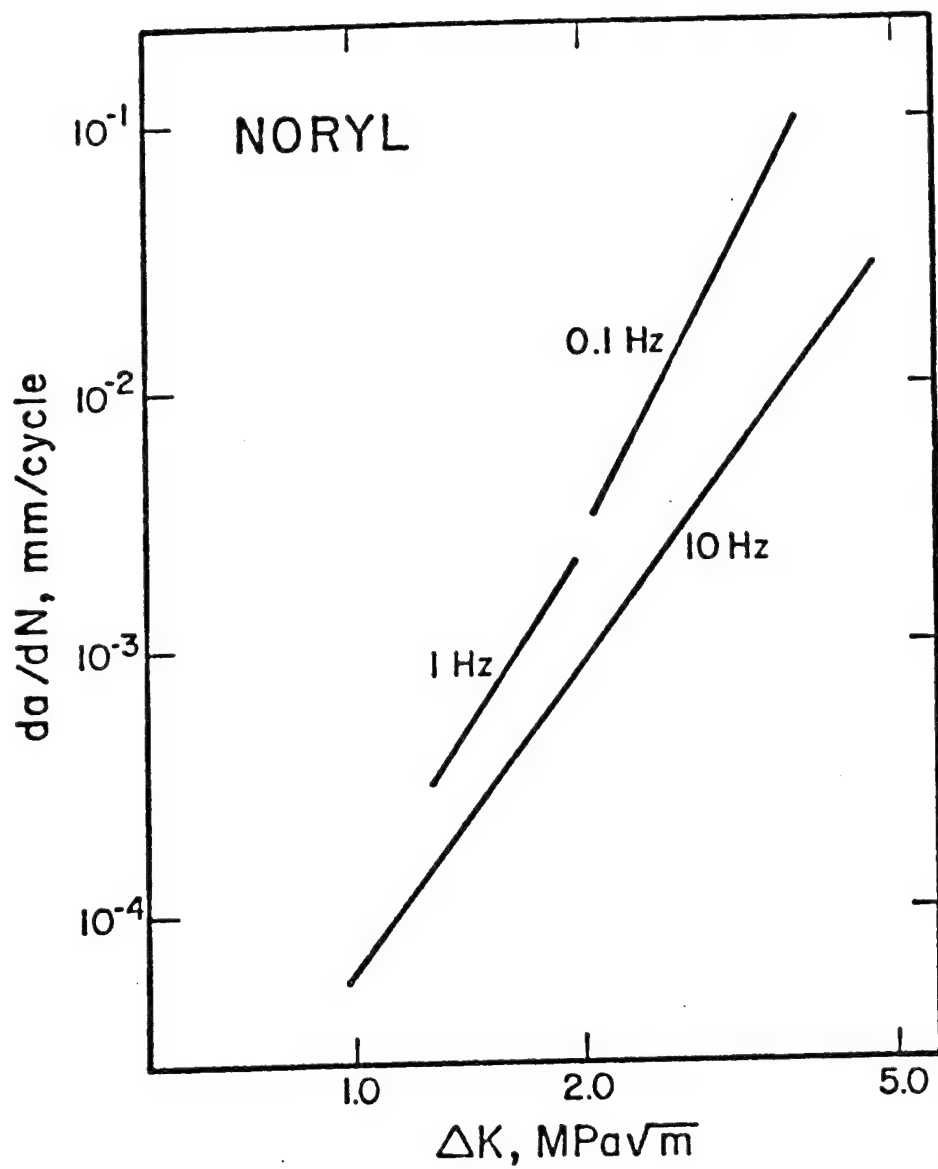
Figure 3.6 The effect of test frequency on FCP in Noryl.[A1]

the touch. No crack growth occurred under these conditions.

3.2.2 The Importance of Creep in FCP

A characteristic of all polymers which show some sensitivity to frequency is the shape of the crack growth curve (see Figures 3.3, 3.4, 3.5a, and 3.6). Over an intermediate crack growth range, the slopes of the growth rate curves for different frequencies are nearly equal. Below this range the data converge (i.e. FCP rates become somewhat less sensitive to test frequency) while above this range, test frequency plays an increasingly more important role in determining crack growth rates. This fatigue behavior is postulated to be related to the existence of a variable creep component. It has been reasoned that crack growth rates may be considered to be the sum of a pure fatigue component $da/dN_{(fat)}$ and a pure viscous creep component $da/dt_{(cr)}$ where

$$da/dN_{(tot)} = da/dN_{(fat)} + da/dt_{(cr)}.$$

At low ΔK where $da/dt_{(cr)}$ is small, $da/dN_{(tot)}$ approaches $da/dN_{(fat)}$ which accounts for the lower frequency sensitivity in this test range. At high ΔK where da/dt is believed large, the latter component represents a greater portion of $da/dN_{(tot)}$, thus explaining the increased frequency sensitivity. At intermediate levels of ΔK, $da/dN_{(fat)}$ and $da/dt_{(cr)}$ are presumed to be of comparable magnitude, thereby accounting for the simple displacement of the crack growth rate curves with changing frequency. This

32

hypothesis is supported in part by the CLPS data shown in Figure 3.5b. The presence of chemical crosslinks acts to suppress viscous flow, causing the frequency sensitivity of CLPS to be much less than linear PS (Figure 3.5a). However, further laboratory studies suggest that this model may not be generally applicable to all polymers. Fatigue tests of selected polymers have shown a strong frequency sensitivity at stress intensity levels where no creep crack growth was measureable. This does not rule out the possiblity that a synergistic relationship may exist between fatigue and creep crack growth where the cyclic nature of fatigue deformation induces creep. For example, studies of vibrocreep have shown a significant increase in creep rates when minute cyclic loads are superimposed on the major static stress.[41,42] At any rate, it seems clear that a simple superposition model involving pure fatigue and creep components is both unreasonable and oversimplistic.

3.2.3 Strain Rate Effect

Recognizing the large effect that strain rate changes have on the mechanical properties of polymers in general, one must appreciate the fact that an increase in the cyclic frequency is tantamount to an increase in strain rate. Since many polymers are highly viscoelastic over certain time and temperature ranges, their mechanical properties should be sensitive to strain rate or frequency in these regimes. Consequently, an increase in the frequency should increase the modulus and strength and enhance FCP resistance.

33

While the end result is consistent with the frequency response of certain polymers, it is a fact that the mechanical properties of all polymers studied in this dissertation lie close to or above the plateau in the mechanical properties - time/temperature curve (i.e. a change in frequency of 2-3 orders of magnitude could not dramatically alter any mechanical property). One can only conclude that strain rate effects alone should not be wholly responsible for the observed frequency sensitivity of FCP. A thorough analysis of strain rate will be offerred in the section on waveform.

3.2.4 β - Transition - Frequency Sensitivity Hypothesis

The β peak, representing a maximum in loss modulus in the dynamic mechanical spectrum of certain polymers, has been related to main chain segmental motion. Since specific mechanical properties have been linked to the β transition,[43] an attempt was made to relate the frequency sensitivity of a polymer to its β peak or associated jump frequency. It was possible through extrapolation and interpolation to estimate the jump frequencies of PS,[44] PMMA,[44] PC,[44] nylon,[44] poly(vinylidene fluoride)[44] and PSF[45] at room temperature. The relative change in da/dN per decade decrease in frequency, calculated from the linear and parallel portions of the crack growth rate curves in Figures 3.3-3.6 was given by the "frequency sensitivity factor" (FSF) and is listed for each polymer in Table 3.1. The comparison of the room temperature jump frequency and FSF yielded a very interesting and profound relationship (Figure 3.7).

34

Table 3.1 FSF of FCP in Polymers at Room
Temperature

Material	FSF
PMMA	2.5-3.3
PS	2.3
Noryl	2
PVC	1.8
CLPS	<1.5
PC	1
PSF	1
Nylon	1
PVDF	1

35
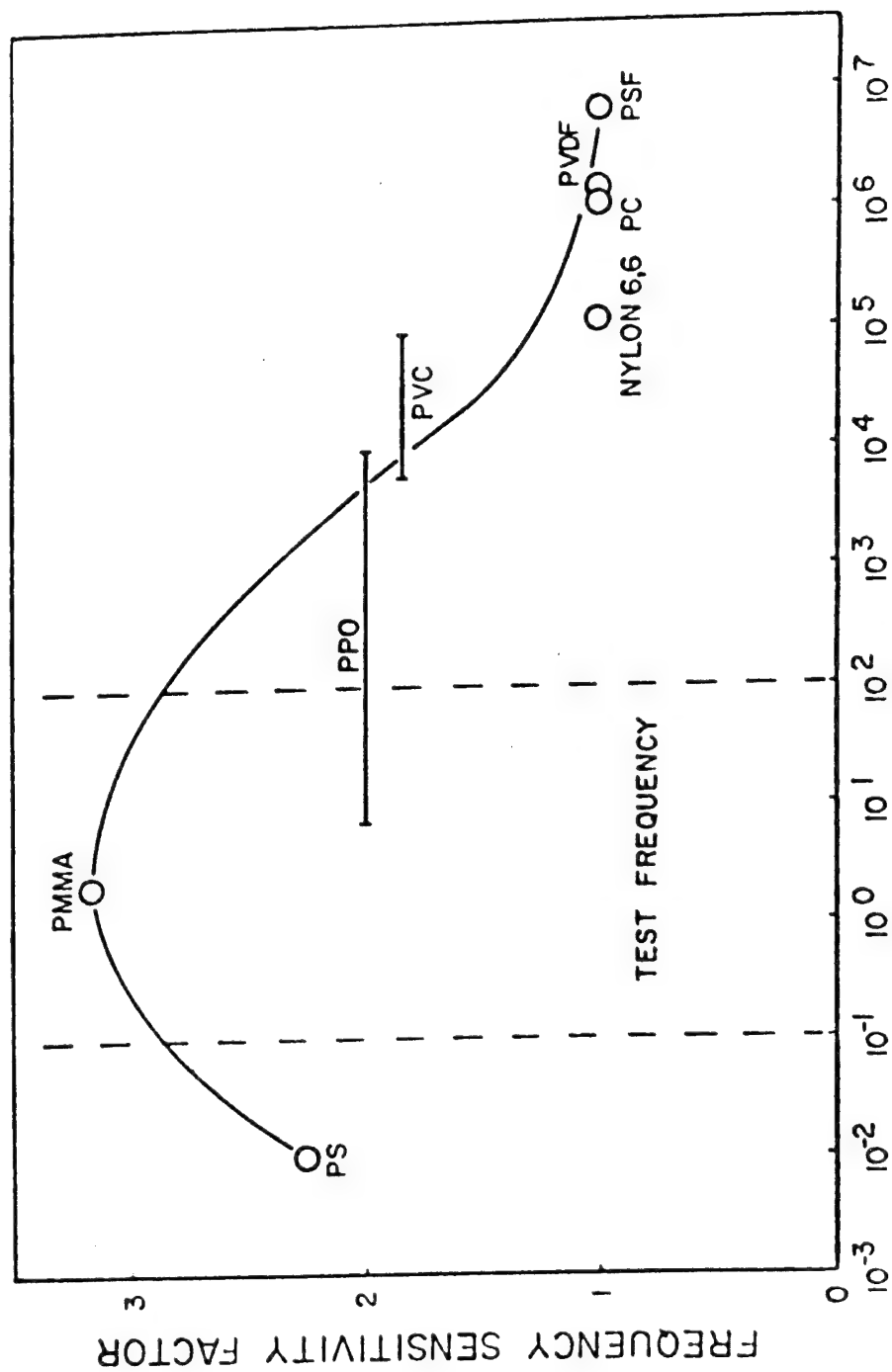
Figure 3.7 Relationship between FCP frequency sensitivity and the room temperature jump frequency for several polymers.

It is evident that the polymers which exhibited a jump frequency close to the mechanical test frequency regime showed a high frequency sensitivity factor, while those polymers with a jump frequency much greater than the test frequency range had no frequency sensitivity (FSF = 1). Although no polymer with a jump frequency much less than the test frequency has been tested, a frequency sensitivity factor at about 1 for such a material would be expected. This relationship suggests a condition of resonance of the externally imposed test machine frequency with the material's internal segmental mobility corresponding to the β peak.

On the basis of the correlation shown in Figure 3.7, one would expect the room temperature frequency sensitivity factor of PC, PSF, nylon 66, and PVDF to increase were it possible to excite these materials at test frequencies in the range of 10^6 Hz. Unfortunately, this could not be studied directly because of test machine limitations. However, since the segmental motion jump frequency varies with temperature, it should be possible to choose a particular test temperature for each material that will bring the jump frequency into the cyclic frequency range permitted by our test machine. For this case, the frequency sensitivity should be maximized. Correspondingly, the frequency sensitivity of PMMA should be attenuated at test temperatures below ambient.

Therefore to further clarify this correlation between cyclic frequency and jump frequency, the FSF was evaluated at different

37

test temperatures. The polymers chosen for this study were PMMA, PSF, and PC. Polycarbonate and polysulfone which showed no frequency sensitivity at room temperature, were tested at lower temperatures where the β peak at the test frequency is maximized. Correspondingly, PMMA, a polymer with a high frequency sensitivity factor at room temperature, was tested at lower temperatures where the test frequency and the jump frequency differ by orders of magnitude. In this manner, the FSF for this material should be reduced. (With all specimens, it should be noted that since each frequency corresponds to a somewhat different value of the temperature for the β-process, experiments at constant temperature are not rigorously comparable. However, inspection of typical β-peak data[47] shows that the consequent error in the frequency sensitivity factor will not affect the conclusions.)

Frequency sensitivity factors were calculated for all test specimens from fatigue crack propagation data obtained at 1 and 100 Hz. The values of the frequency sensitivity factor were then plotted as a function of temperature and are shown in Figures 3.8-3.10. Polysulfone and polycarbonate, two polymers which showed negligible frequency sensitivity at room temperature, exhibited a maximum in frequency sensitivity factor (>2.4) at temperatures corresponding to a jump frequency between 1 and 100 Hz for both materials. PMMA which demonstrated a maximum FSF at room temperature (jump frequency ~ test frequency) responded to a lowering of test temperature with a

38
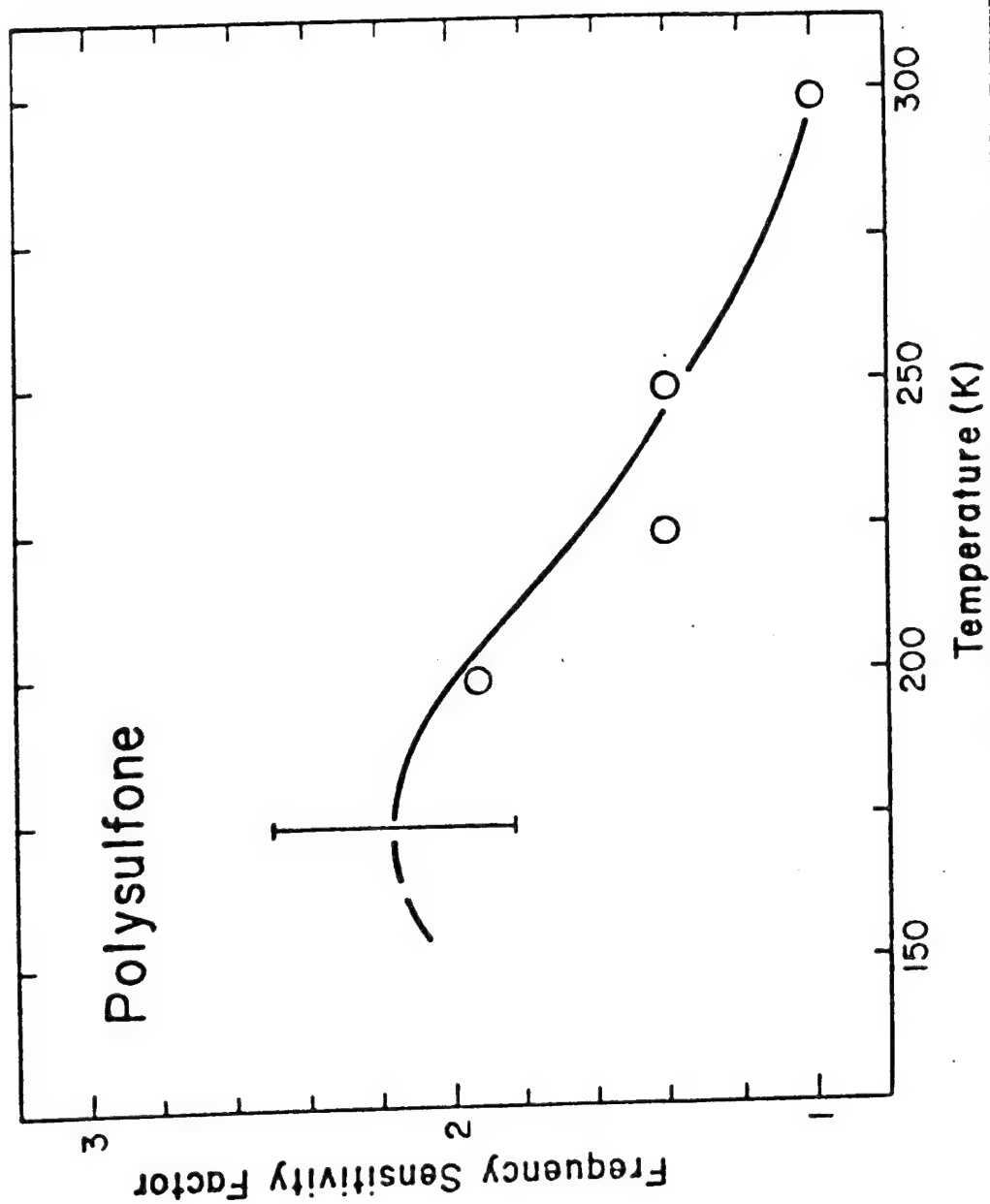
Figure 3.8 Relationship between the frequency sensitivity factor and temperature in polysulfone.[A4]
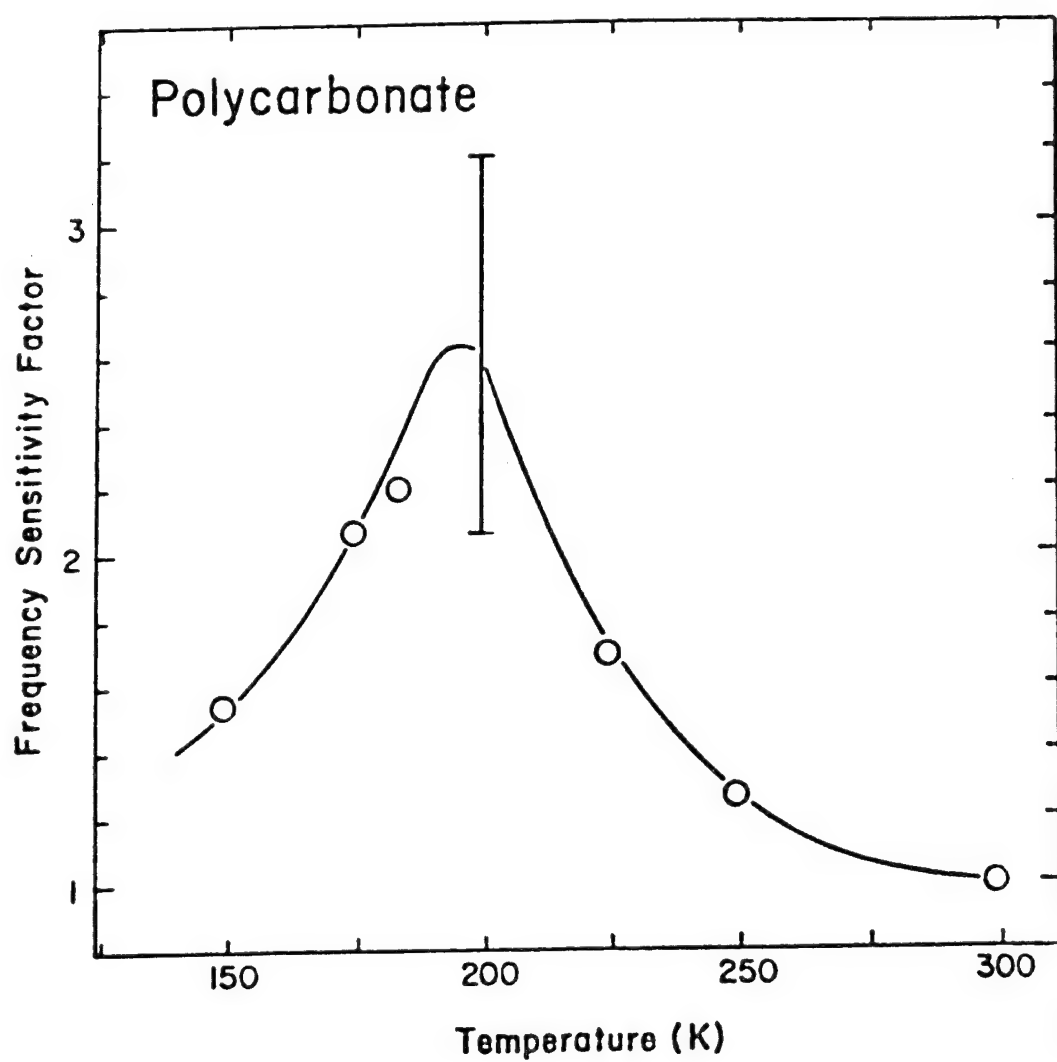
Figure 3.9   Relationship between the frequency sensitivity factor
and temperature in polycarbonate.
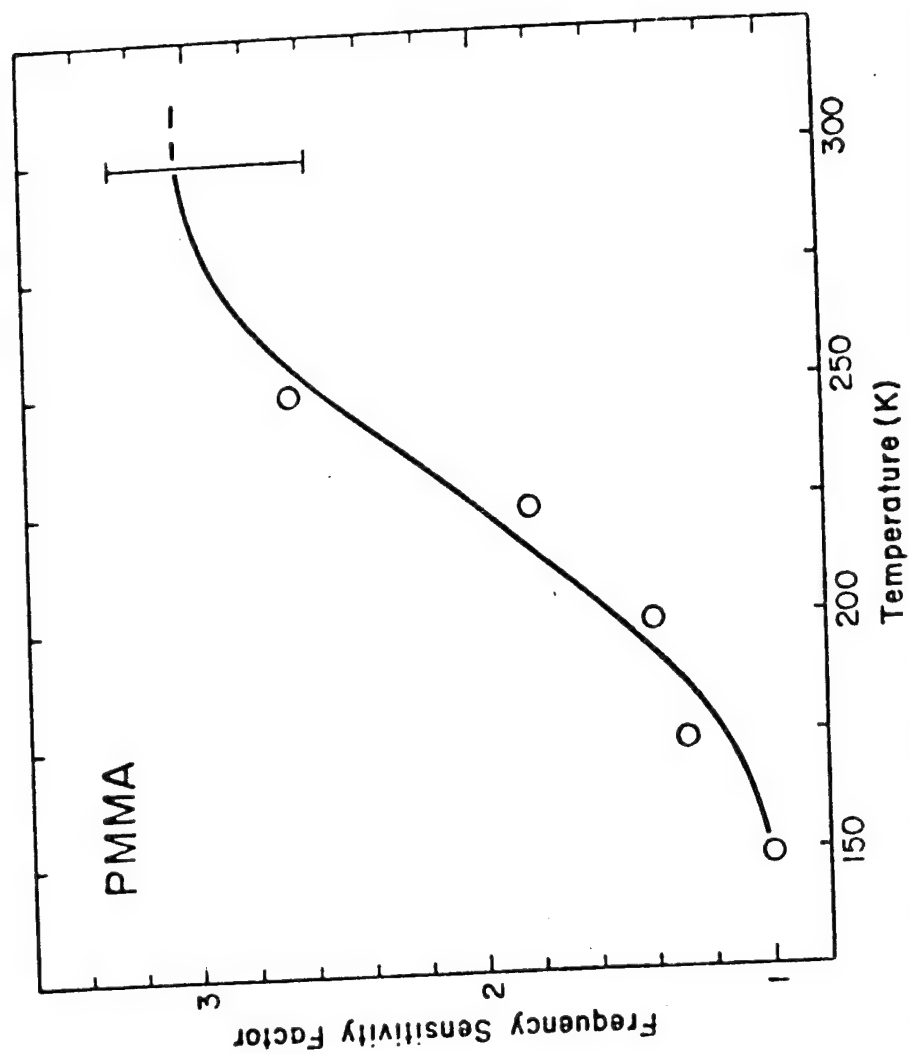
Figure 3.10. Relationship between the frequency sensitivity factor and temperature in PMMA.[A4]

considerable decrease in FSF as the jump frequency became much lower than the test frequency. These data lend further support to the correctness of the β-jump-frequency-test frequency correlation. Such a correlation is not without precedent, for the β-process may be associated with yielding, creep, crazing and crack growth phenomena.[43] Carrying this relationship one step further, it is possible to normalize the previous data with respect to the temperature of the β-maximum. Figure 3.11 shows the relationship between the FSF for PSF, PC, PMMA, and some preliminary PS data and the normalizing factor $T-T_\beta$. Note that all data points fall approximately on the same curve evincing the generality of this correlation.

A physical interpretation of this correlation may be seen with the following model. It is generally accepted that the β-peak represents a region of maximum loss compliance, associated with a high level of damping or energy dissipation. This increase in damping leads to a corresponding increase in hysteretic energy and a localized temperature rise. In the notched samples utilized in this study and others, the maximum heat rise is restricted to the minute plastic zone near the crack tip while the bulk of the specimen experiences lower cyclical stresses and remains essentially at ambient temperature. Although heat transfer from the plastic zone to its cooler surrounding environment might limit the rate of crack tip heating, fatigue testing at high frequencies (100 Hz) should nevertheless produce a considerable temperature rise at the crack tip.

42
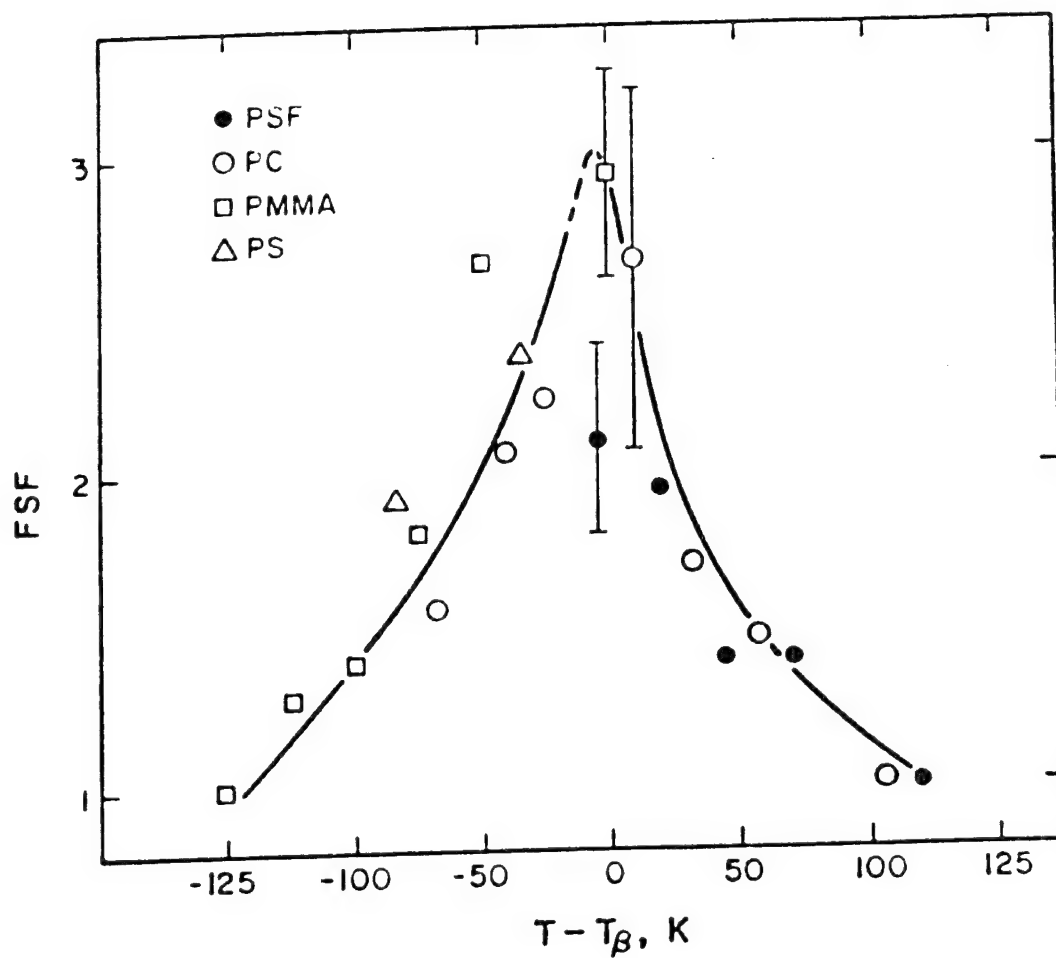
Figure 3.11 Relationship between FSF and the normalized β-transition temperature, $T - T_{\beta}$.

43

This has been confirmed by Attermo and Östberg[39] who recorded a max-imum increase in crack tip temperature of 30 K in fatigue testing of polymers at only 11 Hz. With a significant increase in temperature, yielding processes in the material surrounding the crack tip should be enhanced. This should lead to an increase in the crack tip radi-us. This greater radius of curvature at the crack tip should result in a lower effective ΔK. As the effective ΔK decreases, da/dN is expected to decrease accordingly. While no attempt was made to meas-ure crack tip radii or temperatures in this study, high frequency fatigue tests performed on another polymer (internally plasticized PMMA) with a very high value of J" caused the crack tip region to rapidly become hot to the touch. In addition, the crack tip became visibly rounded. At this point, stable crack growth ceased.

It is conceivable then that the frequency sensitivity factor is maximized when the rate of crack tip heating is greatest since crack growth rates will be slowest in comparison. This should oc-cur at temperatures where extensive energy dissipation or damping is present within a polymer, and would occur in resonance with the test frequency.

3.2.5 The Effect of Waveform on FCP in Polymers

In the previous section, the effect of frequency on the FCP be-havior of plastics was carefully analyzed under conditions of sinus-oidal loading. Since strain rate $(\dot{\epsilon})$ was identified as one of sev-

44

eral possible mechanisms controlling the frequency sensitivity, it seems appropriate to isolate the effect of this basic parameter on FCP. To isolate the effect of strain rate on FCP, cyclic tests of certain polymers were conducted at fixed frequencies but different load waveforms: the square wave, triangle, positive and negative sawtooth. In addition to the previous waveforms, baseline sinusoidal da/dN vs. ΔK data was available for all materials. The above mentioned waveforms may be listed in order of decreasing strain rate as follows: square and negative sawtooth, triangle and positive sawtooth.

In testing under variable waveform conditions, another parameter, time under load or creep, becomes an important variable that may affect the fatigue crack growth process. By maintaining constant strain rate and varying the integrate time under load, creep crack growth may also be isolated. Experimentally, this could be accomplished by comparing crack growth rates obtained under the square and negative sawtooth waveforms where the ascending strain rate is equal but the square wave exhibits twice the time under load as compared with the sawtooth waveform.
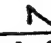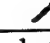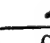
The overall test frequency was maintained at 1 or 10 Hz to minimize the possibility of extensive crack tip heating. However, considering the exceedingly high strain rate of the rapid ramping functions, some heating may occur during the initial portion of each cycle.

45

The results of the variable waveform fatigue tests of PC, PMMA, PVDF, PS and epoxy are listed in Table 3.2. These crack growth rates were obtained at a constant ΔK which was chosen to yield conveniently obtainable crack growth rates. From Table 3.2, PMMA, PS and PVC exhibit some changes in da/dN as a function of waveform, while PC, PVDF and epoxy showed no variation.

While the changes in da/dN with waveform are small in comparison to the frequency effect shown earlier, they accurately reveal the true but minor effect of strain rate. It is more than coincidence that the same polymers which exhibit a strong frequency sensitivity also are sensitive to waveform. One can only speculate that the β transition may also be responsible for waveform effects. This is consistent with the possibility of maximum strain rate effects and creep rates occurring around the β transition.[43] It is therefore quite interesting to note that the polymers sensitive to waveform, PS, PMMA and PVC, also exhibit strong β peaks in the test frequency range.

Of those polymers which revealed changes in da/dN with waveform, two distinct responses are evident. PVC and PS showed a continuous increase in crack growth rates with increasing loading rate and area under the load-time curve (note in Table 3.2, da/dN $\sqcap$ > da/dN $\wedge$ > da/dN $\wedge$ > da/dN $\wedge$). Conversely, PMMA was insensitive to varying strain rate but was affected only by time under the curve (da/dN $\sqcap$ ~ 2.5 (da/dN $\wedge$, $\wedge$, $\wedge$)). The latter response indicates the importance of creep crack growth. However, it is clear that the

46

Table 3.2 Crack Growth Rates as a Function
of Waveform

Material	ΔK MPa/m	Frequency Hz	da/dN x 10^4				
			$\sim$	$\sqcap$	$\wedge$	$\wedge$	$\wedge$
PVC	.72	1	1.17	1.41	1.02	1.08	0.8
"	"	10	0.8	0.9	0.7	0.8	0.68
"	.77	1			2.03	1.96	1.7
"	.77	10			1.33	1.3	1.14
PMMA	.83	1		19.2	7.8	8.2	7.8
PS	.77	1		21.6	17.8	14.5	13.9
Epoxy 1.6:1	.70	1	2.26	2.20		2.30	
PVDF	2.0	1	No Change				
PC	-	1 + 10	No Change				

square waveform with its maximum loading rate and time under load, generally yields the highest da/dN.

If the waveform - da/dN relationship is linked to the β transition, the shape of the β peak, or more specifically the slope of the damping curve at this maximum may account for the specific waveform response observed. A positive slope would signify an increase in damping with increasing temperature and a negative slope, the reverse. The loss modulus vs. temperature curve for PMMA (Figure 3.12a) shows a maximum at room temperature corresponding to the β peak. With a slight temperature rise, the slope becomes negative and damping decreases. If PMMA is cycled under a waveform involving a rapid initial strain rate, some crack tip heating may occur, but the increase in temperature should be quickly balanced by decreasing damping. Therefore, it may be argued that strain rate, per se, should not affect da/dN in PMMA. However, the β peak has been related to a maximum in static load-related creep rates. Consequently, the fatigue response of PMMA should be highly sensitive to time under load which is consistent with the maximum FCP rates being associated with the square waveform of loading. PS and PVC also exhibit β peaks near room temperature (Figures 3.12b,c), but both curves show positive slopes in their damping (G" or tan δ) - temperature curves. In these materials, a waveform with a higher ascending strain rate should induce a real temperature rise at the crack tip.

It seems apparent from the previous discussion that the strain

48
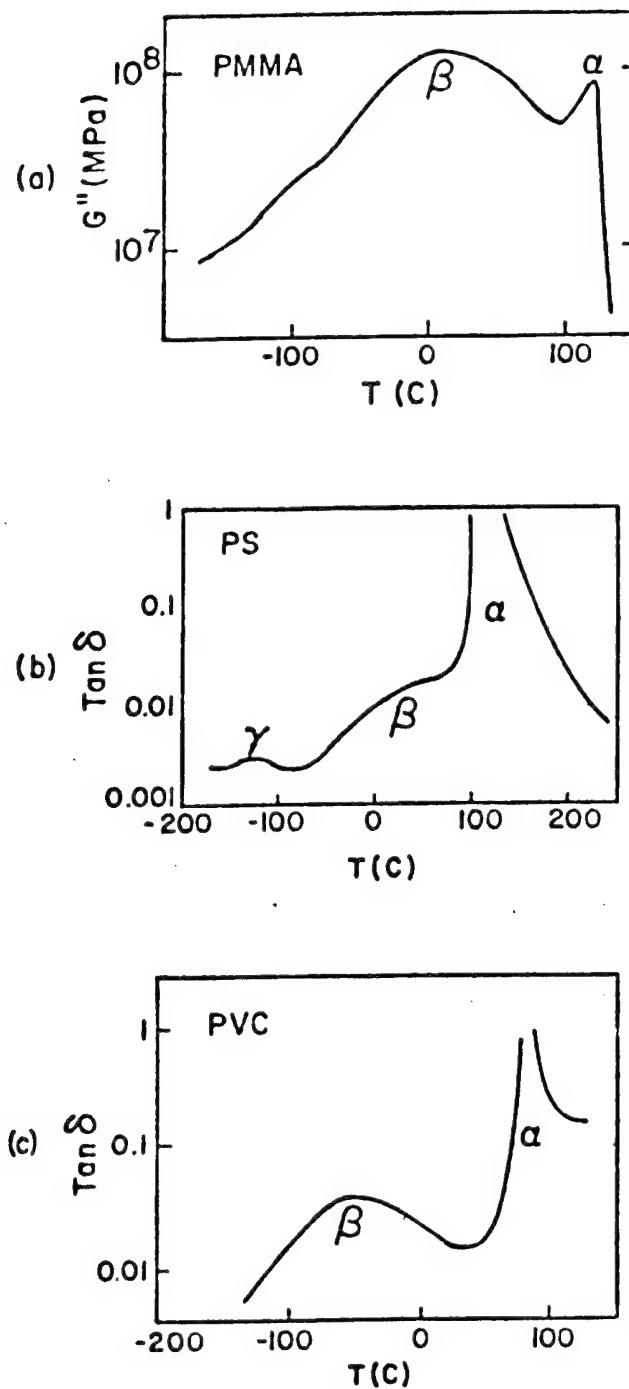
Figure 3.12   Temperature sensitivity of loss modulus and tan δ
in a) PMMA[44], b) PS[44], and c) PVC.[46]

49

rate serves to modify crack tip conditions in a manner which could affect creep crack growth. Consistent with this argument is the total lack of waveform sensitivity in the heavily crosslinked epoxy, a material where creep caused by molecular chain sliding is highly restricted. Now consider the waveform response of PS-PU reported by Harris and Ward.[40] Although the exact composition of PS-PU is not known to the author, the authors indicated that this material consisted of a 2 component structure of glassy PS and crosslinked rubbery PU. If this material behaves in a manner similar to other interpenetrating network polymers, one might expect the mechanical properties of both components to be evident. Under the rapid loading associated with the square waveform, the rubbery component should exhibit increased rigidity and yield strength which would account for a drop in crack growth rates. Conversely, the square waveform would tend to produce more creep cracking in the PS component of the material. In fact, Harris and Ward found the square waveform to yield a minimum in crack growth rates. This suggests that the strain rate sensitivity of this two phase material was dominated by the rubbery PU phase.

3.2.6 The Effect of Temperature on FCP in PSF, PC and PMMA.

Figures 3.13-3.15 show crack growth data for PC, PSF and PMMA, respectively, at 1 and 100 Hz over a temperature range of 150 K to 300 K. A comparison of the 1 Hz crack growth curves shown in

50
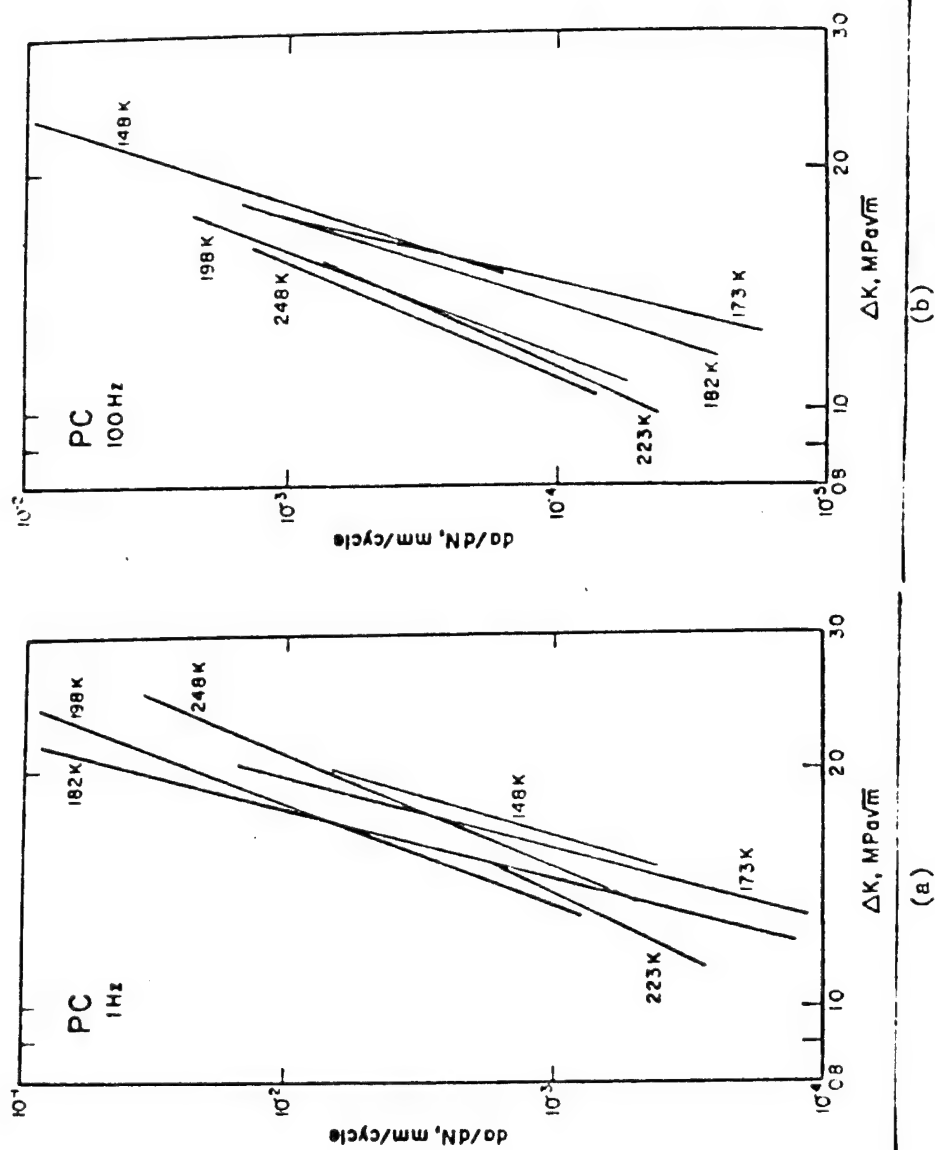
Figure 3.13 Effect of temperature on fatigue crack growth rates in polycarbonate at a) 1 Hz and b) 100 Hz.

51
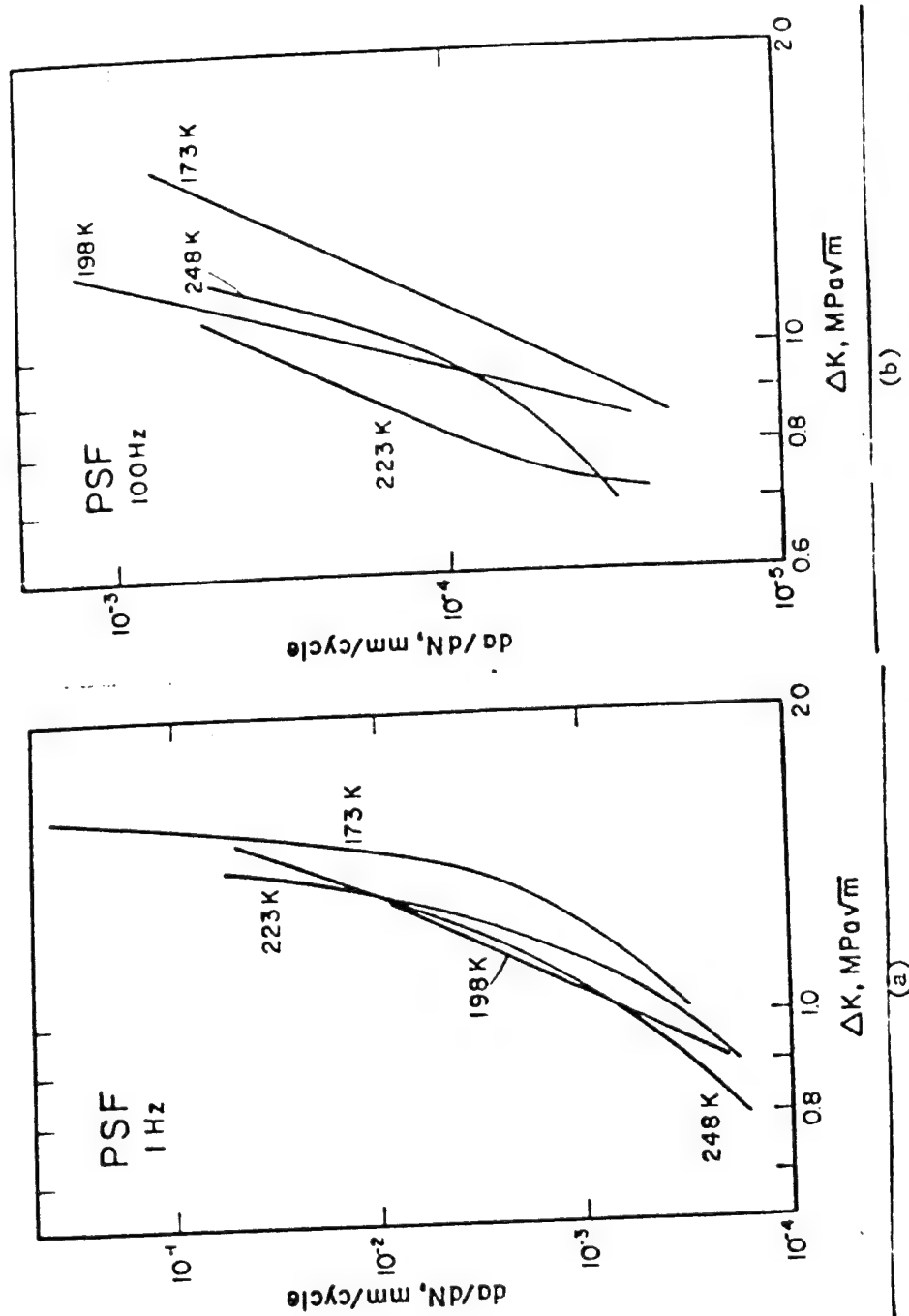
Figure 3.14 Effect of temperature on fatigue crack growth rates in polysulfone at a) 1 Hz and b) 100 Hz.
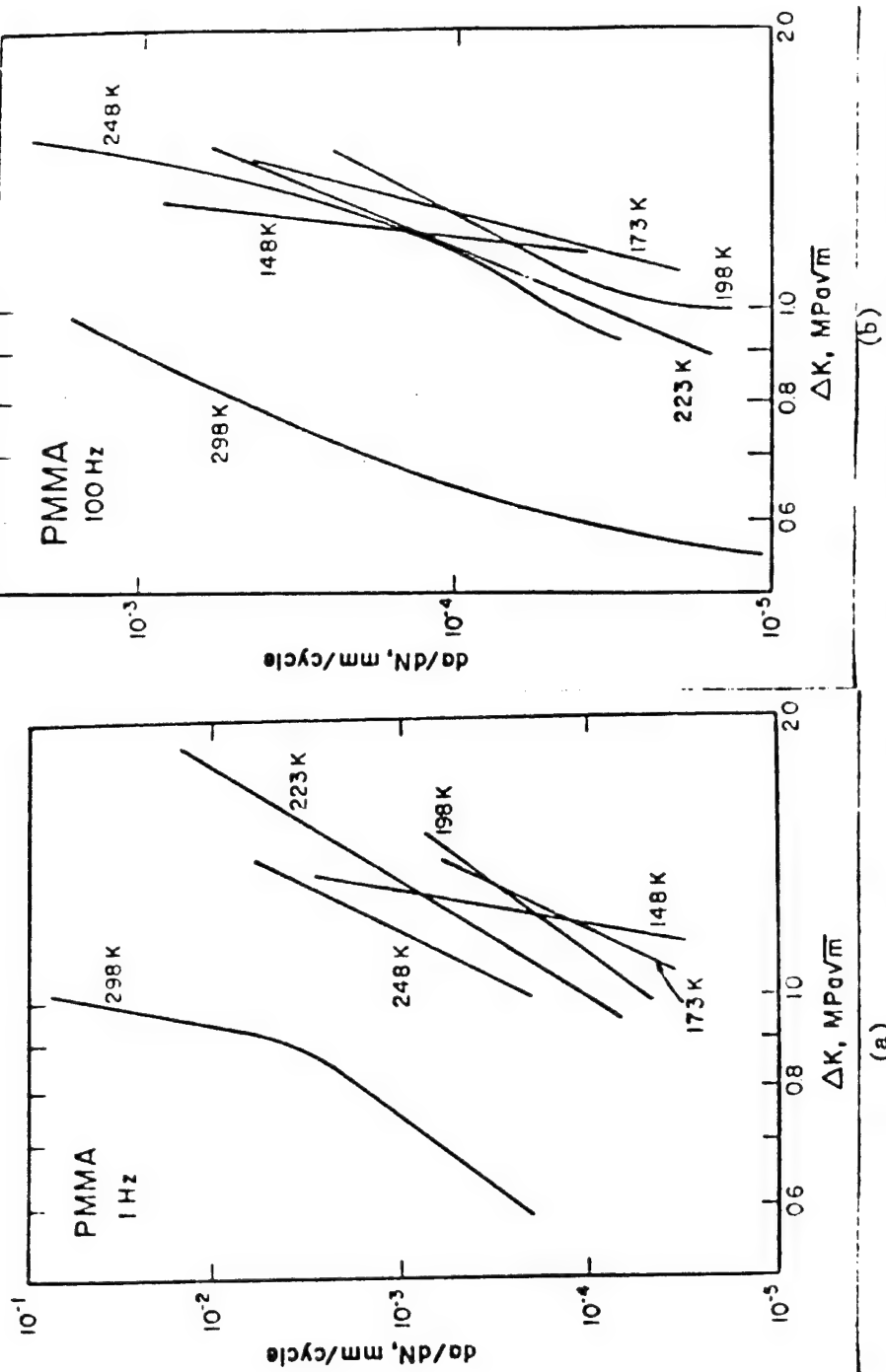
Figure 3.15 Effect of temperature on fatigue crack growth rates in PMMA at a) 1 Hz and b) 100 Hz.

Figure 3.13a with the 1 Hz data reported by Martin and Gerberich[26] gives good agreement from room temperature to 223 K. Below this temperature, the curves diverge yet maintain a similar trend with temperature.

In Figures 3.16-3.18, da/dN is evaluated at an arbitrarily chosen ΔK as a function of temperature for PC, PSF and PMMA, respectively. A characteristic of each polymer is a general increase in crack growth rates with increasing temperature. This is consistent with the normal decrease in mechanical properties such as modulus and strength which one encounters with increasing temperature. It is appropriate to mention that the FCP results for PMMA shown in Figures 3.15 and 3.18 directly contradict those published by Kurobe and Wakashima[24,25] who reported an increase in crack growth rates with decreasing temperature. This apparent anomaly may be explained by the basic difference in testing methods between the two studies. The fatigue testing in this report is load controlled while Kurobe and Wakashima utilized constant displacement fatigue equipment. With decreasing temperature (300 K to 225 K), the modulus of PMMA rises considerably. If the loading stroke remains constant as temperature is decreased, the fatigue specimen will fail sooner at lower temperatures due to effectively higher loads being applied.

Closer inspection of Figures 3.16-3.18 revealed a relative maximum in 1 Hz data around the β transition. Since the β peak

54
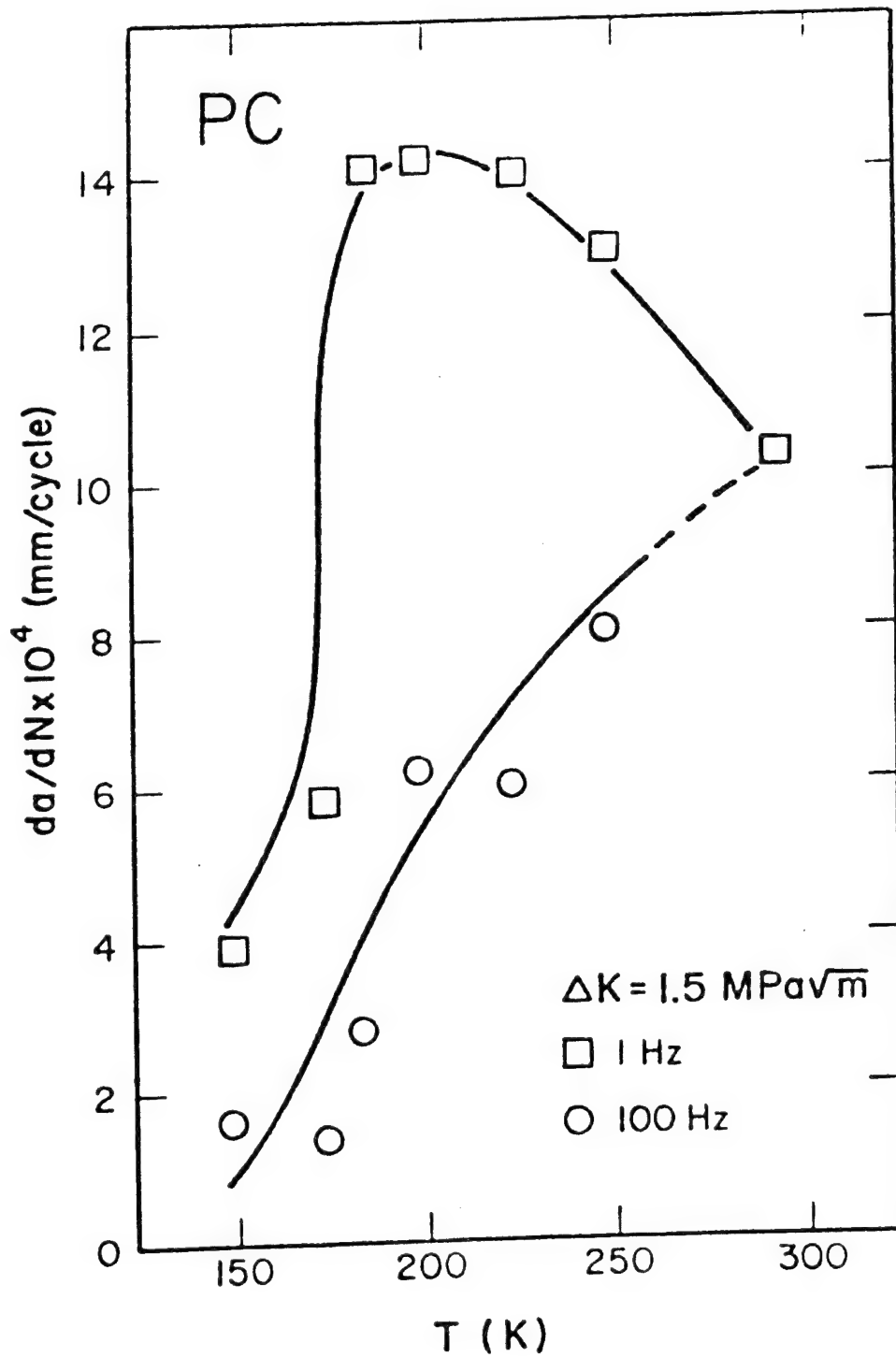
Figure 3.16   Crack growth rates at 1 and 100 Hz as a function of
temperature at constant ΔK in polycarbonate.

55
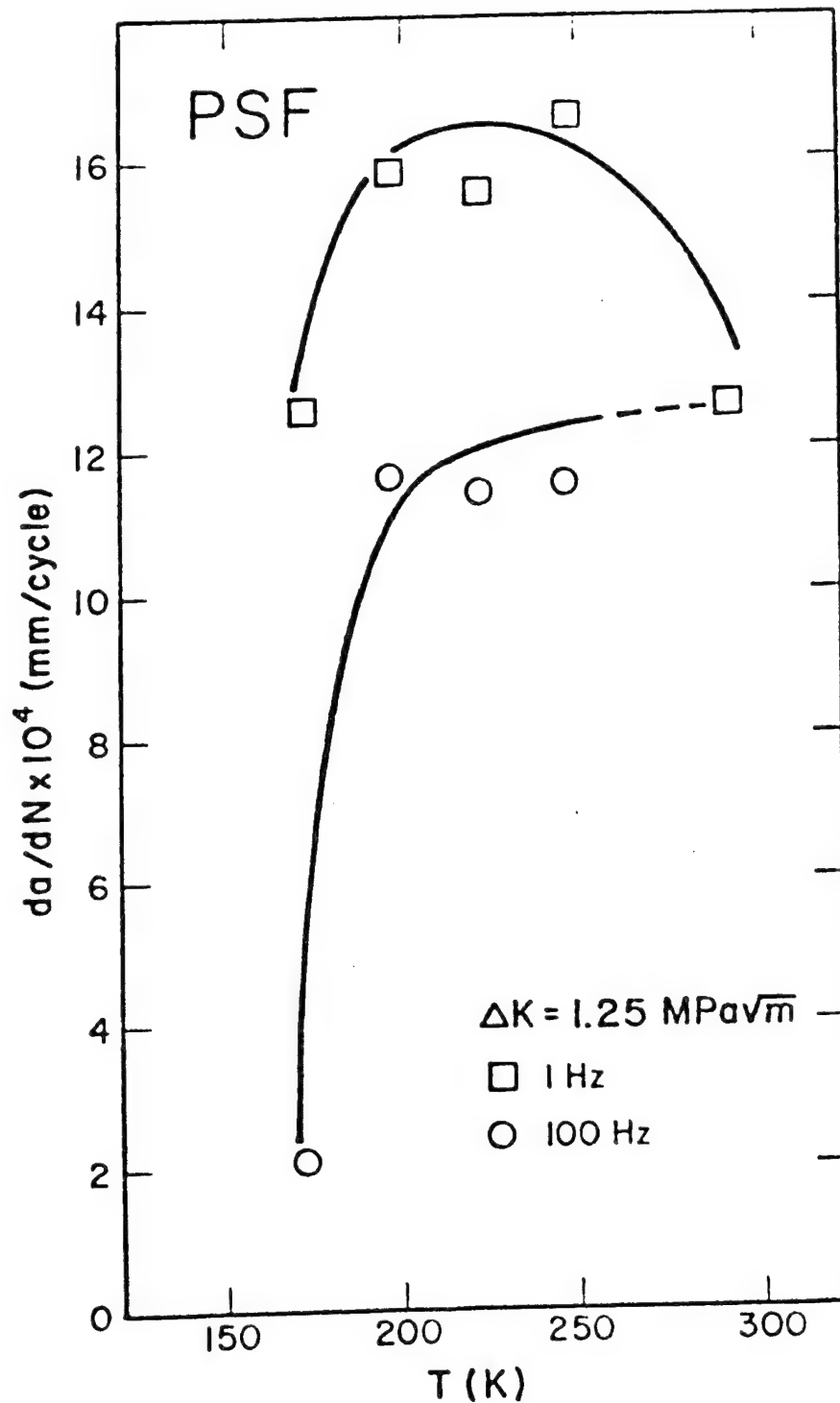
Figure 3.17 Effect of temperature on crack growth rates at 1 and 100 Hz at constant ΔK in polysulfone.
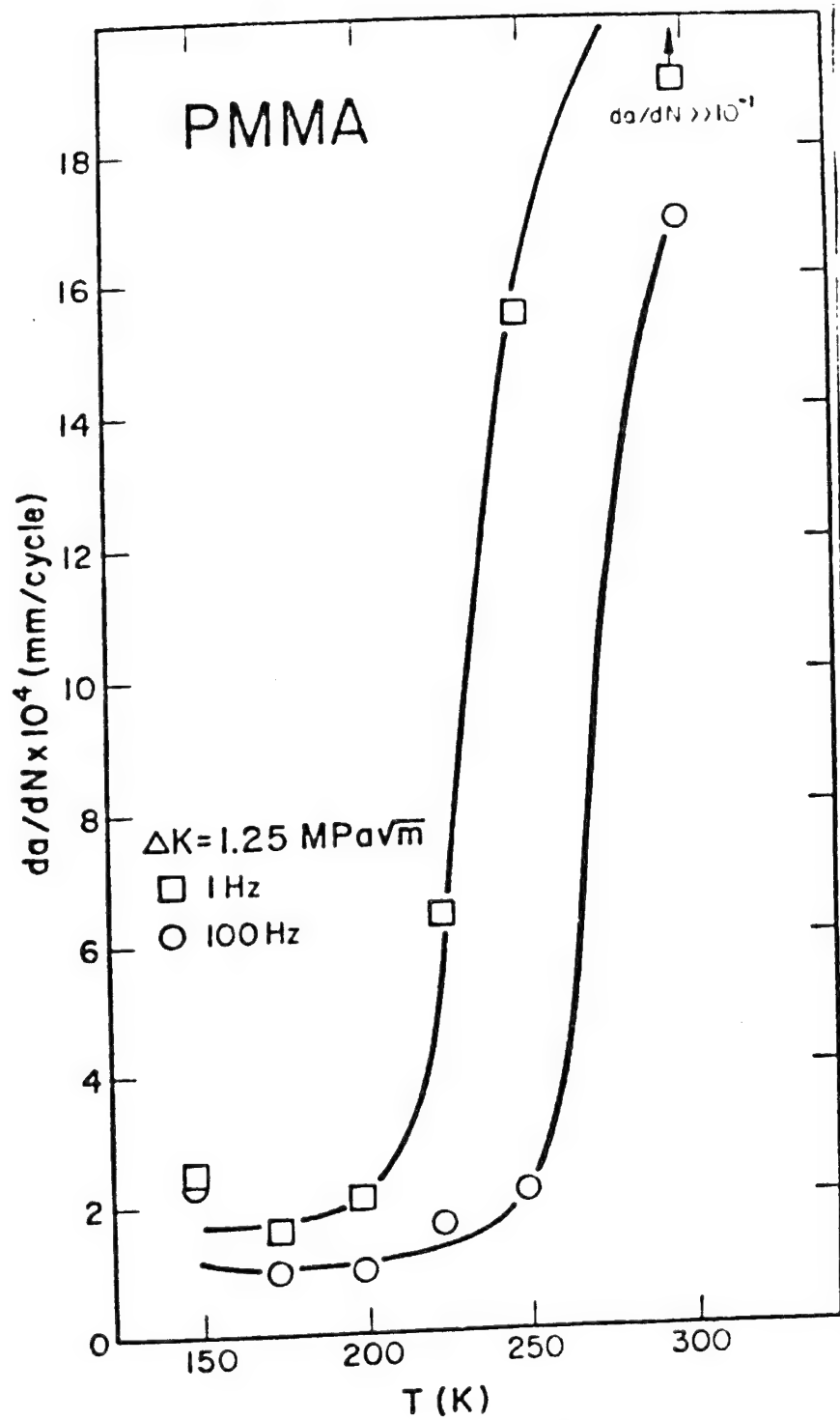
Figure 3.18 Crack growth rates at 1 and 100 Hz as a function of temperature at constant ΔK in PMMA.

57

has been related to a maximum in creep, the creep component of FCP will be larger at 1 than 100 Hz. Simultaneously, fatigue testing at 100 Hz should generate considerable hysteretic heating and result in a relative diminution in FCP. Consequently, the relative difference in FCP at this temperature as a function of test frequency (i.e., the frequency sensitivity factor) should be maximized.

A relationship between the β-peak and the absolute fatigue crack growth rates in PC and PSF has been hypothesized by Gerberich and Martin.[26,27] They obtained good correlation between da/dN and a minimum in the integrated E" ($\int_{T}^{T+100} E''dT$) where the analysis is based on the assumption of a 100 K rise in crack tip temperature at 1 Hz. Such crack tip heating is conceivable under conditions of rapid fracture, but the temperature rise at 1 Hz should be negligible. Attermo and Östberg reported an increase in crack tip temperature in PC of less than 30 K at 11 Hz. At 1 Hz, a much smaller rise would be expected. If the initial assumption of a 100 K crack tip temperature rise in unsupported, the remaining analysis becomes questionable.

3.3 Conclusions

The frequency sensitivity of crack growth rates in polymers is a function of several, sometimes competing, factors. Based on results presented in this chapter, the dominance of the β transition is apparent with frequency sensitivity being at a maximum where the β transition at room temperature occurs in the range of experimental

58

test frequency. This correlation between β jump frequency and test temperature is convincingly supported by fatigue crack propagation data obtained for PMMA, PC and PSF over a range of temperatures. This behavior may be reasonably explained in terms of hysteretic heating at the crack tip which is maximized at the β peak. The resulting crack blunting causes a drop in da/dN which is believed to be responsible for the observed frequency sensitivity in numerous polymeric solids.

Waveform studies performed on a variety of polymers indicate the only effect of increasing strain rate on FCP was the inducement of a minor increase in crack growth rates. This was related to a slight crack tip temperature rise which may have been responsible for aiding creep. Those polymers with low damping or crosslinked structures were insensitive to strain rate and creep crack growth under cyclic loading.

Crack growth rates were seen to be a strong function of temperature. FCP tests of PMMA, PSF, and PC demonstrated a general increase in crack growth rates with temperature. In all three materials, a maximum in da/dN at low frequency was evident near the β transition temperature. This is believed to be related to a relative maximum in creep rates which is usually found near the β peak.

IV. The Importance of Internal Structure in Fatigue Crack Propagation in Polymers

4.1 Crystallinity

4.1.1 Introduction

Of all polymeric materials, the semi-crystalline plastics offer the most desirable mechanical properties. Their impressive combination of high strength and toughness exceed that of most single component polymers. Similarly, the FCP response of crystalline plastics such as nylon and PVDF are far superior to typical amorphous polymers[1] (see Figure 1.2). At this time the mechanisms governing FCP in crystalline polymers are not clearly understood. It is believed that the strong crystalline spherulites play a major role in hindering crack propagation. Apparently, much energy is required for the initial breakdown of a spherulite. Once deformed, the molecular chains recombine to form a crystalline structure oriented parallel to the load direction. The manifestation of this deformation may be seen in the strong whitening of the fatigue fracture surface.[1,12] Considerable resistance to crack growth should be encountered when such a structure is present just ahead of the crack tip. Spherulitic deformation may not represent the only mode of fatigue crack propagation in crystalline polymers. In a study of FCP in polyethylene, Andrews and Walker[48] reported evidence which suggested that both intercrystalline and transcrystalline mechanisms of crack growth may be operable, depending on the crack driving force.

60

Fatigue crack propagation studies have been performed on the common crystalline polymers such as Nylon 6, Nylon 6,6, PVDF, PE,[48] chlorinated polyether, and polypropylene;[1,12] however, crack growth data in polyacetal (PA) and polytetrafluoroethylene which are believed to be fatigue resistant polymers have not been published.[5-8] An attempt will be made to generate FCP data in two commercial PA resins, the homopolymer Delrin and the copolymer Celcon (copolymerized with ethylene oxide).

4.1.2 Results and Discussion

Fatigue crack growth rates as a function of stress intensity at 10 and 50 or 100 Hz in Celcon and Delrin are shown in Figures 4.1 and 4.2, respectively. Note in Figure 24 the good agreement between all Celcon data and Delrin tested at 50 and 100 Hz. Due to the low inherent toughness (K_c) and the strong fatigue resistance (low da/dN for a given ΔK), the data base is small. If one compares the fatigue response of Delrin to PVDF and Nylon 6,6, the most FCP resistant polymers identified to date, (Figure 4.3), the superiority of polyacetal at a low da/dN range is clearly evident. Through comprehensive studies of fatigue crack growth in common engineering metals, researchers have concluded that by normalizing ΔK with respect to the elastic modulus, E, crack growth data for all metallic alloys lie on the same curve. If a similar comparison is made between the normalized fatigue behavior of metals and crystalline polymers (Figure 4.4), the FCP response of all metals is seen to be far inferior to crystalline polymers.

61
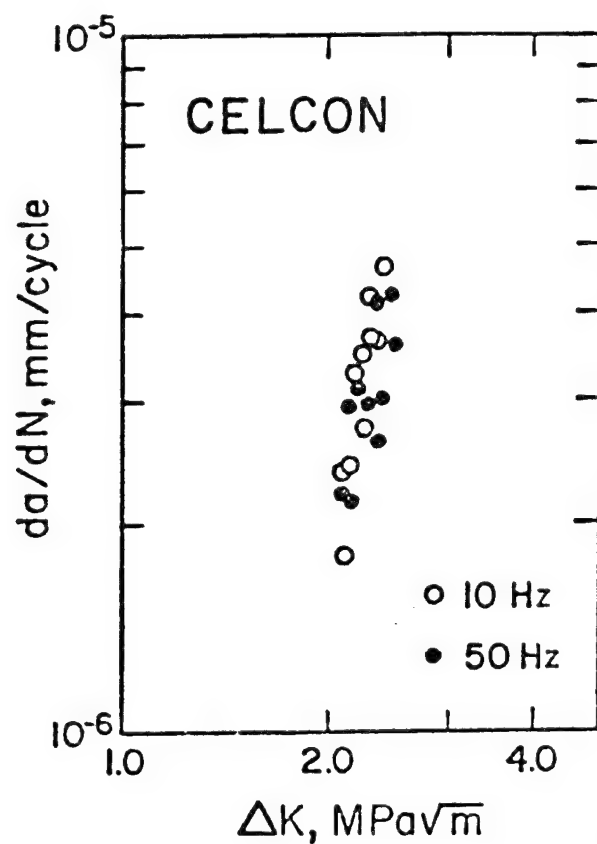
Figure 4.1 Fatigue crack growth rates as a function of frequency
in Celcon.

62
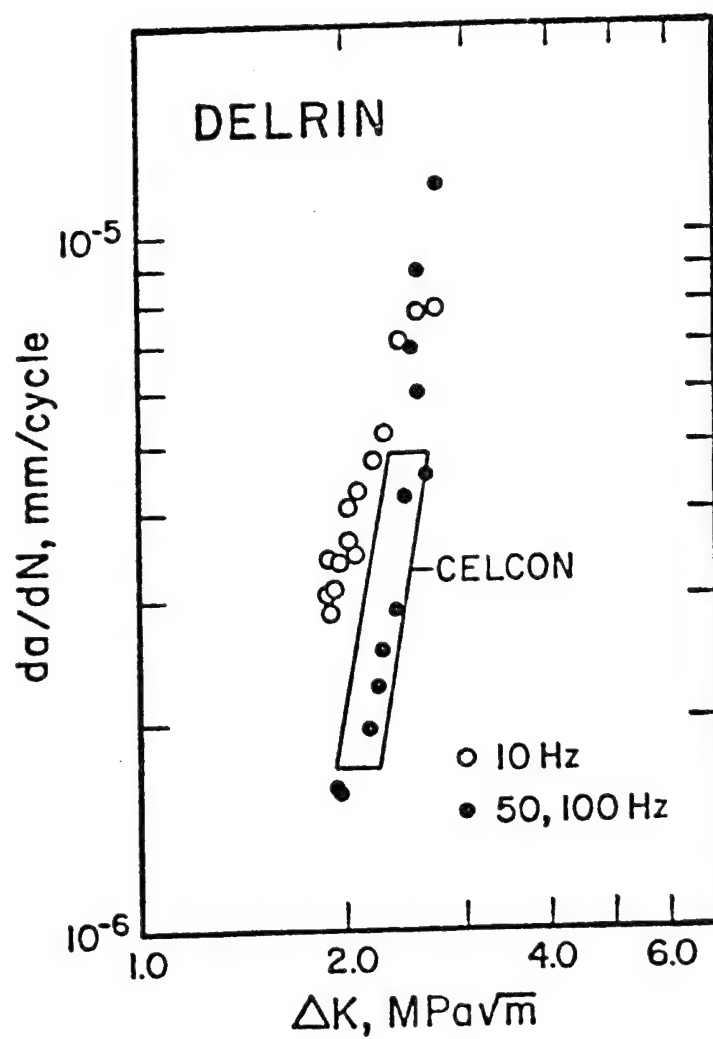
Figure 4.2 Fatigue crack growth rates as a function of frequency in Delrin.

63
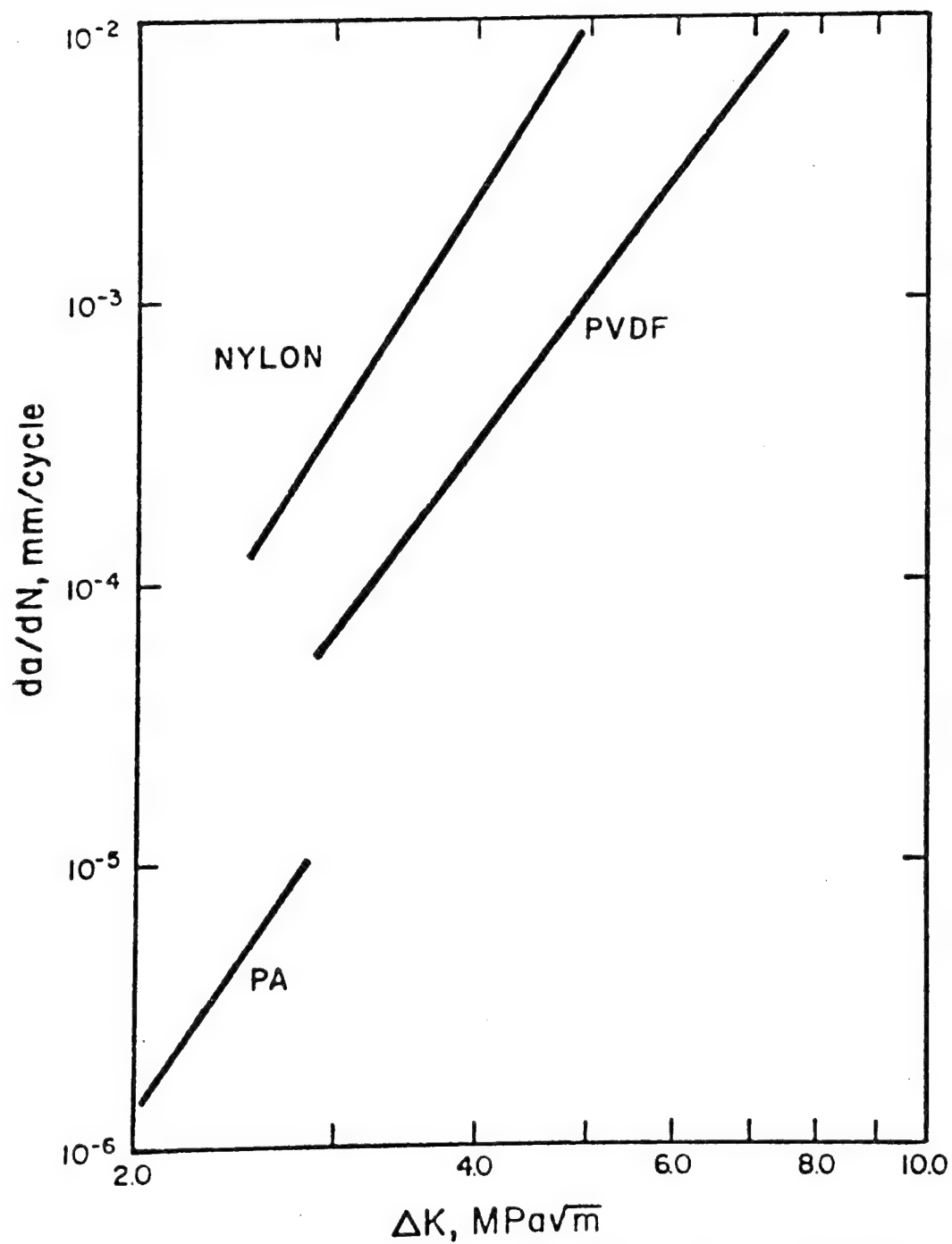
Figure 4.3 Comparison of fatigue crack growth rates at 10 Hz in
Nylon 6,6, PVDF and Delrin.

64
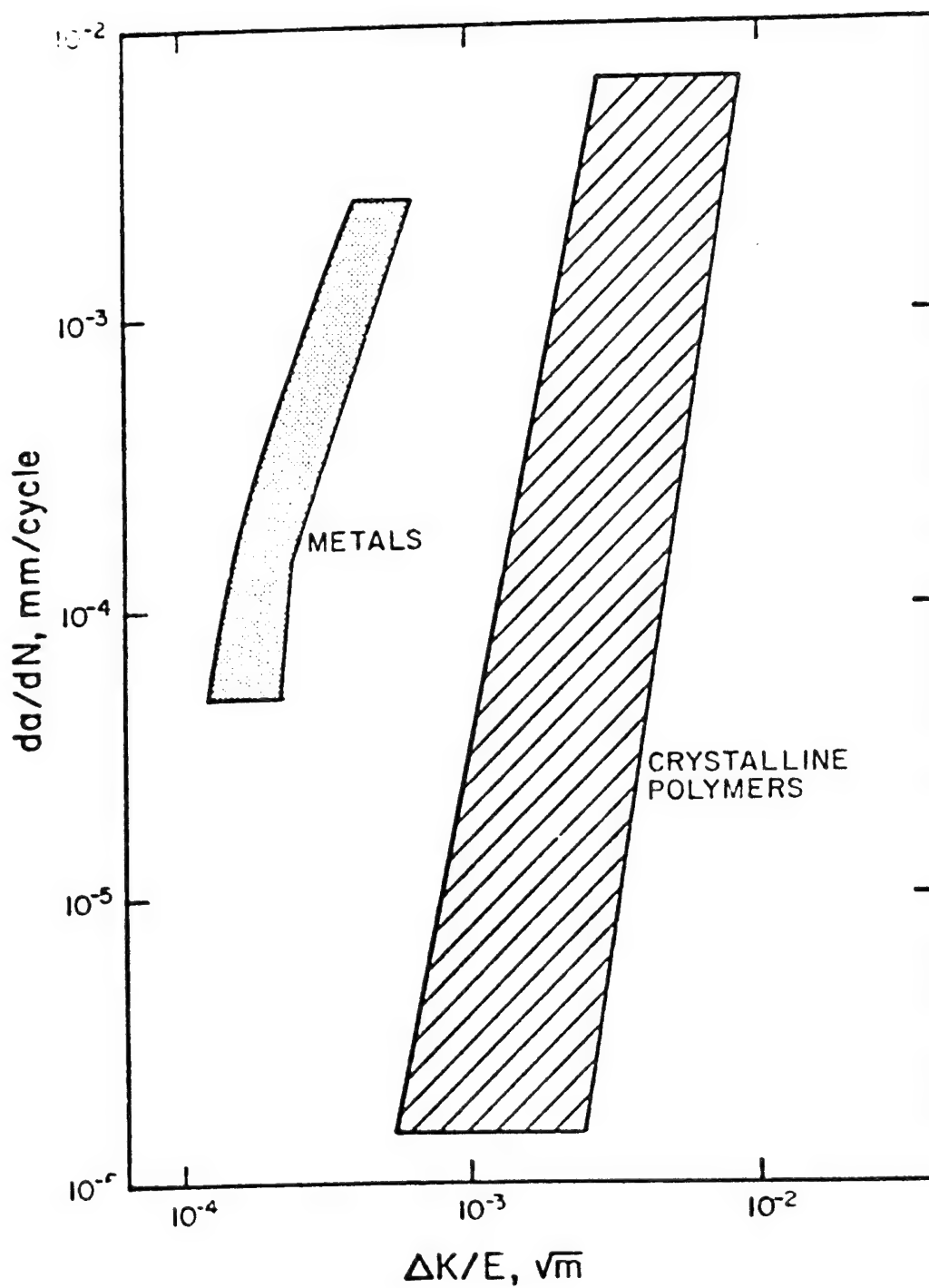
Figure 4.4 Comparison of crack growth rates in metals and crystal-
line polymers as a function of the normalized stress in-
tensity factor, $\Delta K/E$.

65

By increasing the frequency from 10 to 100 Hz, a change was noted in the slope of the da/dN vs ΔK curve in Delrin (Figure 4.2) while Celcon was unaffected. This result contradicts previous FCP studies of crystalline polymers where no frequency sensitivity was evident. The increased slope of the crack growth rate-ΔK plot at high test frequencies in Delrin appears to be related to a change in the mechanism of fatigue crack growth. At the higher frequencies a series of macrobands perpendicular to the direction of crack growth are evident while none were observed under 10 Hz testing conditions. Similar bands have been seen in PS[13] and PVC[20,23] and have been attributed to a discontinuous crack growth process with crack advance occurring in bursts after remaining sessile for thousands of cycles. (This mechanism will be discussed in greater detail in Chapter V.) Evidence for a discontinuous crack advance process is shown in Figure 4.5 where the large scatter in crack growth rates at 100 Hz is apparent. This is compared with the monotonic increase in FCP with ΔK for the Delrin samples tested at 10 Hz where no fracture bands were observed. Since the increment of crack advance following each stationary period was comparable to the typical increment over which crack extension data were collected, one would expect to find more scatter in the FCP data. Celcon exhibited discontinuous crack growth at both 10 and 50 Hz test conditions. Note the excellent correlation between Celcon and 100 Hz Delrin fatigue data (Figure 4.2). (The mechanisms of fatigue crack propagation in PA will be discussed further in Chapter V.)

66
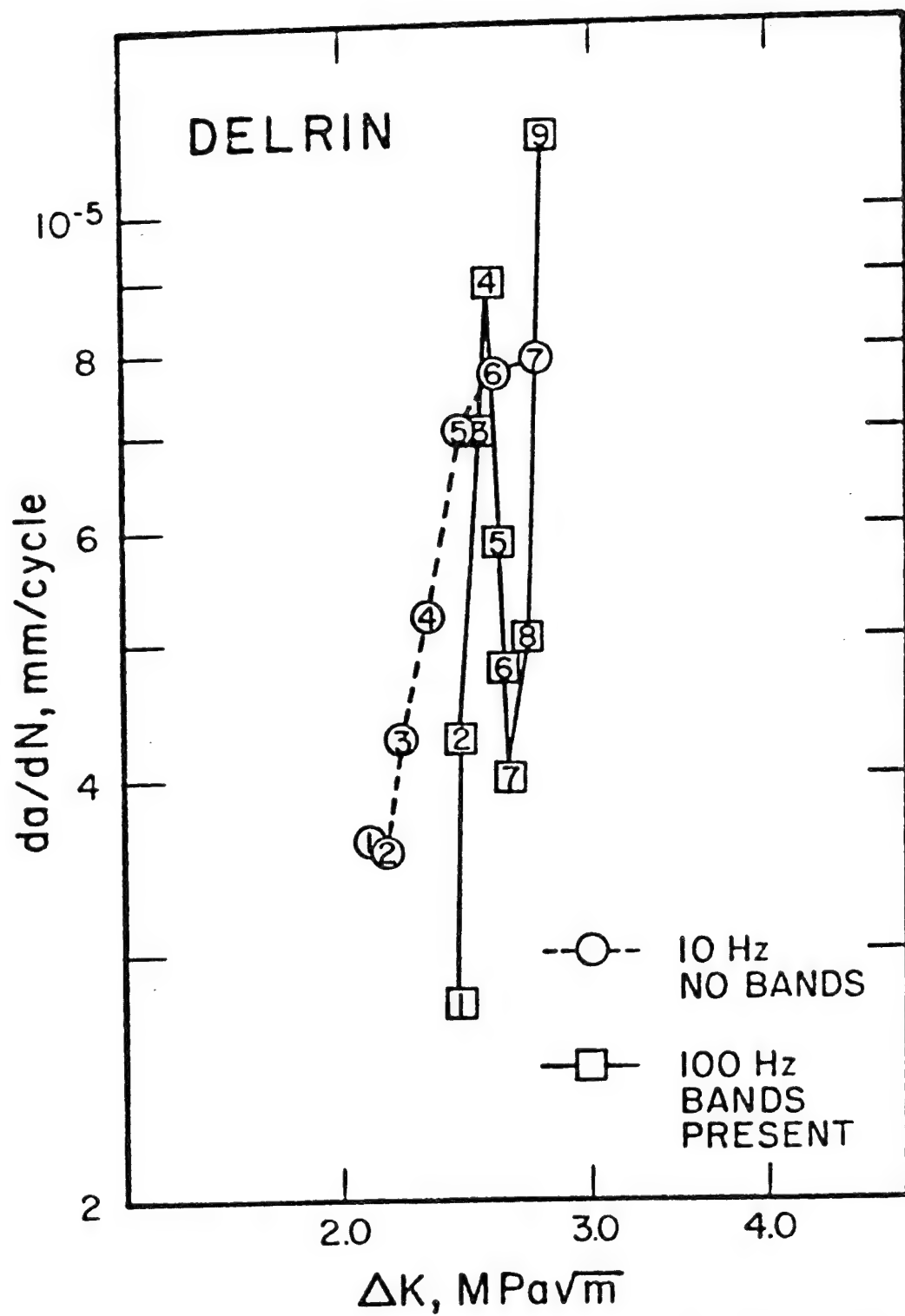
Figure 4.5 Comparison of crack growth rates as a function of frequency in Delrin. Note large scatter at 100 Hz.

4.2 The Effect of Molecular Weight on FCP and Fracture in PMMA and PVC

4.2.1 Introduction

The mechanical properties of a polymer are known to be a strong function of molecular weight (M) and molecular weight distribution (MWD).[49] These tensile properties which increase with M tend to reach a plateau at some high value of M. The tensile strength as well as the fracture energy continue to increase slightly beyond this M while the elastic modulus appears to remain constant.[50,51]

At present the effect of M on fatigue crack propagation has not been evaluated in any polymer. Fatigue life studies of unnotched test bars as a function of M have shown a dramatic decrease in fatigue life with decreasing M in PS $(1.6 \times 10^5 < \bar{M}_w < 8.6 \times 10^5)$[29,30] and PVC $(5 \times 10^4 < \bar{M}_w < 2 \times 10^5)$.[31,32] Unfortunately, crack growth rates are not available from studies of the type referenced above. An attempt will be made to evaluate the fatigue response of PMMA and PVC as a function of M.

4.2.2 Results and Discussion

Fatigue crack growth rates in PVC as a function of ΔK for $\bar{M}_w$ ranging from 225,000 to 60,500 are shown in Figure 4.6. Analogous data for bulk and emulsion polymerized PMMA over the range in $\bar{M}_v$ between 1×10^5 and 8×10^6 are shown in Figures 4.7a and b, respectively. Although the growth rate curves are not quite linear, they are generally parallel to one another. The continuous shift to higher growth rates with decreasing M in both PVC and PMMA is obvious.

68
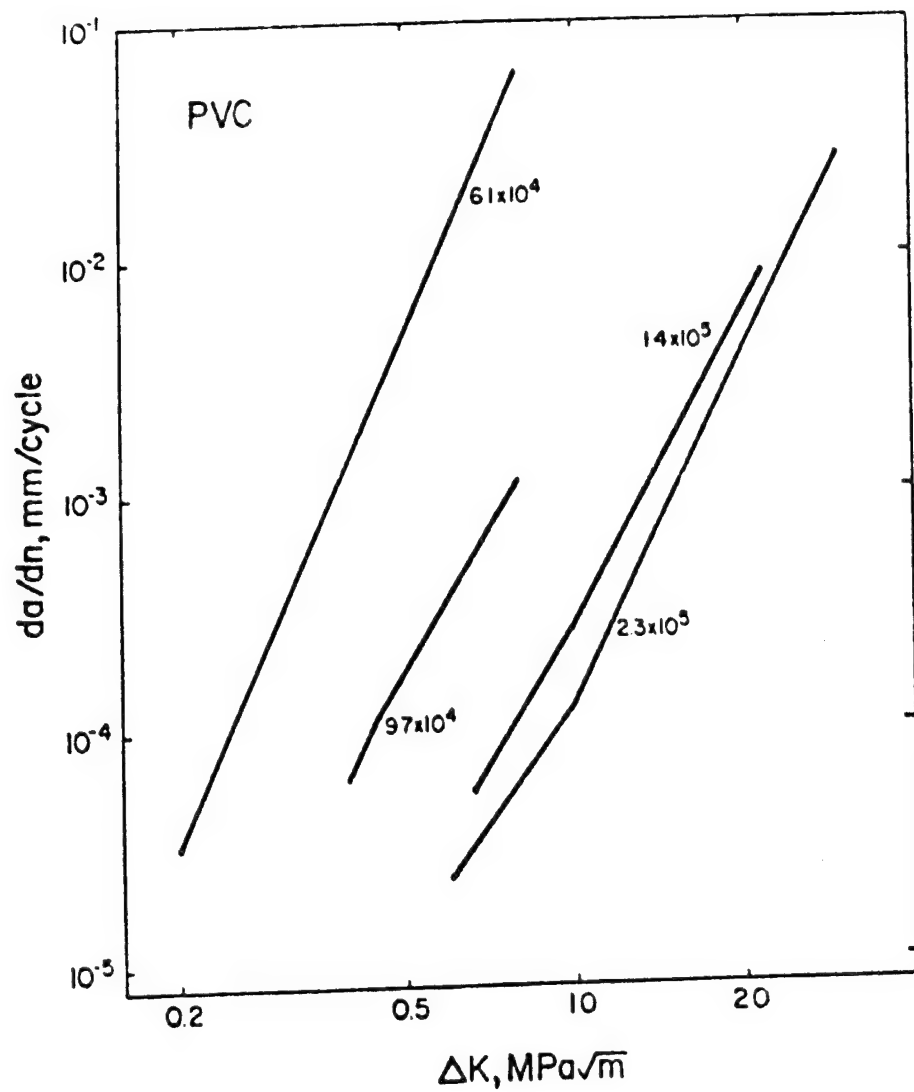
Figure 4.6 Fatigue crack growth curves as a function of $\overline{M}_W$ at 10 Hz in PVC.[A7]
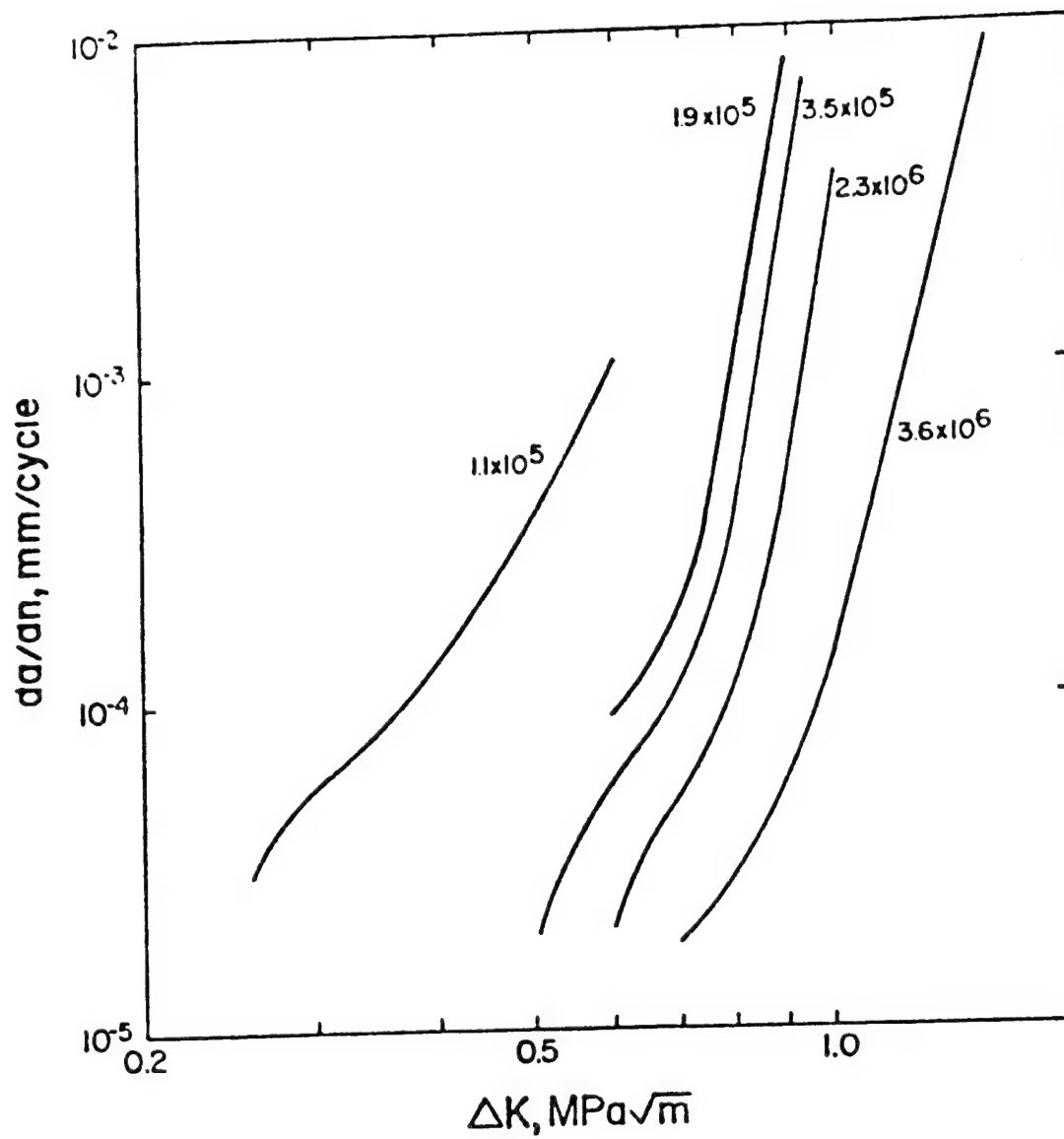
Figure 4.7a Fatigue crack growth as a function of $\overline{M}_v$ in bulk poly-
merized PMMA.[A6]
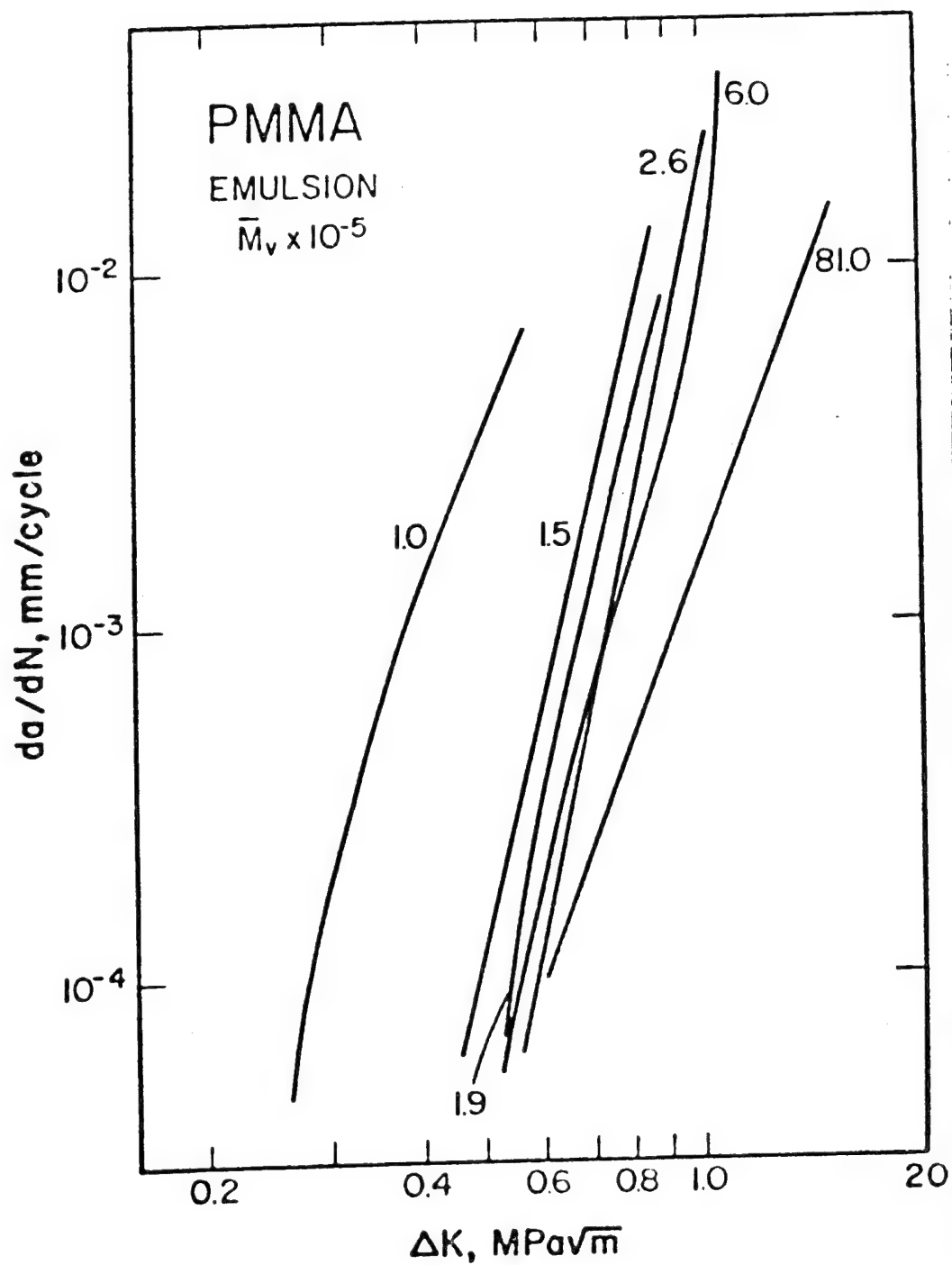
Figure 4.7b The effect of $\overline{M}_V$ on fatigue crack growth rates in emulsion polymerized PMMA.

71

These results can also be depicted by comparing da/dN for different values of M at an arbitrarily chosen value of ΔK (0.6 MPa $\sqrt{m}$). The results for PMMA, shown in Figure 4.8, indicate an increase in da/dN with decreasing $\overline{M}_v$. Below $\overline{M}_v \cong 2 \times 10^5$, the crack growth rate sensitivity to $\overline{M}_v$ is greatest. Crack growth rates vs M in PVC at constant ΔK are shown in Figure 4.9. A change of nearly 3 orders of magnitude in da/dN is apparent over the range of M tested. In both PVC and PMMA, the strong relationship between da/dN and M is exponential with da/dN varying with exp (1/M) (Figure 4.10). Although the effect of M on da/dN is greatest at low M, it persists to the highest processable values of M, usually above the point where static properties are relatively insensitive to further changes is M.

Figure 4.8 also shows that at a given value of M, emulsion polymerized PMMA specimens exhibit higher rates of crack growth than those polymerized in the bulk. This was not believed to be related to unsatisfactory primary particle bonding since preliminary inspection of the fracture surface revealed no evidence of decohesion along original particle boundaries. Often the emulsion polymerization process leaves small amounts of emulsifier in the bulk polymer. It is possible, however, that traces of diluent can deleteriously affect crack growth rates.

Values of K_c were considered approximately equal to K_{max} calculated from the last stable value of ΔK prior to fast fracture. These data are shown for PVC and PMMA in Figure 4.11 and 4.12, respectively. Here K_c is seen to increase as M is increased. With

72
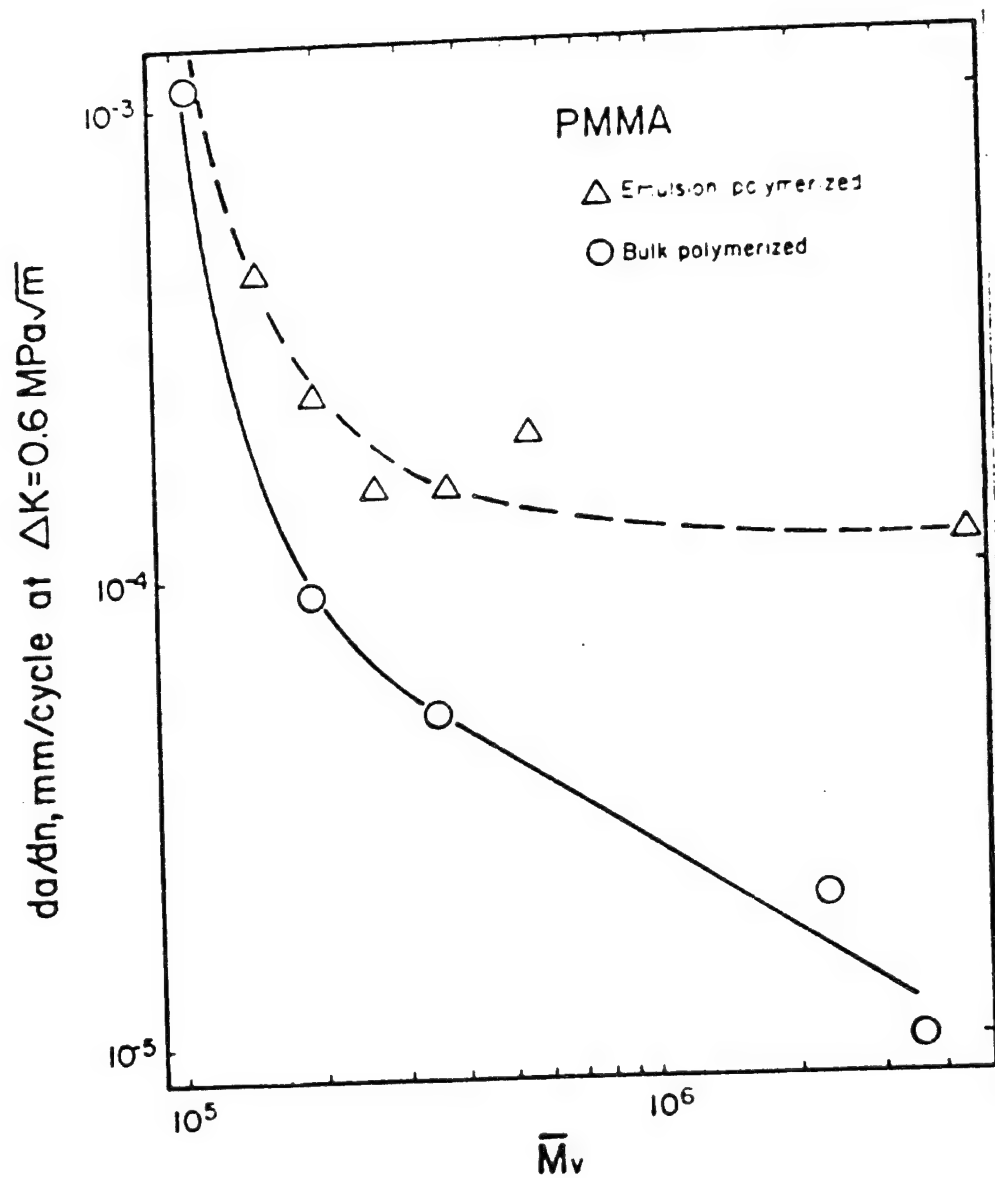
Figure 4.8 Effect of M on FCP rate (at $\Delta K_{A6} = 0.6$ MPa$\sqrt{m}$) in bulk and emulsion polymerized PMMA.[A6]

73
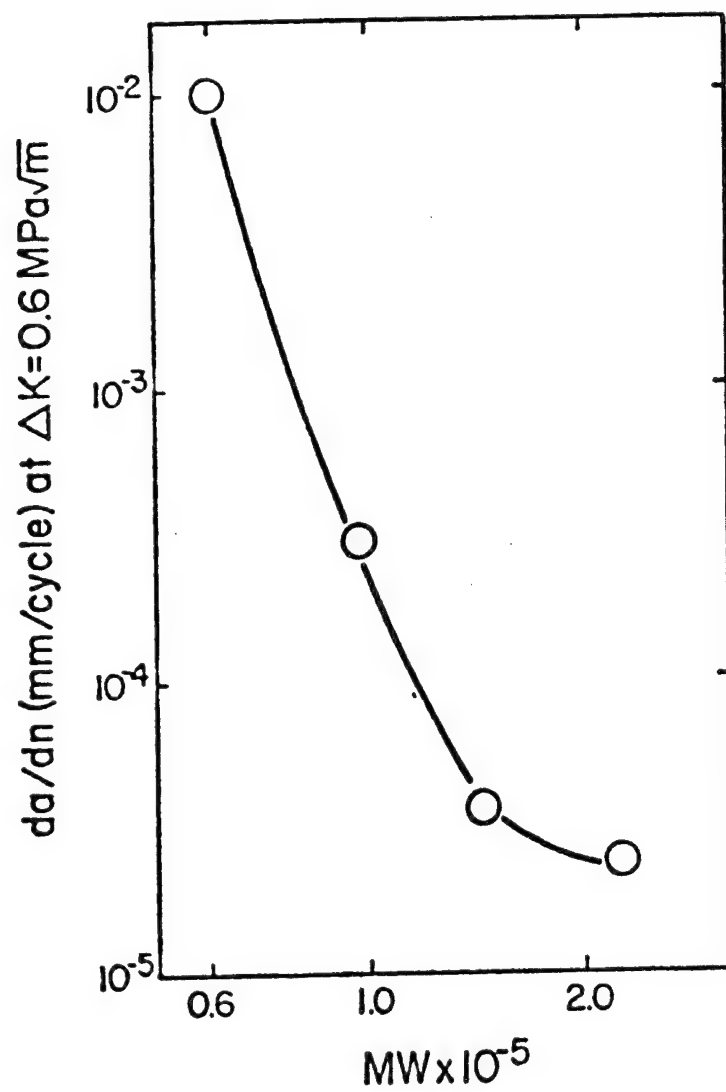
Figure 4.9 Effect of M on FCP rate (at ΔK = 0.6 MPa$\sqrt{m}$) in PVC.[A7]

74
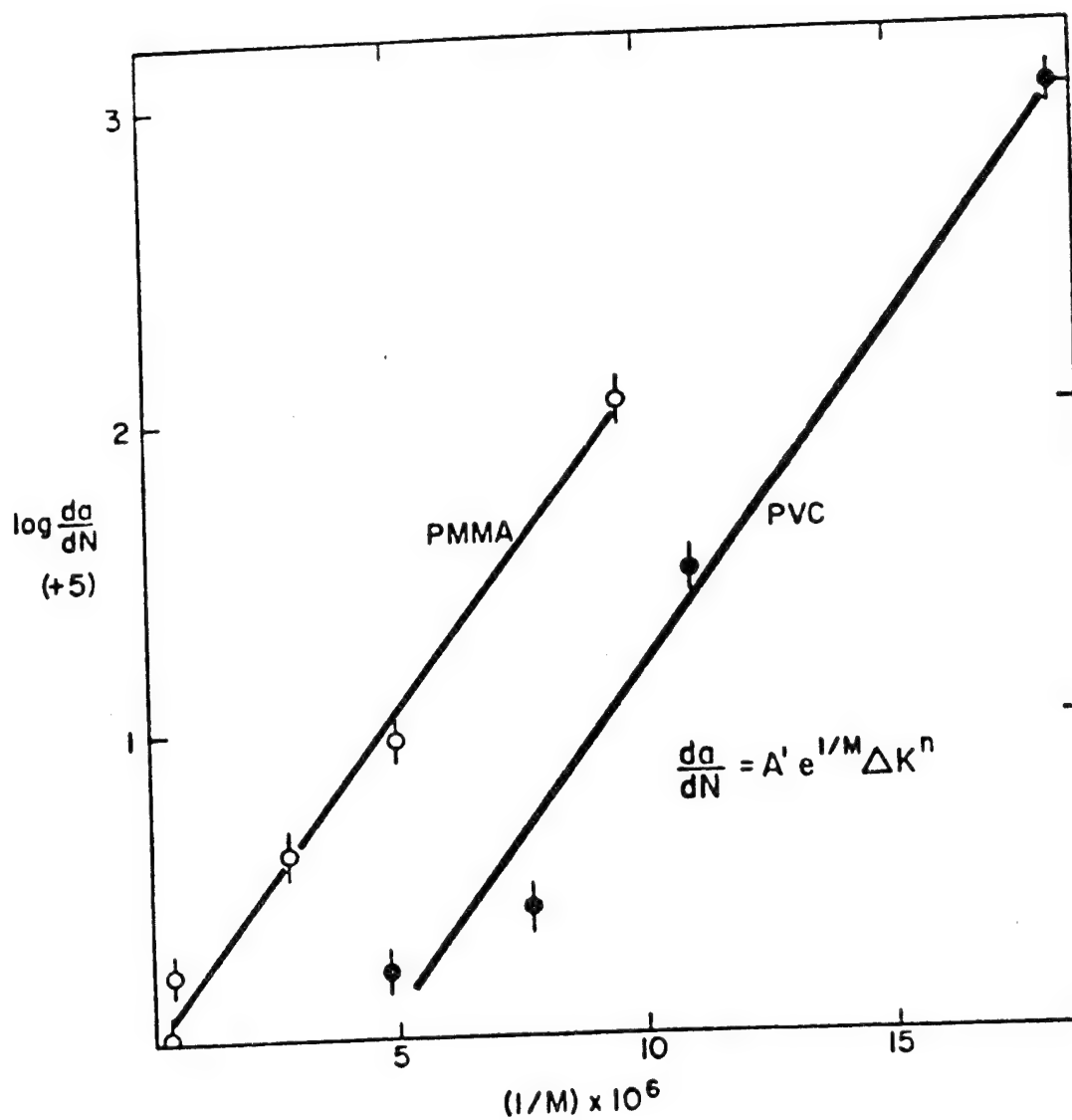
Figure 4.10   Exponential relationship between da/dN and 1/M in PMMA and PVC.[A7,A6]
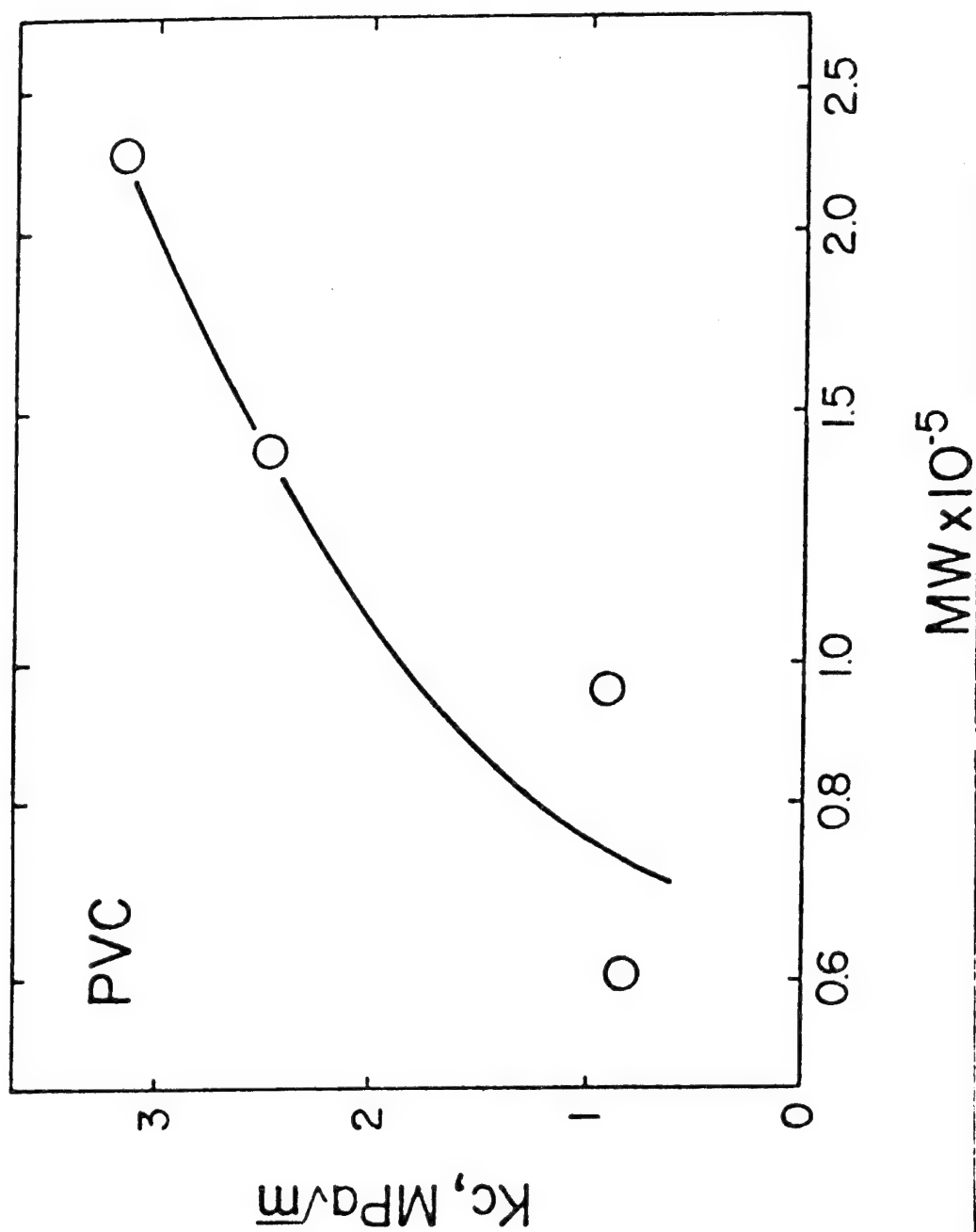
Figure 4.11 Effect of M on fracture toughness of PVC.

76
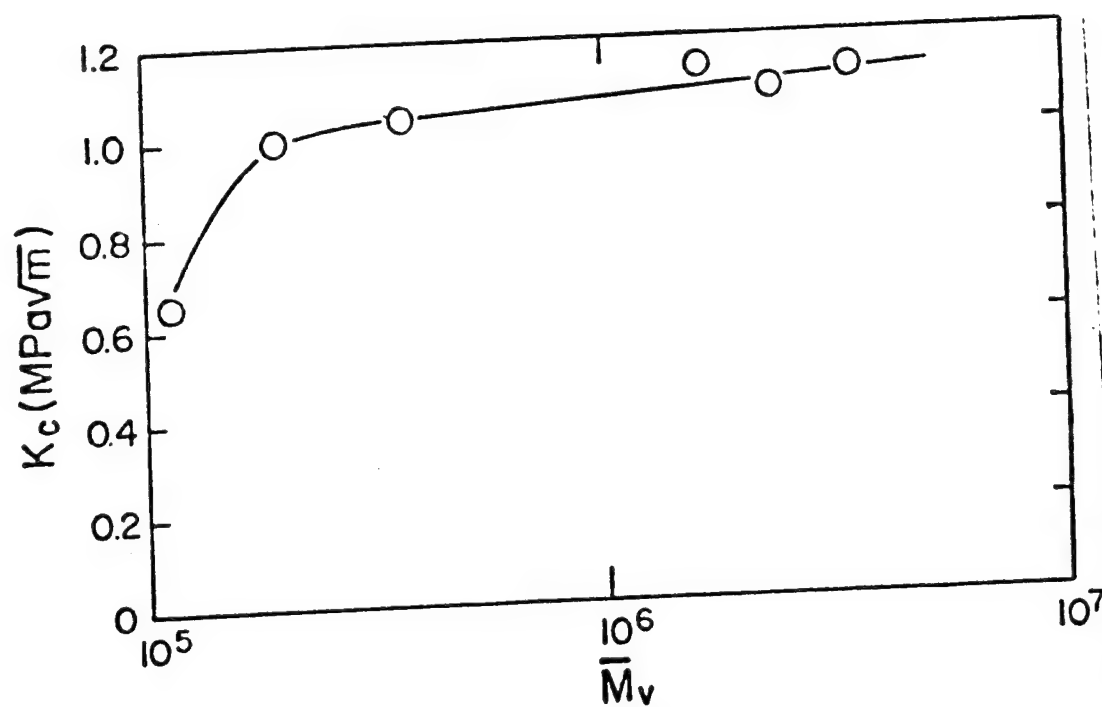
Figure 4.12 Effect of M on fracture toughness of PMMA.[A6]

77

PVC, only a slight decrease in the slope of the K_c-$\bar{M}_w$ curve is evident as all polymers tested are still on the rapidly rising portion of the curve. PMMA, however, demonstrates a leveling-off of toughness above $\bar{M}_v \sim 10^5$. From Figure 4.13, it may be seen that values of fracture energy obtained for all PMMA specimens, regardless of method of preparation, show a similar trend.

These data are also in agreement with those published by Berry[53] and Kusy and Turner.[50,59] Note again that although K_c is relatively insensitive to M above $\bar{M}_v = 2 \times 10^5$, FCP rates continue to decrease by an order of magnitude.

The effect of M on K_c and FCP rates must now be explained in more detail. It is generally accepted that crack growth in PVC and PMMA as well as most glassy polymers is almost always preceded by some craze growth. It is, therefore, the stability of the craze and not the properties of the bulk material which should determine the FCP response of a polymer. In 1964, Berry[53] suggested that a stable craze would develop if the molecular weight were sufficiently high for molecular chains to span the craze. Similarly, Gent and Thomas[60] reported that the development of strength and toughness can only occur when M exceeds a critical value for chain entanglements. Kambour[61] concluded that some higher level of M (2×10^5 in PMMA) is required to produce maximum craze stability. Both statements are in agreement with the observation by Fellers and Kee[62] that low values of M lead to weak crazes in PS. Martin and Johnson[31,32] noted an increase in craze thickness (an indicator of greater craze

78
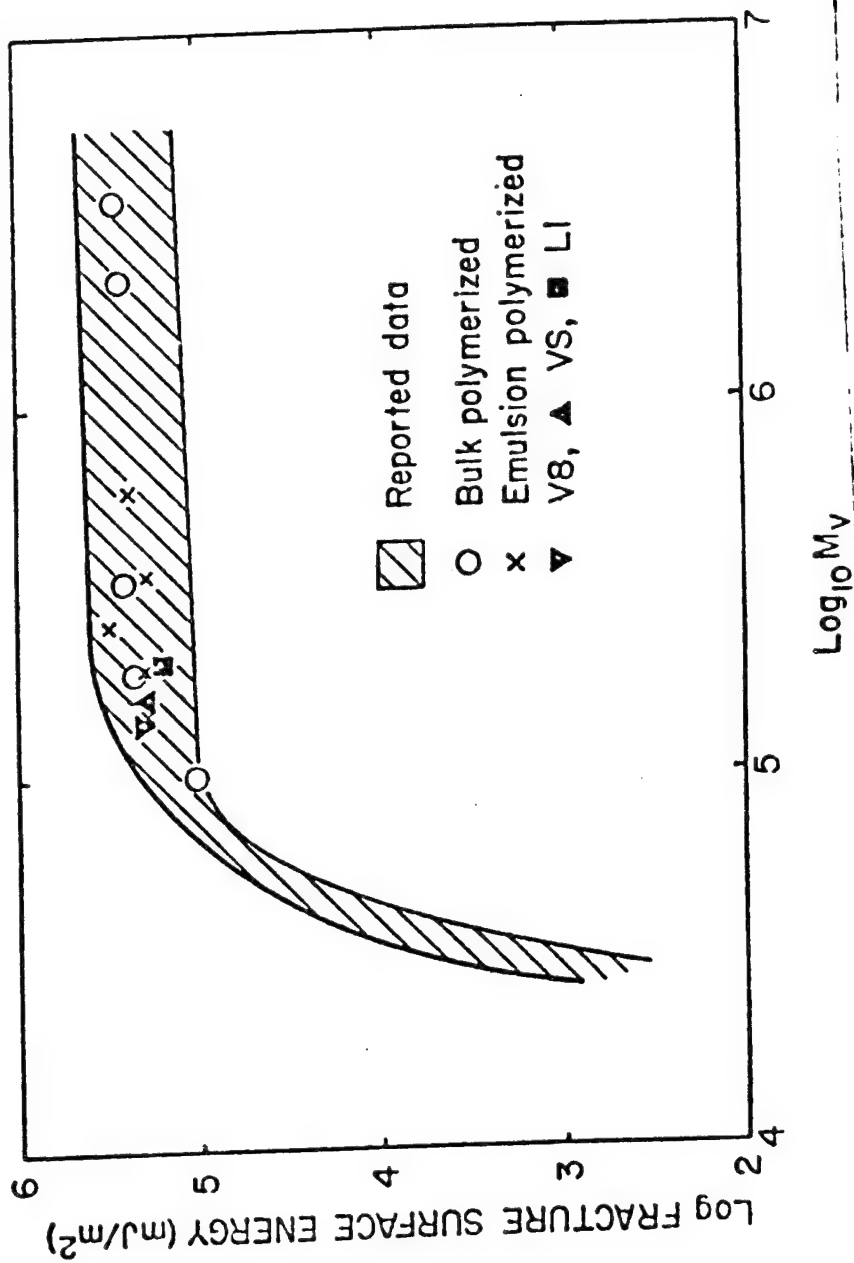
Figure 4.13 Effect of M on fracture energy of PMMA. Band indicates the range of values obtained by other investigators.[50,53,59,86]

79

stability) with M in PVC.

Recently, Weidmann and Doll[63] and Kusy and Turner[50] have given further support to Berry's hypothesis that craze stability is related to the ability of molecular chains to span the craze at the crack tip. Wellinghoff and Baer[64] have shown that only a small fraction of high M polymer (long chains) can greatly enhance the spanning of crazes. However, the concept of complete extension of single molecular chains spanning the craze has been found by Kausch[65] to be somewhat unrealistic. He concludes that crazes are spanned by coils comprised of many entangled molecular chains. At high molecular weight, the coils contain more entanglements. In static fracture tests, the improvement of K_c with M will tend to saturate when further entanglements do not measureably strengthen the craze.

While the above argument may rationalize the leveling off of fracture properties with increasing M, the continuous improvement in FCP behavior with M has not been explained. One may hypothesize that the nature of fatigue loading may tend to disentangle progressively a molecular network. Therefore, a low M polymer with few entanglements should disentangle most readily and as a result lead to premature craze breakdown; this in turn, would lead to accelerated fatigue crack propagation rates. Conversely, a high M polymer with many entanglements should offer superior resistance to any disentanglement which may occur during cyclic loading. Consequently, crack growth rates should decrease.

From the previous discussion, the importance of M on fatigue

80

crack growth rates is clearly evident. This effect is so great that changes in M can overshadow the inherent variation in FCP properties in different polymers.

4.3 The Effect of Plasticizer on the Fatigue and Fracture Properties of PVC and PMMA

4.3.1 Introduction

The role of plasticizer content on the cyclic response of polymeric solids is almost unknown. Only in two studies has the effect of plasticizer on FCP been examined. Suzuki et al.[33] have shown that fatigue crack growth rates at low test frequency in PVC increased with dioctyl pthalate (DOP) content. Manson and Hertzberg reported similar results in nylon plasticized with H_2O.

4.3.2 Results and Discussion of External Plasticization of PVC

The effect of DOP on the FCP response of PVC was quite surprising. Figure 4.14 shows that a change in DOP content from 0 to 13% produces a minimal change in crack growth rates. It is important to note that these data contradict those reported by Suzuki[33] who found a significant increase in da/dN when DOP was increased from 0 to 20%. While the reason for this discrepancy is not known, the test by Suzuki were performed at a frequency of 0.25 Hz, much lower than the 10 Hz used in this study. It is known that an increase in DOP content decreases the Tg while increasing damping and an increase in the viscoelastic nature of deformation in PVC. Conceivably, with increasing % DOP, localized crack tip heating may occur at the
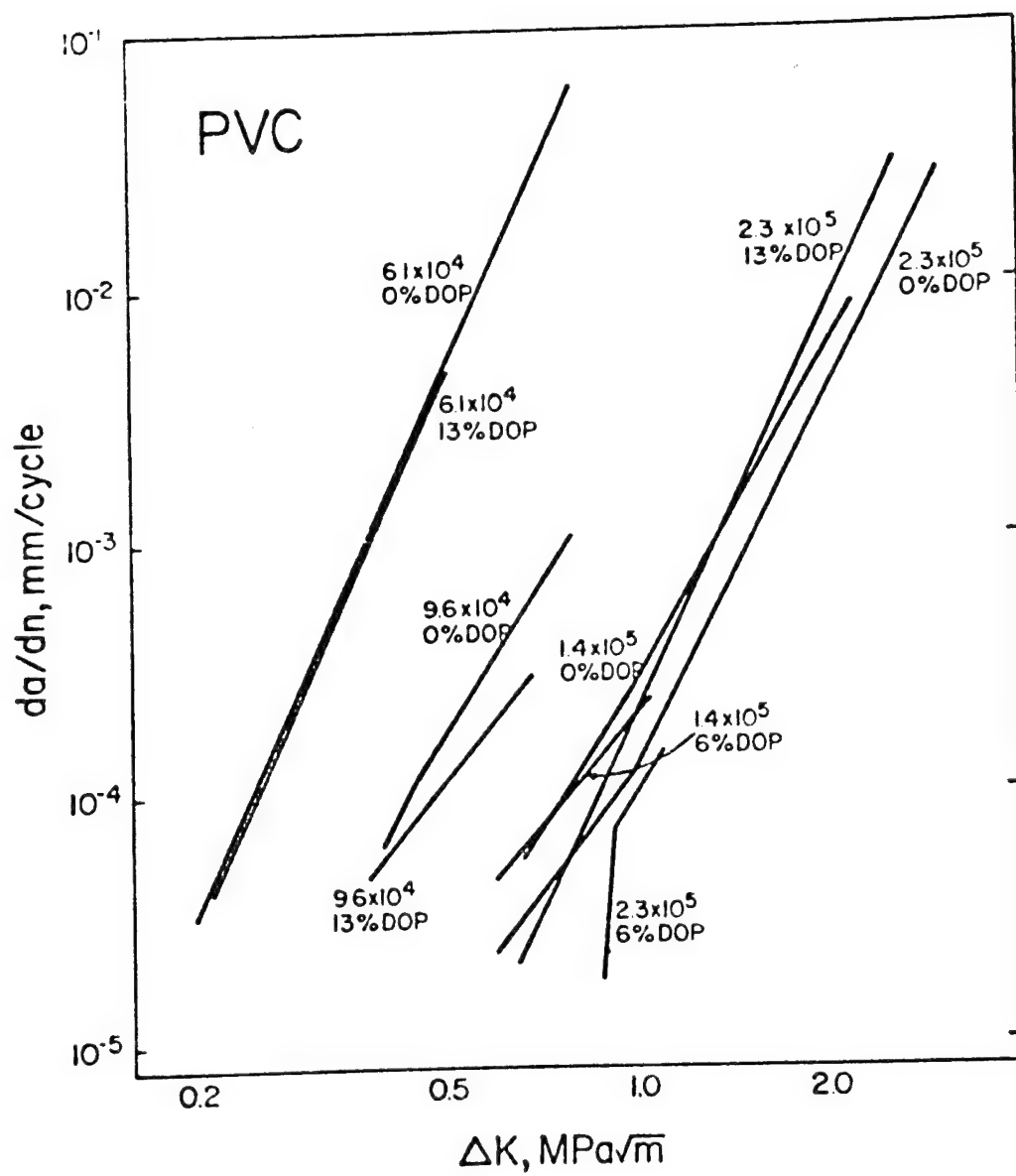
Figure 4.14   Fatigue crack growth rates in PVC as a function of
M and percent DOP. [A7]

82

higher frequency which will lead to crack tip blunting and lower crack growth rates. This effect may mask any real decrease in fatigue strength which may occur by diluting the polymer network.

While FCP tests at a frequency of 10 Hz were easily performed at DOP contents from 0 - 13%, no FCP data were obtained from specimens containing 20% DOP. The sensible crack tip heating and blunting caused crack growth to cease after some minor crack advance. Apparently, the low Tg and high damping of heavily plasticized PVC causes excessive hysteretic heating at even moderate frequencies.

The effect of % DOP on K_c is rather complex. At 6% DOP, PVC suffers a massive drop in toughness at all molecular weights (Figure 4.15). This embrittling effect of DOP closely parallels the antiplasticizer effect wherein small concentrations of plasticizer are believed to inhibit segmental mobility by filling free volume and increasing polymer stiffness while simultaneously decreasing toughness.[55] When DOP content is increased to 13%, K_c is only slightly reduced from the unplasticized specimens (Figure 4.15). This minimal effect may reflect a slight dilution of the PVC network.

4.3.3 Results and Discussion of Internal Plasticization in BA-PMMA Copolymers

The FCP response of PMMA internally plasticized (copolymerized) with butyl acrylate (BA) is quite apart from the externally plasticized PVC results discussed earlier. From Figure 4.16, increasing amounts of BA in PMMA (at constant $\bar{M}_v$) is seen to have a pronounced

83
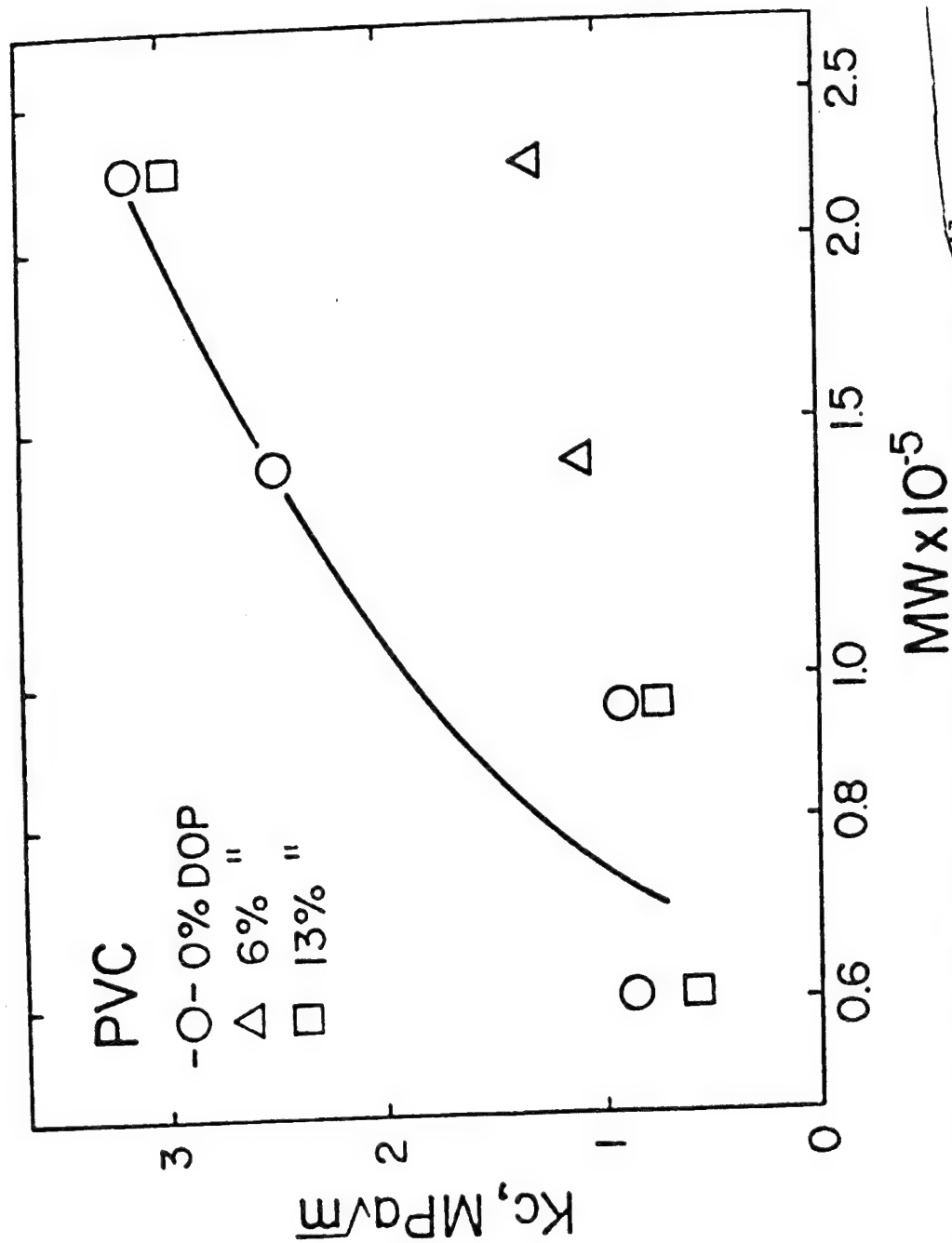
Figure 4.15 Effect of percent dioctyl phthalate on toughness in PVC.A7

84
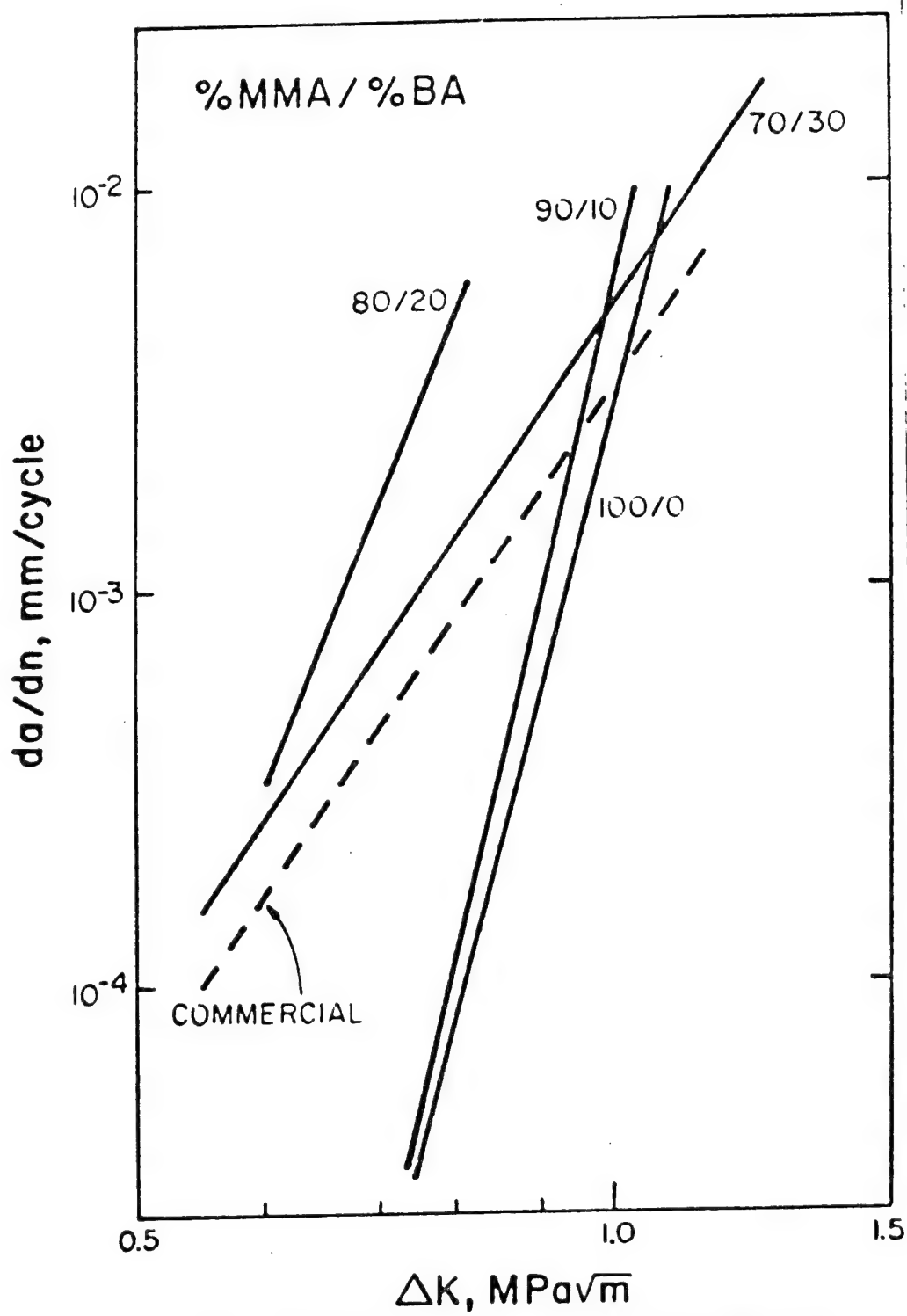
Figure 4.16 Effect of copolymerization with a plasticizing co-
monomer, BA, on the FCP behavior of PMMA.[A6]

85

but complex effect on fatigue crack growth rates. As % BA is increased initially, growth rates approach a maximum while toughness is lowest at approximately 80% MMA-BA. Upon increasing BA to 30%, the FCP growth rates decreased for any given ΔK level while the toughness became superior to values associated with the unplasticized material. A comparison of this copolymer with commercially available PMMA indicates similar fatigue and fracture properties. Although it is unlikely that commercial PMMA contains 30% of some copolymer, clearly it is not pure homopolymer. A study of the slopes of the growth rate curves shows no definite trend as a function of BA. As was noted in PVC, above a certain plasticizer content, 30% BA, fatigue crack growth was not experienced and was believed to be due to the observed localized heating and presumed crack tip blunting. Total crack growth in these specimens was negligible.

The fatigue response of BA-MMA copolymers indicates the possibility of several competitive fatigue processes. Since values of damping (tan δ) are unchanged up to 20% BA (see Table III), the differences in FCP at low BA must be related to changes in the mechanical properties rather than thermal softening. Consequently, at low BA contents, increasing BA improves ductility at the expense of strength. This effect would be consistent with the tendency of molecules with large effective cross-sectional areas to be weaker than those which are smaller.[56] As % BA is further increased, crack blunting due to controlled localized thermal softening decreases

86

da/dN and increases apparent toughness. At still higher BA contents, thermal softening prevents any stable fatigue crack growth.

4.4 The Effect of Crosslinking on Fatigue Crack Propagation in Epoxies

4.4.1 Introduction

With increasing interest being directed toward materials with high strength and modulus but low density, the crosslinked polymers are receiving renewed attention. Of greatest importance are the heavily crosslinked epoxies. They are used most often in adhesive joints or composite matrices where their low inherent toughness is not necessarily detrimental.

The mechanical properties of crosslinked materials have been related to the crosslink density or molecular distance between cross-links (M_c). While the elastic modulus and strength reach a maximum at the smallest M_c, the toughness reaches a minumum.[54,55]

The FCP response of crosslinked polymers has received little attention. Hertzberg and Manson[1] reported the FCP response of linear PS to be somewhat superior to CLPS. The crosslinks in CLPS were believed to reduce the capacity of PS to craze. Without crazing as a mechanism of energy dissipation, crack growth rates increased. It has been reported that crack growth rates in uncross-linked polymers are seen to vary with a linear function of ΔK[56] and are also sensitive to mean stress.[57] Tomkins and Biggs have indi-cated the possibility of limited crazing preceding crack growth.

87

The effect of M_c on FCP is completely unknown.

4.4.2 Results and Discussion

Figure 4.17 shows the effect of crosslinking density (M_c) on crack growth rates in methyl dianiline cured epoxies (see Appendix II for details of sample preparation). Note the constant shift to higher crack growth rates with increasing epoxy content (decreasing M_c). The most unusual aspect of these growth rate curves are the exceedingly high slopes (7.7 to > 20) (Figure 4.18). Closely paralleling the fatigue behavior is toughness, K_c, which shows a continuous increase with decreasing epoxy content (Figure 4.19).

Considering the improvement in fatigue properties which occurs with increasing M_c, a correlation between molecular chain mobility and fatigue resistance may exist. Given that some plastic deformation at the crack tip is required for FCP in any material, those materials which offer the greatest energy dissipation during deformation should exhibit the most resistant fatigue behavior. Clearly, a low M_c produces a tightly constrained structure intolerant of plastic deformation. Under these conditions, the crack tip is believed to be quite sharp inducing a high effective ΔK and consequently crack growth rates when subjected to cyclic loading. Conversely, as M_c is increased and the structure assumes that of a nearly linear polymer, the loose molecular network permits greater molecular flow. With increased capacity for energy dissipation and crack tip yielding, the effective ΔK and da/dN should drop. The increase in plastic deformation with increasing M_c is apparent by inspection of the fracture

88
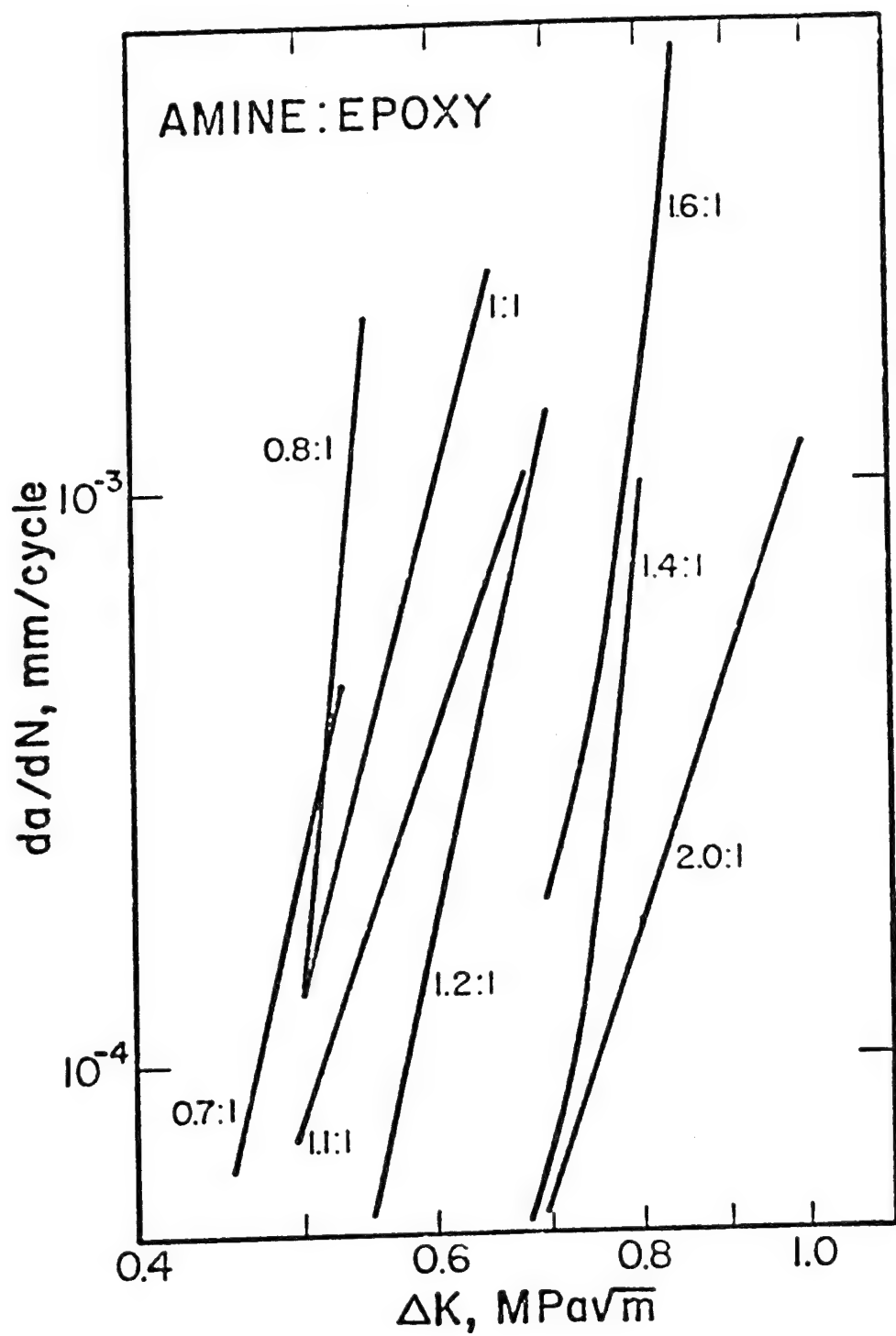
Figure 4.17   Effect of amine:epoxy ratio on fatigue crack growth rates as a function of ΔK in Series A epoxies.

89
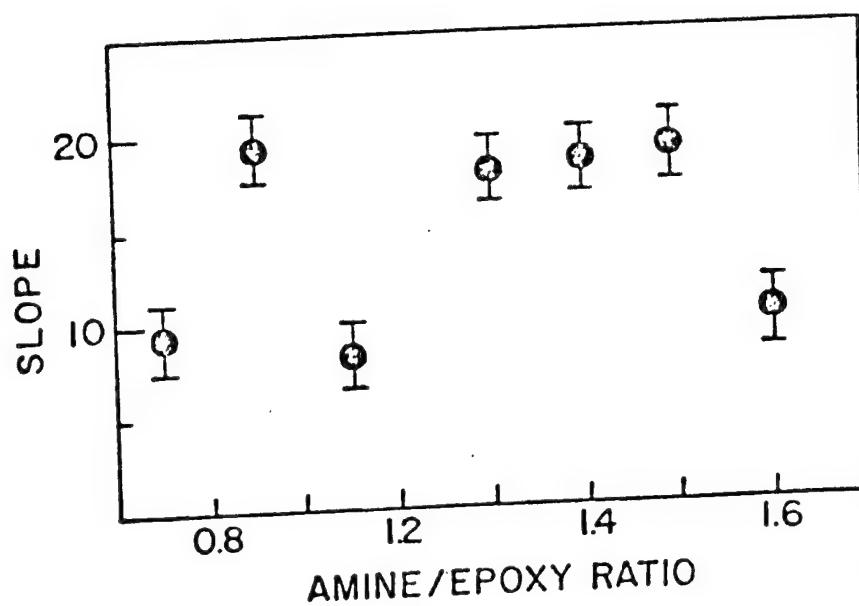
Figure 4.18 Slopes of fatigue crack growth rate curves shown in
Figure 4.17 as a function of amine: epoxy ratio.
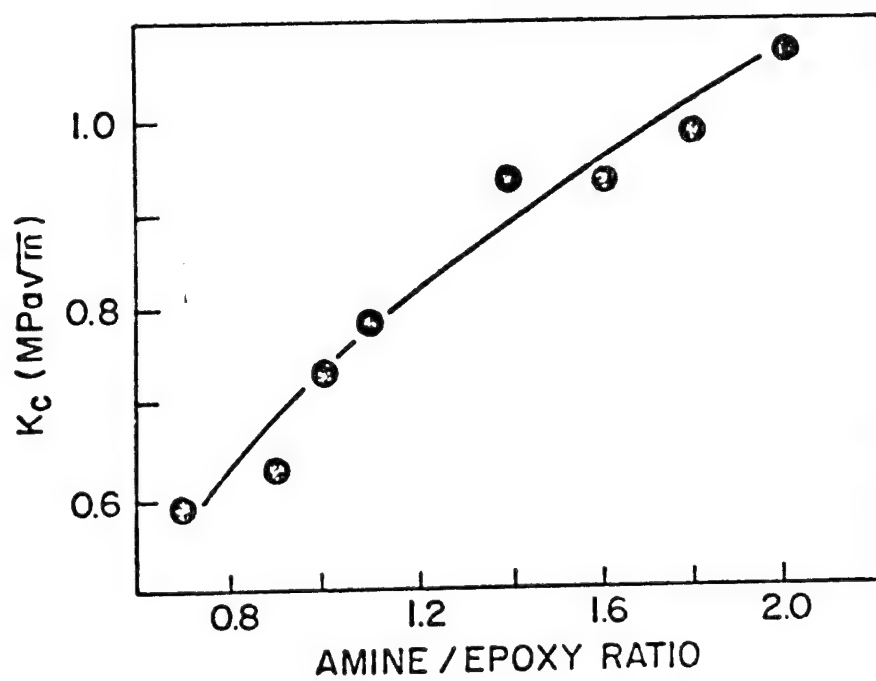
Figure 4.19 Effect of amine:epoxy ratio on the toughness of series
A epoxies.

91

surface where a gradual roughening with M_c is noted.

The continuous increase in toughness with M_c also seems consistent with the previous argument. Increasing the capacity for plastic deformation should enhance the total fracture energy; consequently, toughness should rise. However, these data contradict those published by Selby and Miller[43] which showed toughness to reach a maximum at an intermediate M_c. No rationalization can account for this discrepancy.

Figure 4.20 shows the effect of M_c distribution on crack growth in epoxies where the average M_c was maintained at stoichiometry (M_c = 326). Note that no clearly discernible trend in crack growth rates or toughness is evident. Since the M_c distribution may be of insufficient width to produce a real effect, the importance of this variable in controlling fatigue resistance is not yet clearly understood.

4.5 Conclusions

1. The fatigue response of polyacetal was found to be superior to all known polymers. A slight frequency effect related to a fracture mode transition was evidenced by an increase in the slope of the crack growth rate curve with increasing frequency.

2. Both fracture, toughness and fatigue response in both PMMA and PVC were affected by changes in molecular weight. While toughness was increased by a factor of 2.5, da/dN decreased by 10^3 with

92
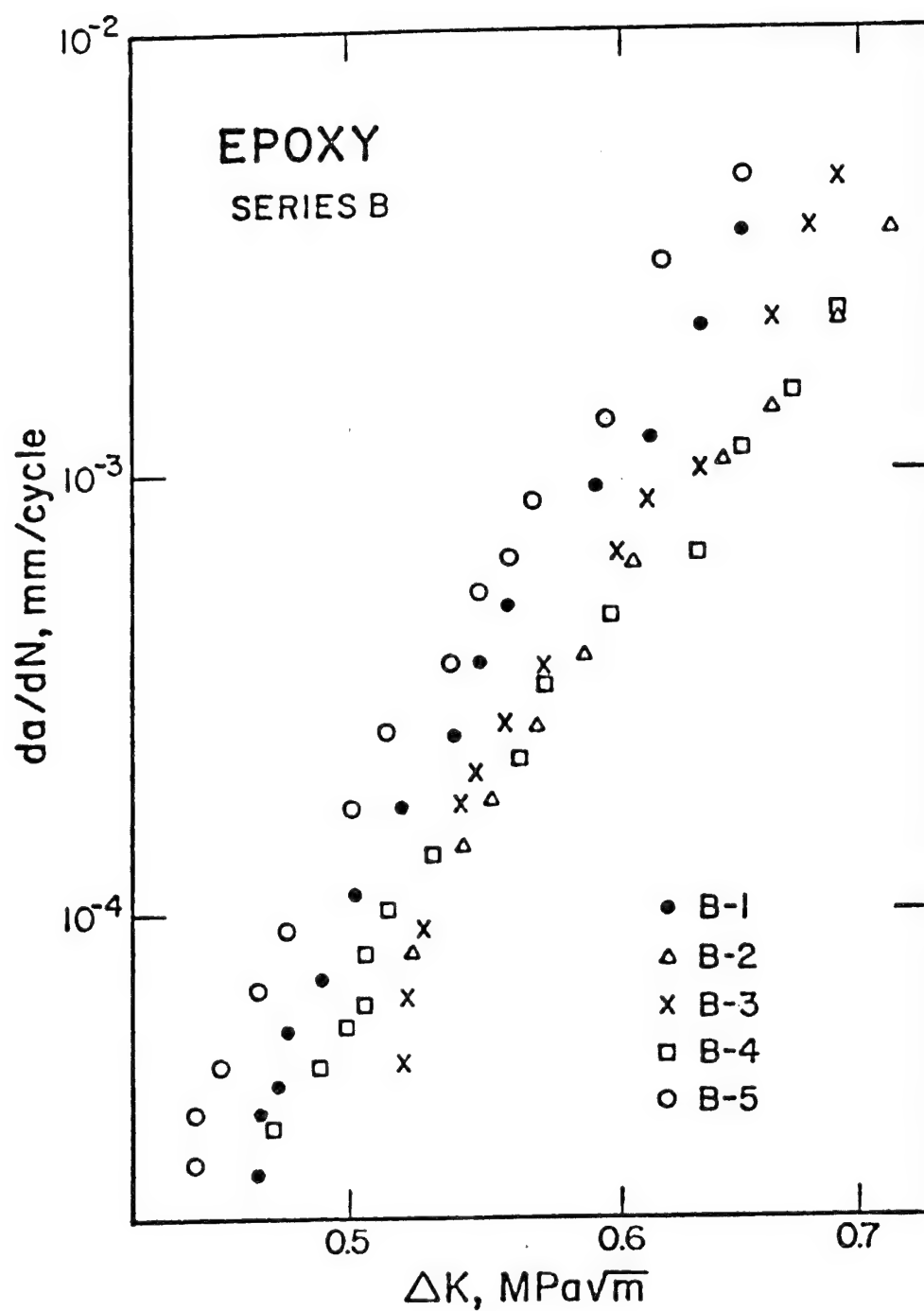
Figure 4.20 Effect of M_c distribution on fatigue crack propagation
in series B epoxies. B-5 has the widest distribution.
(See Appendix II)

93

increasing M over the same M range. A similar but lesser effect was noted in PMMA. Apparently, static properties such as toughness reach a limiting value when increase in the extent of chain entanglements does little to increase the strength of the craze preceding the crack. Under cyclic loading conditions, the molecules spanning the craze will become disentangled. By increasing the number of entanglements at high M, disentanglement is partially suppressed; consequently, da/dN is lower.

3. The effect of plasticizer content on the fatigue and fracture properties of externally plasticized PVC (with DOP) and internally plasticized PMMA (BA copolymerized PMMA) were dissimilar. Except for a reduction in toughness in PVC at 6% DOP, an external plasticizer had relatively little effect on K_c or FCP in PVC. With increasing BA contents in PMMA crack growth rates increased while toughness decreased. At 30% BA, the FCP response and toughness had improved. This behavior was explained in terms of interrelated mechanical and thermal processes.

4. A decrease in M_c was seen to increase da/dN and decrease toughness. One may speculate that the increase in structure rigidity incurred at low M_c is incapable of enduring large scale plastic deformation. With any

94

cyclic loading, the crosslinked crack tip network is

damaged. FCP is then enhanced.

V. Fatigue Fracture Surface Analysis of Polymers

5.1 Introduction

Considerable effort has been directed toward the identification of fatigue fracture mechanisms through fracture surface analysis. Much of this work had been performed previously under monotonic loading conditions. Such researchers as Kambour[34] and Murray and Hull[35-37] demonstrated the importance of crazing and craze-crack interactions in the static fracture of PS. However, less emphasis has been placed on mechanistic studies of fatigue fracture. Yet to understand why one polymer is more fatigue resistant than another, requires additional information about the actual fracture processes in each material. One of the most useful methods of analyzing these mechanisms has been through the interpretation of morphological features observed in fatigue fracture surfaces. Transmission and scanning electron microscopes are used extensively for this purpose.

Several previous studies of fatigue fracture surfaces in glassy polymers have shown the presence of many different markings[1,13,20, 23,68-77] The best understood of these are the parallel striations, oriented perpendicular to the direction of crack growth, which increase in size with increasing stress intensity factor range. When the width of these bands were compared with the macroscopic crack growth rate (measured along the specimen surface) in polycarbonate, good correlation was noted[1] Therefore, one fracture band must have

96

been formed during each load cycle, thereby reflecting the total crack front advance as a result of each load excursion. Under these conditions, it has become common practice to refer to these markings as striations.

These fatigue striations become smaller and eventually disappear as one moves back toward the origin of crack growth (i.e., smaller crack sizes and lower ΔK levels). At very low ΔK levels, the fracture surface appearance becomes smooth and mirror-like.[13,72-76] In this region another series of parallel markings becomes evident. Like the fatigue striations, these bands are also perpendicular to the direction of crack growth and increase in size with increasing ΔK. However, a comparison of the band spacing and the macroscopic crack growth rate reveals that each band was not formed during one load cycle but rather over hundreds or even thousands of load excursions. The mechanism for the formation of these bands has been shown to involve a discontinuous crack growth process with craze formation playing a dominant role.[13,20,71] These markings have been found in PVC,[20] PS,[13] and PS-PU,[40] all uncrosslinked glassy polymers with a strong propensity for crazing. It has been suggested that the width of these bands represents the size of the local plastic zone ahead of the crack tip.[13,20,23] Employing the Dugdale[78] plastic zone model, a yield strength was inferred which agreed well with the reported craze stress for the material.[13,23] A further discussion of this analysis will be given later.

97

Fatigue fracture surface analysis of crystalline polymers is complicated by the two phase structure comprised of both crystallites and amorphous regions. However, some evidence of the presence of fatigue striations in nylon has been reported by Manson and Hertzberg[1] and Tomkins and Biggs.[79] In studies of FCP in PE at low growth rates, Andrews and Walker[48] found crack growth to progress by a transspherulitic mechanism. With increasing ΔK, crack advance became interspherulitic indicating the weakness of the spherulite - spherulite boundaries under more extreme loading conditions. Only one known paper by Crawford and Benham[5] discusses the appearance of the fatigue fracture surface of PA. They reported the presence of many regions of irregular-shaped striations or ripples. Since their width (200-500 $\overset{o}{A}$) is about the same as the dimension of a typical lamellae in a crystalline spherulite, interpretation of these markings as striations is open to question without macroscopic crack growth rate information.

5.2 Results and Discussion

5.2.1 Macroscopic Evidence of Discontinuous Growth Bands

At low ΔK levels in glassy polymers with $\overline{M}_v \approx 2 \times 10^5$, the characteristic macroscopic appearance of the fatigue fracture surface is smooth and mirror-like as shown in Figure 5.1. A higher magnification of these regions (Figure 5.2) reveals hundreds of parallel bands lying perpendicular to the direction of crack growth. These bands are found in PVC, PC, PSF, PS and low $\overline{M}_v$ PMMA (see below for discussion of effects of M on band formation). The fracture surface of PA is considerably rougher; however, similar fracture surface markings are evident (Figure 5.3). In each polymer, the band size increases monotonically with ΔK. From Figure 5.4, it is evident that this increase follows a second power relationship for PVC, PMMA, PS, and PA throughout the ΔK range where the bands exist. For the case of PC and PSF, the data conform to a second power correlation only over a small ΔK range. This deviation occurs simultaneously with a transition in the fracture surface appearance from smooth to a rough texture as shown in Figures 5.1b and c. During crack growth the rough region associated with multiple crazing (in which the main crack jumps from one craze to another) is observed to lag behind the smooth region as shown schematically in Figure 5.5. This perturbation of the crack front profile may be responsible for hindering the development of each band and as a consequence may cause the observed complex dependence of band size on

99
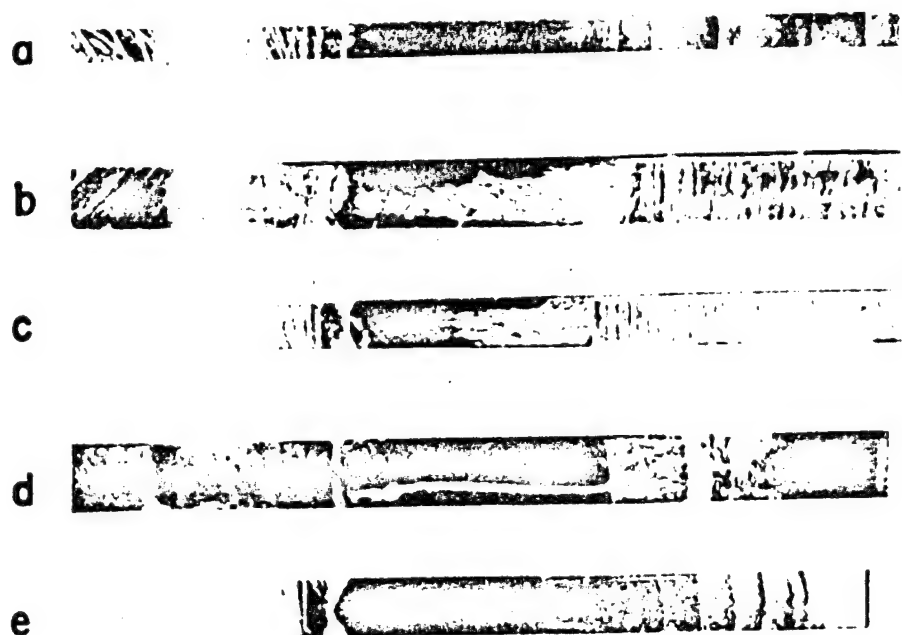
Figure 5.1   Fracture surfaces of a) poly(vinyl chloride), b) poly-
carbonate, c) polysulfone, d) polystyrene and e) poly(
methyl methacrylate).

100
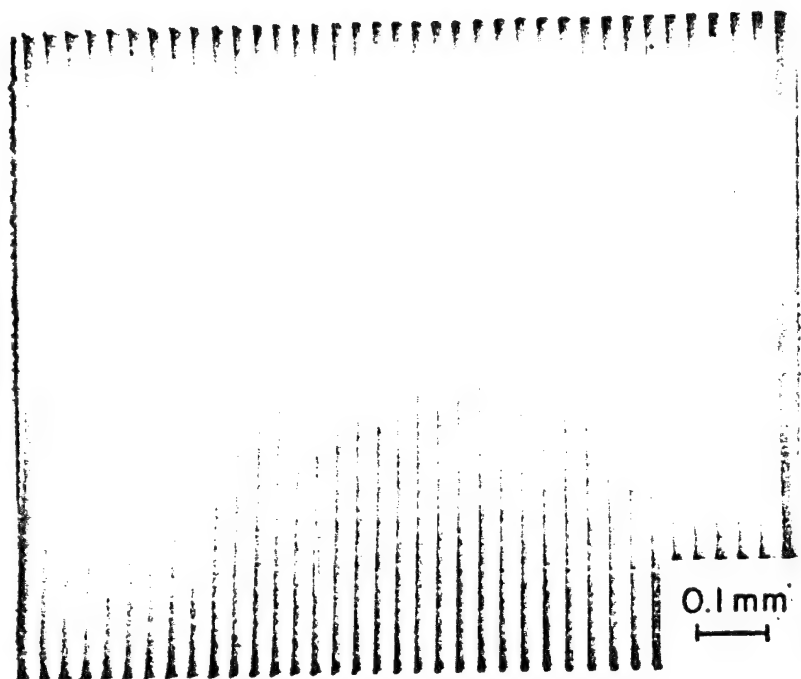
Figure 5.2   Parallel array of discontinuous growth bands in poly-
styrene.   Direction of crack growth indicated by
arrow.A8

101
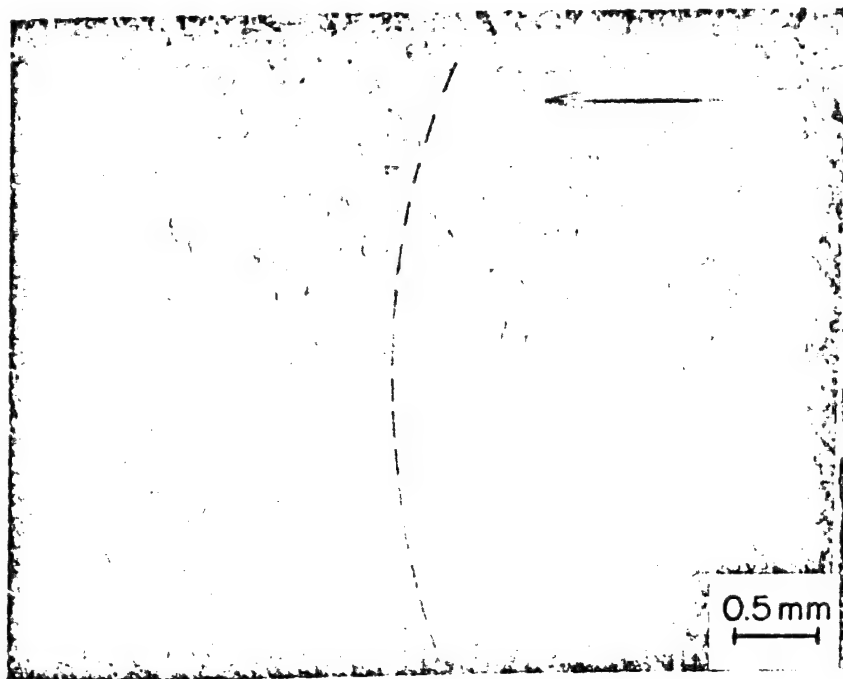
Figure 5.3 Fractograph of PA revealing rough discontinuous growth bands. Dotted line indicates contour of band. Direction of crack growth indicated by arrow.

102
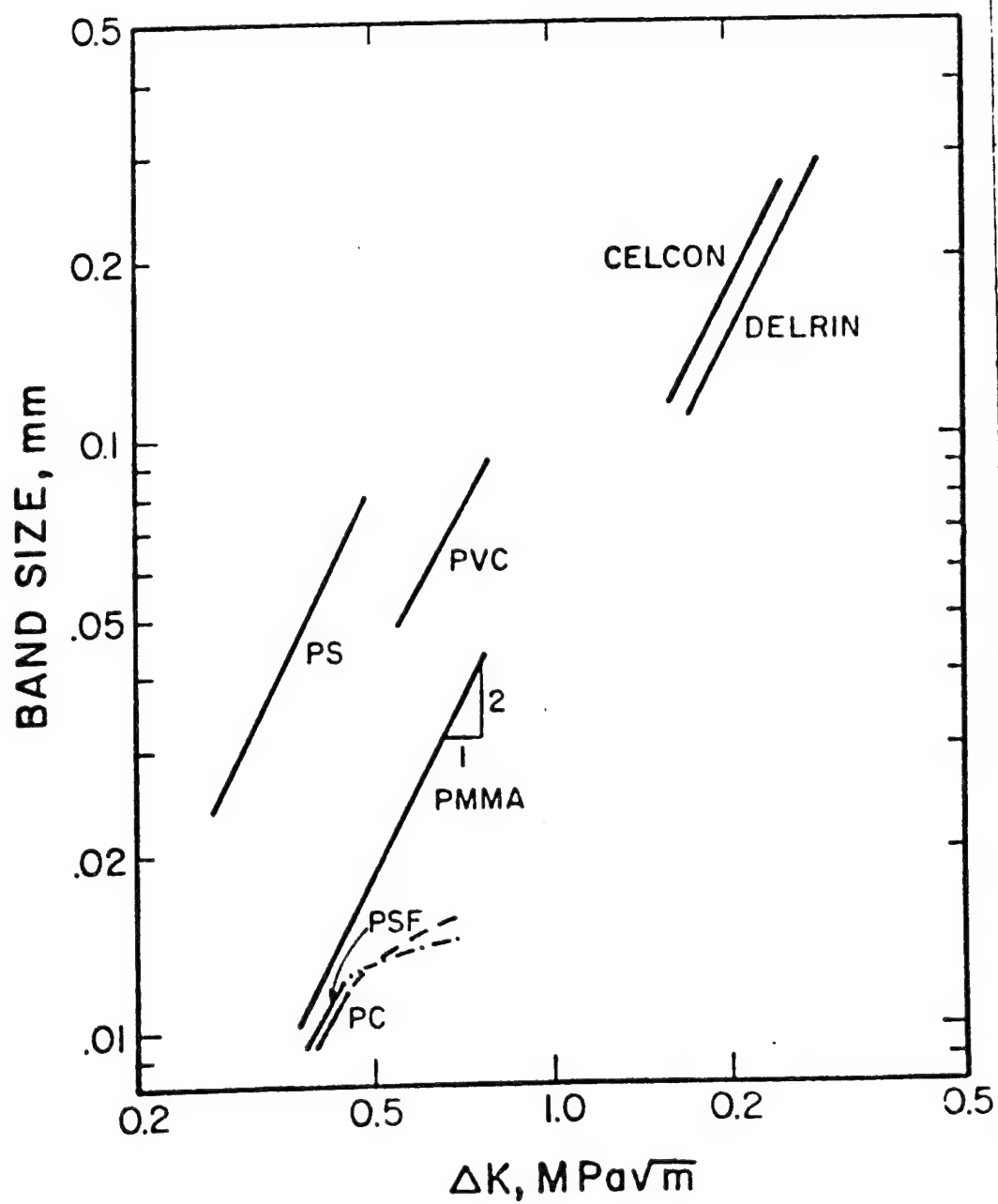
Figure 5.4   Dependence of band size on ΔK for five glassy polymers
and polyacetal.

103
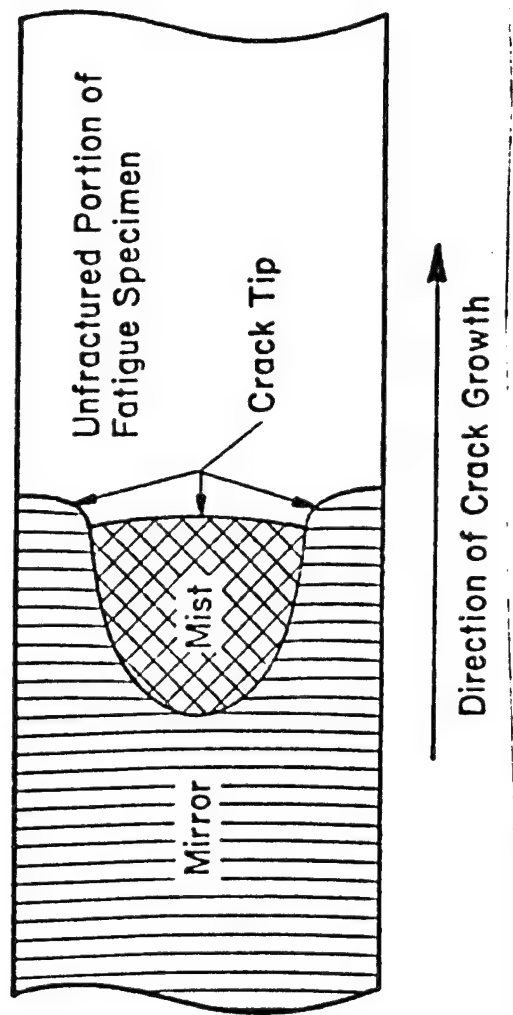
Figure 5.5 Schematic diagram of the crack plane during fatigue testing of PC and PSF. Note that the rough mist region associated with multiple crazing lags behind the smooth mirror region which contains the discontinuous growth bands.

104

It was suggested previously in studies of PS[13] and PVC,[20,23] that the band size represents the extent of stable craze development ahead of the crack tip. Assuming the craze dimension to be equal to the crack tip plastic zone length (r_y), one may infer an apparent yield strength (σ_y) (presumably a constant value) at different K_{max} levels through the use of the Dugdale[78] plastic strip model[80-82] which yields the following equation:

$$r_y \sim \frac{\pi}{8} \frac{K_{max}}{\sigma_y^2} \qquad (5.1)$$

Figure 5.6 shows the inferred yield strength calculated for PS at different ΔK values.[13] This quantity is observed to be relatively invariant over a considerable ΔK span with all data falling within the range of reported craze strength values. Of the data plotted in Figure 5.6, those marked by open points were determined from 100 Hz test specimens and the two solid points were evaluated at 10 Hz. Note the minor effect of cyclic strain rate on craze stress. This behavior is in agreement with the low sensitivity of craze stress to changes in static tensile strain rate.[83] It is to be noted that all data lie considerably below values reported for homogeneous shear yielding. Since PS crazes before general yielding under tensile loading conditions, this result seems reasonable. Similar measurements and calculations were made for PVC, PMMA, PC, and PA (both Celcon and Delrin), taking band size values from the

105
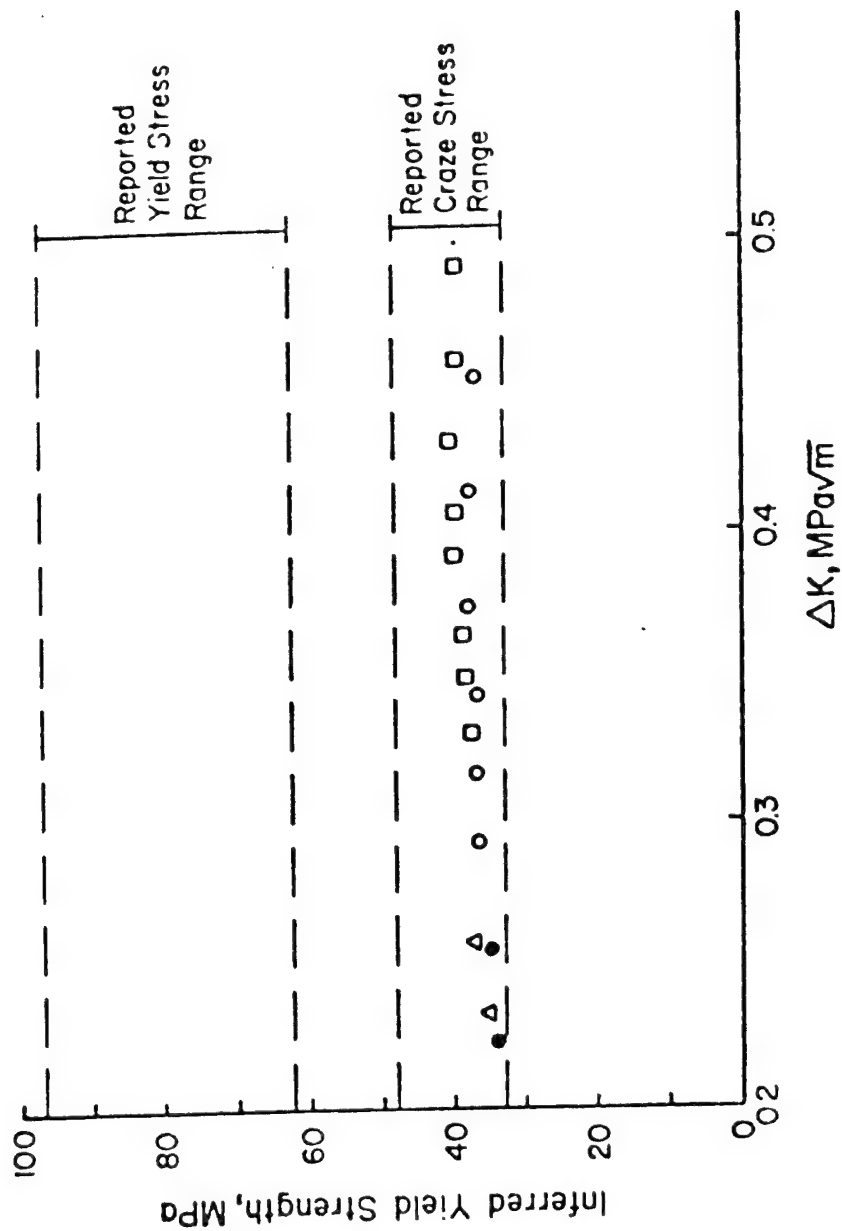
Figure 5.6 Relationship between inferred yield stress from discontinuous growth band meas-
urements and stress intensity range. Also shown are yield and craze stress
values for polystyrene as reported in the literature. 72,83,A8

linear portions of the log-log curves in Figure 5.4. These results are tabulated along with reported triaxial yield strength data in Table 5.1. Again good agreement is noted. On initial reflection, it is surprising to find good agreement between craze strengths obtained from a tensile test and those reported here under fatigue conditions at relatively high frequencies. It should be pointed out, however, that the fatigue crazes associated with DG band formation grow to their stable length only after many cycles. As such, the effective strain rate is actually low. The triaxial yield strength seems to be a more accurate representation of the yielding process at the crack tip at low K values where the plastic zone is small and plastic constraint and tensile triaxiality are at high levels.

Although the macroscopic appearance of these crack growth bands are geometrically similar to fatigue striations which are formed during one load excursion, crack growth measurements indicate that many cycles were required to allow the crack to propagate through each band. In dividing the band width by the macroscopic FCP rate, it is seen that for the test conditions employed in this study, up to 75,000 (for PA) cycles were necessary to advance through a distance equal to the band width (Figure 5.7).

The recognition that such bands exist in these six materials bears directly on failure analyses of components made from these polymers. If such bands were observed and misinterpreted as fatigue

107

TABLE 5.1   YIELD STRENGTHS OF POLYMERS INVESTIGATED

Polymer	Mean Inferred Yield Strength (Standard Deviation) (MPa)		Reported Plane Strain Yield Strength (MPa)
PC	81	(3.6)	61 - 82[80]
PVC (commercial)	51	(3.1)	47 - 65[82]
(suspension polymerized) 0% DOP	70.6	(6.4)	"
" 6% DOP	55		not available
" 3% DOP	37		
PSF	79	(1.5)	67 - 80[80]
PS	38	(1.84)	38[72,83]
PMMA (molded resin)	73	(2.9)	
(bulk polymerized)	81	(0.95)	83[84]
(emulsion polymerized)	87	(1.4)	
PA Celcon	89.6		89[85]
Delrin	99.		97[85]
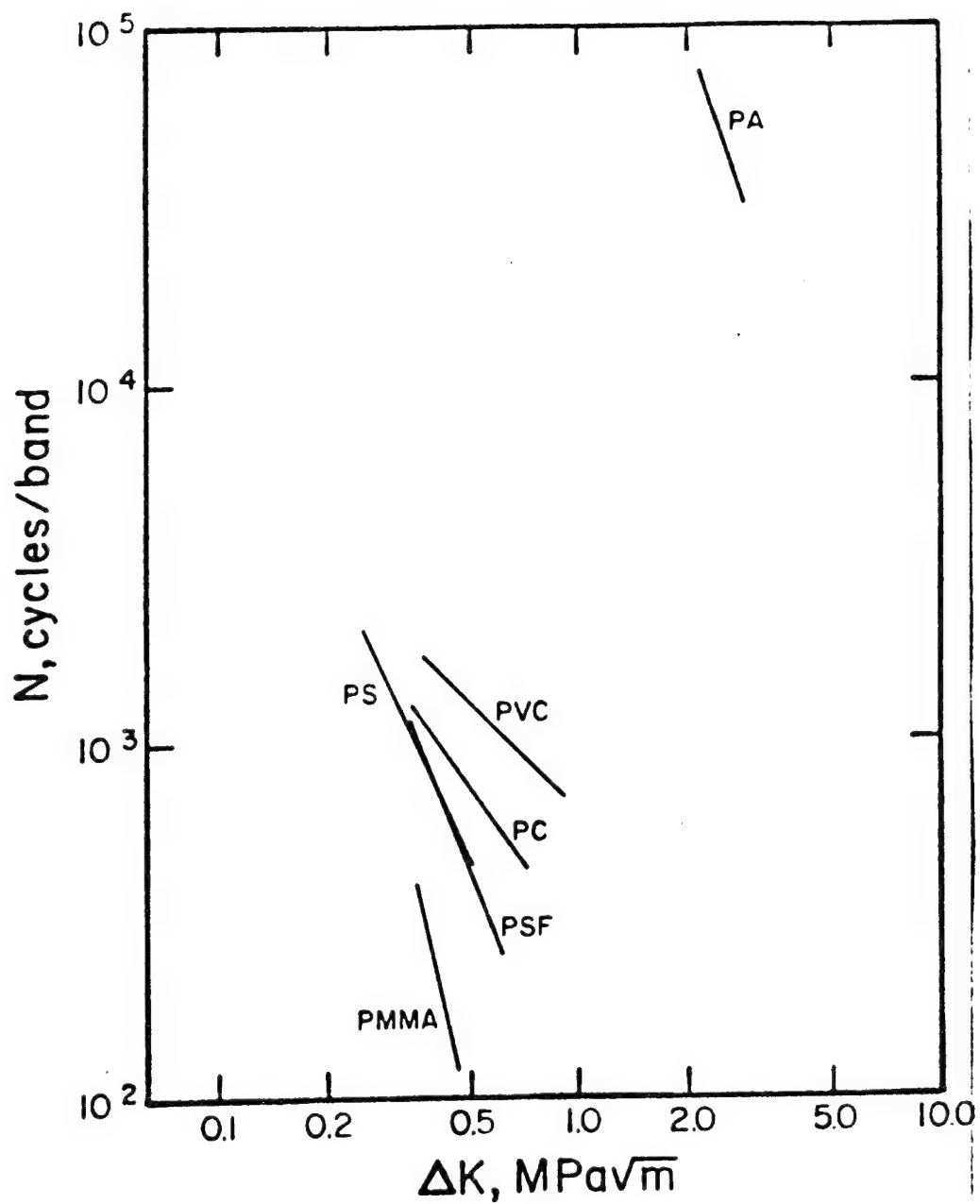
Figure 5.7 Effect of ΔK level on the number of cycles required
for growth through a discontinuous growth band.

striations, one might conclude incorrectly that most of the fatigue life was consumed during fatigue initiation with only a few cycles involving FCP. In fact, this conclusion would underestimate the propagation stage of the fatigue life by more than three orders of magnitude in the amorphous polymers and by almost five orders of magnitude in PA. For this reason, it is extremely important to examine the micromorphological differences between these two markings.

5.2.2 Micromorphology of Discontinuous Growth Bands

A higher magnification of the discontinuous growth bands shows a distinctive morphology common to all amorphous polymers tested.

From Figure 5.8, the surface of each band is seen to contain microvoids, decreasing in size in the direction of crack growth. In a previous study of these markings in PVC, Hertzberg and Manson[20] showed these bands to be formed by a discontinuous crack growth process shown schematically in Figure 5.9a. It was concluded that under cyclic loading conditions, a single craze would grow to a stable limiting size characterized by the Dugdale plastic strip dimension. The crack was then envisioned to propagate rapidly to the tip of the weakened craze. The rapid fracturing of the craze would occur by a void coalescence mechanism with the void size distribution reflecting the internal structure of the craze just prior to crack extension, as determined by the crack opening displacement distribution at the craze tip. Blunting, represented by the

110

(a)

10μm

(b)

2μm
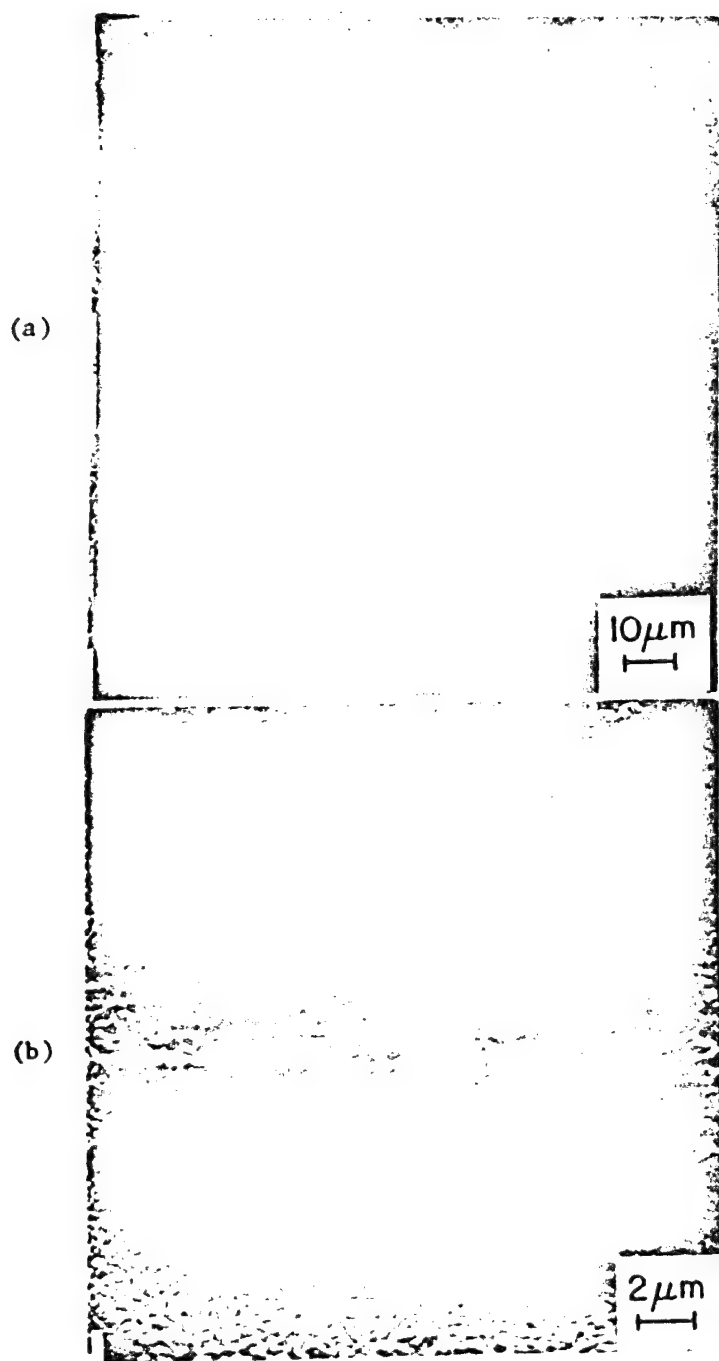
Figure 5.8   Fractographs of discontinuous growth bands in a) PVC,
b) PC, c) PSF, d) PS (SEM micrographs) and e) PMMA
(TEM micrograph). Direction of crack propagation
given by arrow.[A8]

111

(c)

5μm

(d)

10μm

Figure 5.8 continued.

112

(d)

Figure 5.8 continued.

113

CRACK TIP

CRAZE

STRETCH ZONE
NEW CRACK TIP

CRAZE

(a)

N=0

N=100

N=200

N=300

N=450

75μ
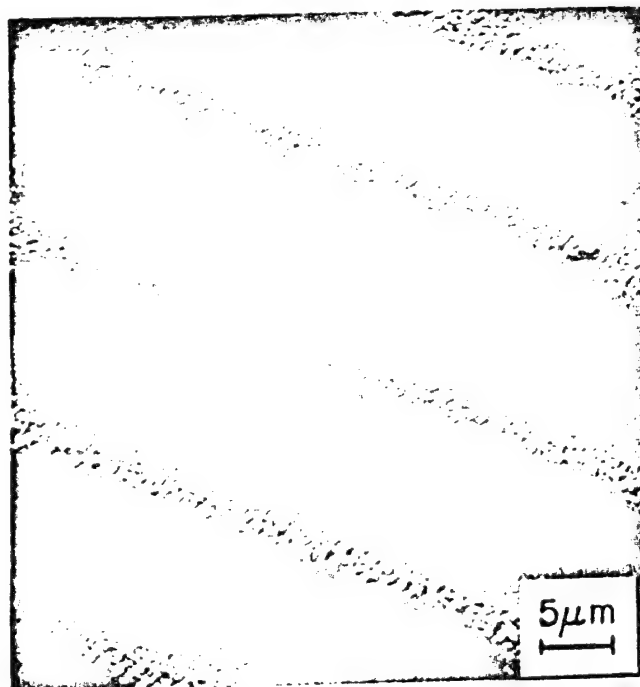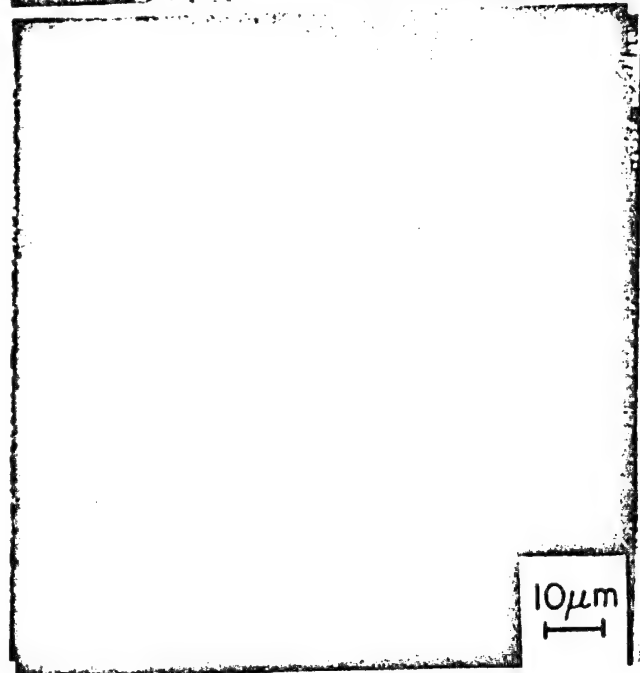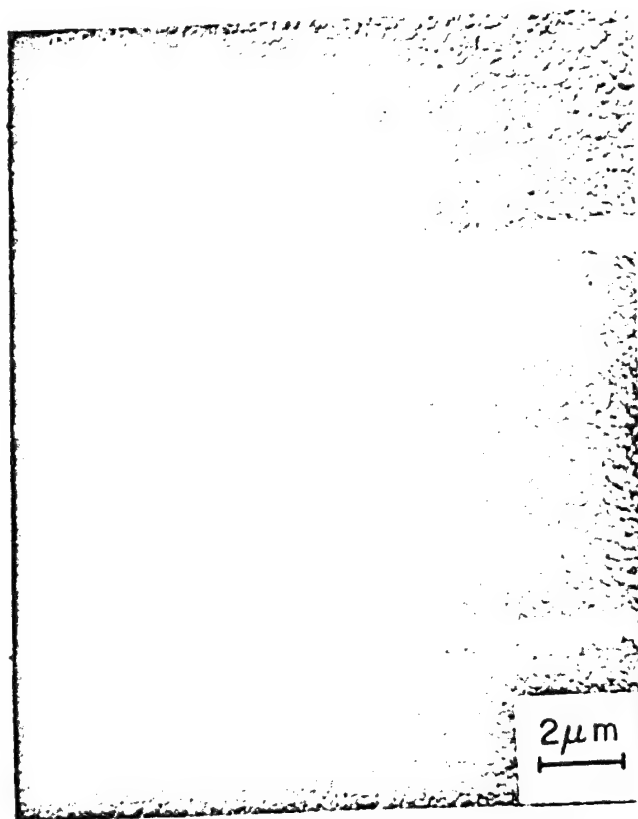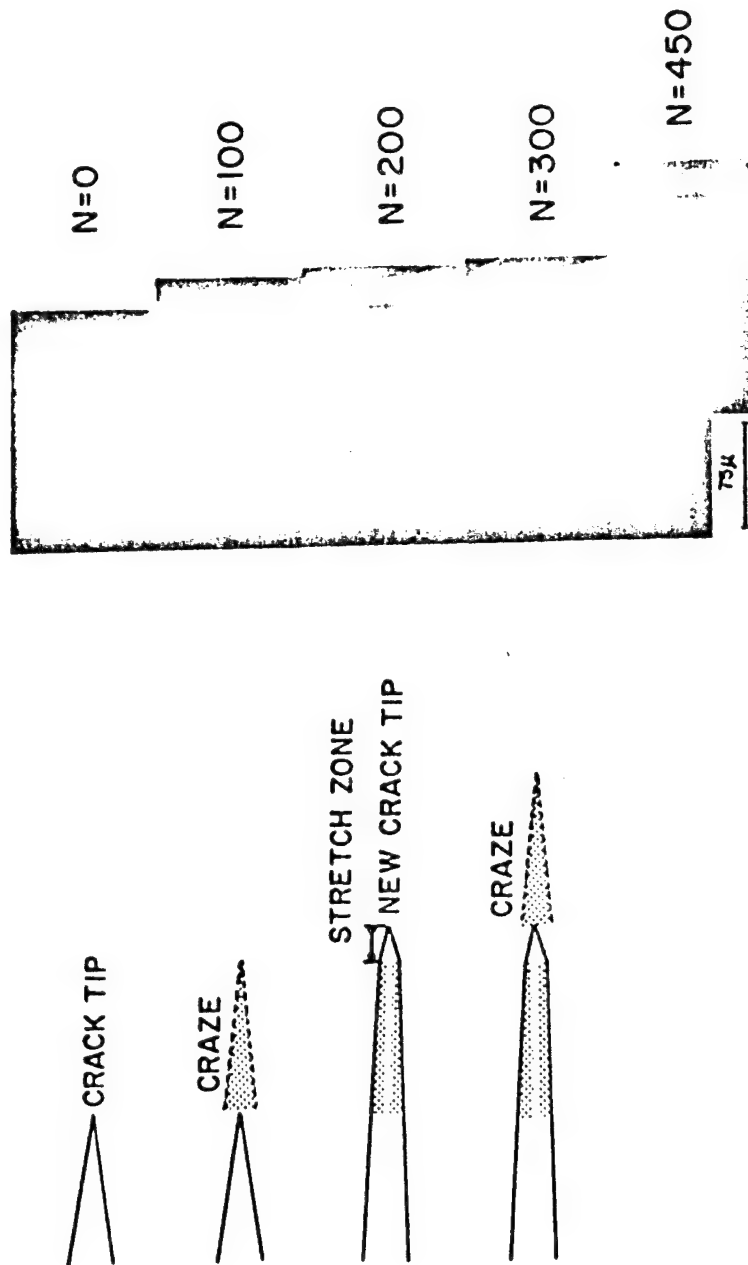
(b)

Figure 5.9 (a) Schematic representation of the discontinuous growth process. (b) Composite micrograph of PVC showing position of craze (↓) and crack (↓) tip at given intervals. A8

114

stretch zone following each band and crack arrest would occur when the crack reached homogeneous uncrazed material. This discontinuous crack growth mechanism was confirmed during the fatigue test by observations of crack tip jumping, which occurred intermittently after the crack tip remained stationary for several hundred loading cycles (Figure 5.9b). In low $\bar{M}_v$, plasticized PVC each jump was accompanied by a slight but audible "click" which confirmed the occurrence of a discontinuous cracking process.

The previous discussion provided a generalized view of the discontinuous crack growth mechanism. A more complete analysis of crack growth through a craze is now required to describe certain variations in discontinuous growth band (DGB) morphology. All polymers examined, and especially PS and PVC, showed a narrow region of coarser microvoids immediately preceding the stretch zone (i.e., at the end of the DGB). Close examination reveals this region to be comprised of intermediate sized voids. It is believed that the presence of these voids reflect changes in the rate of crack growth through the craze. The velocity of crack penetration of the initial portion of the craze is quite high due to the low energy needed to fracture a region consisting predominantly of large voids. As the crack approaches the end of the craze where the void size diminishes and the craze becomes more dense, additional energy would be required for failure. This should result in a decrease in crack velocity prior to blunting, thereby provid-

115

ing additional time for void coalescence at the end of each band.
This region is most prominent in PVC and PS in which crazes develop
readily.

Another aspect of DGB morphology relates to the position of the
largest voids in each band which should correspond to the region of
maximum tensile triaxiality. From Figure 5.8, these voids were
found in all polymers at distances of from 1/6 to 1/3 of the band
width from the origin. For an infinitely sharp crack, maximum tri-
axiality will exist at the crack tip. Since blunting occurs after
craze fracture during discontinuous crack growth, the crack tip ra-
dius is most certain finite. From the results by Creager and Paris,[86]
it can be shown that the region of maximum triaxiality will move
further away from the crack tip the greater the crack tip radius.
Hence, the greatest void size should also occur away from the end
of the stretch zone (i.e., the crack tip). While no attempts to
measure crack tip radii were made in this study, it is interesting
to note that the tougher polymers, PSF and PC, which should exhibit
appreciable blunting, showed maximum void diameters furthest from
the DGB origin.

An additional variant in DGB morphology was found in PVC at
high growth rates just before fracture. As shown in Figure 5.10a,
the last five bands contained smaller parallel markings located to-
ward the end of each DGB. The morphology of these bands (Figure
5.10b) is indicative of crack jumping from one craze interface to
another. Similar fracture markings were reported by Murray and

116

(a)

50μm

(b)

10μm
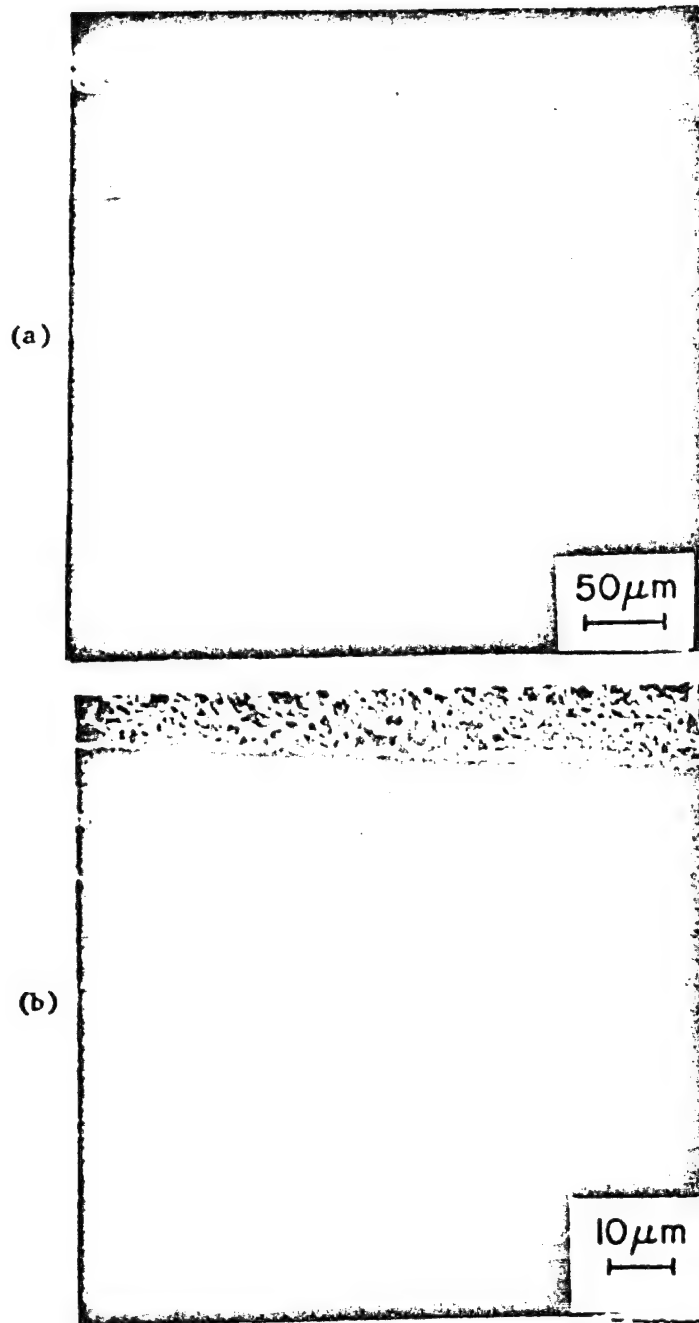
Figure 5.10   (a) SEM fractograph revealing presence of smaller
parallel bands within bands nearest the final stable
crack front location.   (b) Note evidence of crack
jumping between craze interfaces in the layered
structure of the bands. [A8]

117

Hull[35-37] in rapid fracture studies of PS. This PVC fracture surface feature probably reflects the fact that the velocity of crack growth through these last few crazes was approaching conditions associated with rapid fracture. The observation of these markings only in PVC is reasonable since it is the only polymer in the group examined to sustain discontinuous crack growth until final failure.

From the previous discussion, it is apparent that crazing must play a critical role in discontinuous crack growth in amorphous polymers. Consequently it is not surprising that DG bands are found in PS, PMMA and PVC, materials which craze easily; however, PC and PSF are not observed to craze in inert environments under monotonic loading conditions in unnotched samples.[87] One might attribute the presence of crazes in these materials to the large triaxial stresses at the crack tip and perhaps also to the cyclic nature of the loads.

Clearly, the above analysis of discontinuous crack growth in amorphous polymers cannot be applied directly to crystalline polyacetal. The presence of a discontinuous crack growth process in PA is supported by the extensive scatter in crack growth data (Figure 4.5). Since the band spacing was found to be nearly the same as the typical increment over which crack extension data were collected, one would expect to find more scatter in da/dN if the bands in PA were DGB. A higher magnification of these bands (Figure 5.11) reveals them to be ill-defined and dissimilar to those shown in Figure 5.8. From Figure 5.11, no evidence of a void gradient or

118
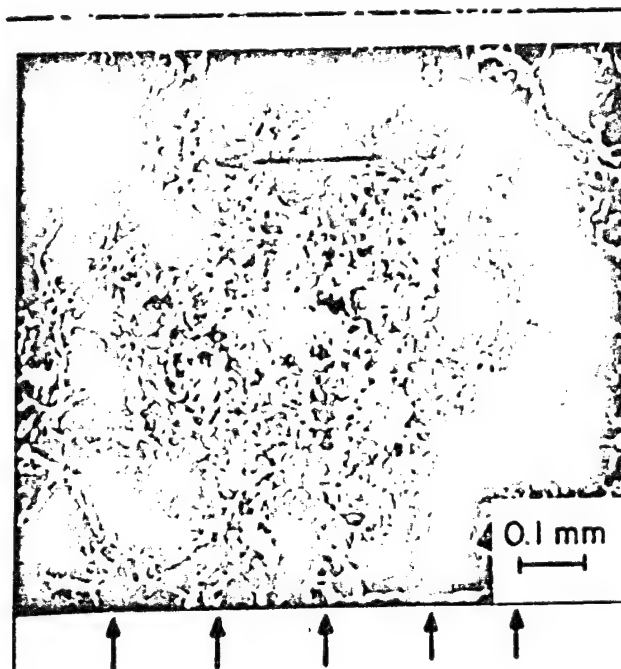
Figure 5.11 SEM fractograph of discontinuous growth bands in Delrin. Vertical arrows indicate the origin of each band and horizontal arrow gives the direction of crack growth.

119

any indication of crack growth through a craze is apparent. It would appear that the ability to form simple crazes is not necessary for the discontinuous crack growth process to occur. Conceivably, any polymer that can develop a narrow region of plastic deformation ahead of the fatigue crack which can be weakened by load cycling may be subject to discontinuous crack growth. Further analysis of the micromorphology of the fracture surface of PA is discussed later.

Since FCP in the discontinuous crack growth regime depends primarily on the characteristics of the plastic zone or craze ahead of the crack, those materials which require a large number of cycles (N) to rupture this zone should prove to be most fatigue resistant. From Figure 5.7, N is observed to decrease with increasing ΔK for all polymers tested. This reflects the increasing amount of damage accumulated in the craze per loading cycle with increasing ΔK level. In Figure 5.7, PA demonstrates a damage zone cyclic stability, two to three orders of magnitude greater than the amorphous polymers. This reflects the well known superior fatigue resistance of crystalline polymers relative to amorphous polymers.

However, if one compares only the amorphous materials in Figure 5.7 with their respective crack growth curves in the ΔK regime where DGB are present (Figure 5.12), it is apparent that the trend in band cyclic stability does not correspond to the observed macroscopic fatigue response of the various materials. This lack of correlation is believed due to the large variation in the yield strength which causes the band size to differ drastically. (Recall that the Dug-

120
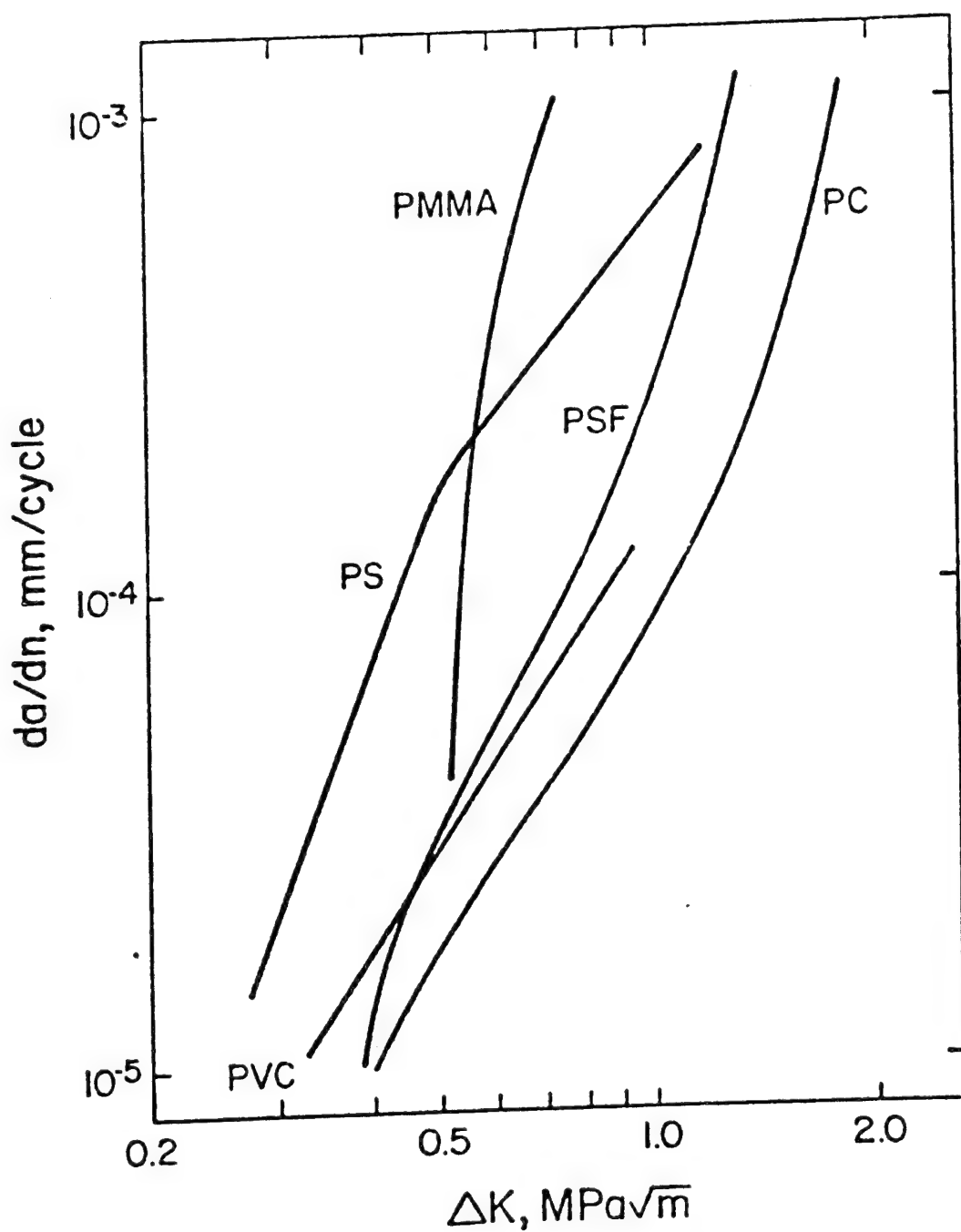
Figure 5.12   Relationship between crack growth rate per cycle in those amorphous polymers which exhibit DG bands as a function of ΔK.[A8]

dale plastic zone dimension varies with inverse square of σ_y.) If two materials could be compared with similar σ_y the effect of craze stability on crack growth rates (da/dn) could be isolated. Such a comparison is made in Figure 5.13. A bulk polymerized PMMA ($\overline{M}_v$ = 1.1 x 10^5) and commercial PC have approximately the same inferred σ_y (approximately 80 MPa). It is apparent that the number of cycles required to fracture the craze in PC is nearly two orders of magnitude higher than PMMA. The effect of this difference in craze stability may be seen in the FCP data in Figure 5.13b where for a given ΔK, PMMA has a crack growth rate about 50 times higher than PC.

5.2.3 Effect of ΔK and Frequency on DGB Formation

Discontinuous growth bands are found to exist near the origin of crack growth where short single crazes are known to precede crack growth. (This generalization may not apply for the case of PA growth bands.) In a majority of the polymers tested, the bands disappear at the point where multiple crazing begins. This suggests that DG bands are more readily generated when ΔK levels are low enough to prevent the development of craze bundles which fragment the crack front.

The effect of frequency on discontinuous crack growth is not the same in all polymers tested. In Celcon, PVC, and low-$\overline{M}_v$ PMMA, DG bands have been found at all test frequencies while Delrin, PS, PC, and PSF require high frequencies (100 Hz) for their formation. The need for high frequency in some polymers may be traced to the effect of frequency on craze formation. At high loading rates which occur during rapid cycling, little time is available for the initi-

122
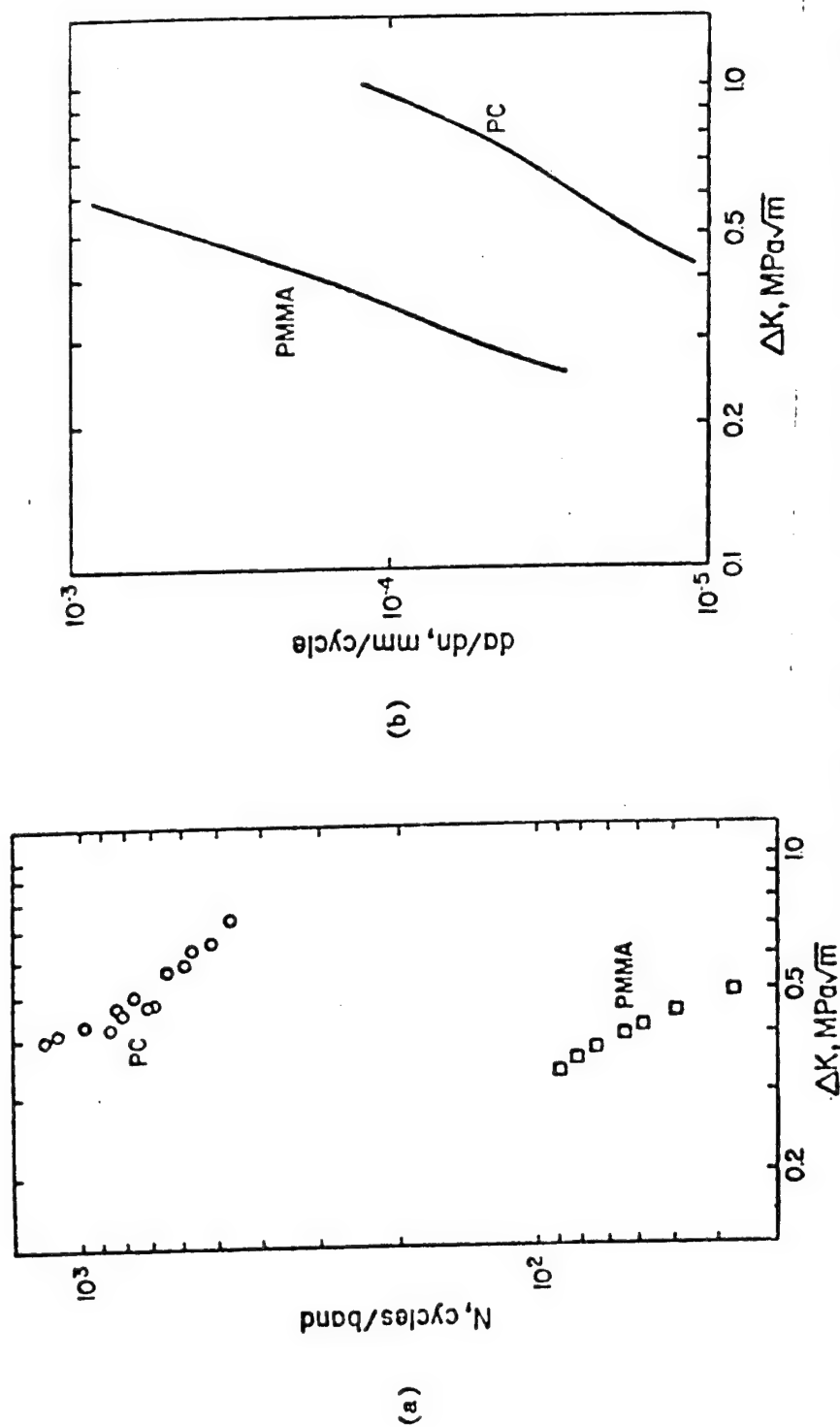
Figure 5.13 (a) A comparison of the number of cycles required for growth through one discontinuous growth band as a function of ΔK in PC and PMMA. (b) Relationship between crack growth rates as a function of ΔK in PMMA and PC. (Both have the same inferred yield strengths.)

123

ation and growth of many crazes. As a consequence, the region asso-
ciated with single craze development is stabilized relative to the
formation of craze bundles. In crystalline Delrin, the high fre-
quency may serve a similar function by producing a narrow zone of
plastic deformation. In both crystalline and amorphous polymers,
this appears to be conducive to the prolonged stability of DC band
formation.

5.2.4 Effect of External Plasticizer and M on Discontinuous Crack Growth

PVC plasticized with DOP shows the presence of DGB at all ΔK
levels from $\bar{M}_w$ = 96,000 to 225,000. While DOP content was seen to
have little effect on da/dN, it has a pronounced effect on DGB size.
From Figure 5.14, the DC band size increased with % DOP, independent
of $\bar{M}_w$. Since band size increases with the second power of the
stress intensity factor, the inferred yield strength is seen to de-
crease as a function of DOP added (see Table 5.1). While triaxial
yield strengths as a function of plasticizer content are not avail-
able for comparison, the observed trend is consistent with the de-
crease in uniaxial yield strengths with % DOP.[33]

Although the effect of M on DGB development is not clearly
understood at this time, a possible trend may be seen. From Table
5.1, all polymers examined in this study which exhibited DG bands
had $\bar{M}_v \leq 2 \times 10^5$ ($\bar{M}_v$ of PA is unknown). No DG bands were visible
in pure bulk polymerized (cast) PMMA over a range of $\bar{M}_v$ = 3 $\times$ 10^6
to 1.9 $\times$ 10^5 nor were any visible in commercially cast PMMA where

124
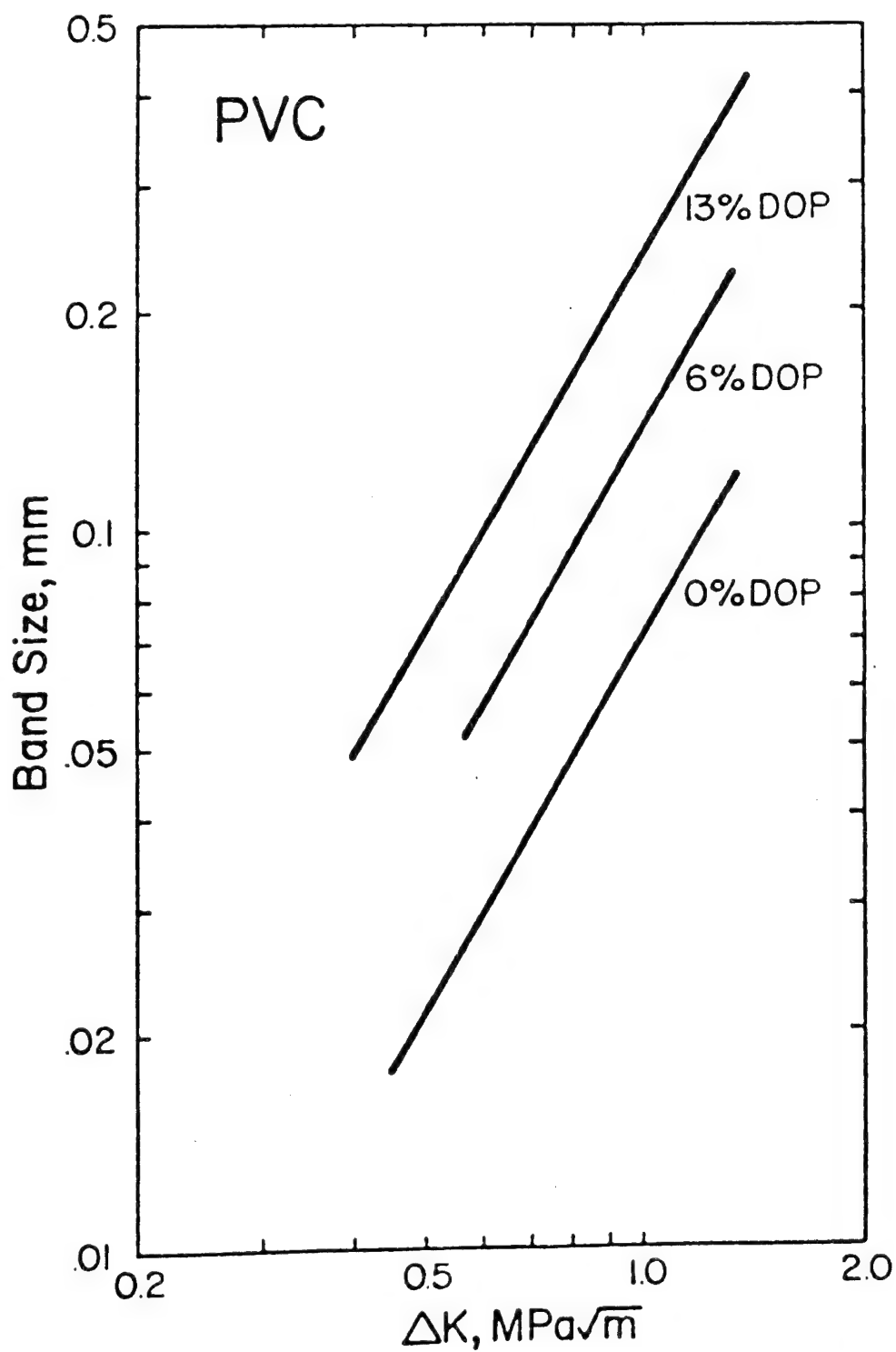
Figure 5.14 Effect of plasticizer content on discontinuous growth band size in PVC as a function of $\Delta K.$[A7]

125

$\overline{M}_v = 1.6 \times 10^6$. However, in bulk and emulsion polymerized PMMA, molded PMMA resins, and all other polymers with $\overline{M}_v \lesssim 2 \times 10^5$, DG bands were visible.

A molecular weight of about 10^5 or 2×10^5 may represent a critical condition for craze stability in the presence of cyclic loading. For low-M polystyrene, Fellers and Kee[88] showed crazes to be short and weak. A similar craze weakness at low M was also reported, Kambour.[89] The cyclic deformations associated with dynamic loading may induce the short molecular chains to disentangle causing failure of the craze to occur at relatively low loads and over a small number of fatigue cycles. At higher M, the molecular chains are longer and chain entanglements more effective in resisting chain sliding during fatigue. The crazes which form in high-M materials should then be stronger, thus requiring a greater driving force (higher ΔK) for failure to occur. Such materials are also seen to form craze bundles readily. All these characteristics of high M crazes will not favor DGB formation, and may account for their absence at M values above approximately 10^5. Although specimens of PSF, PC, PVC, and PS with $\overline{M}_v > 2 \times 10^5$ were not available, one might suspect such materials to be more resistant to DG band formation.

The simple chain disentanglement model offered above can be further developed by utilizing an approach presented originally by Berry[53] and later, in more detail, by Kusy and Turner.[50] They suggested that craze stability could be maximized only if the molecular chains, when extended, were long enough to be anchored at each in-

126

ternal face of a craze. However, Kausch[54] has shown that complete molecular extension is physically unrealistic. In the unstrained condition, the amorphous structure is assumed to consist mainly of interpenetrating coils of molecular chains which elongate upon application of a stress. When crazing occurs, fibrils are formed which consist of a series of these stretched coils. The coils are believed to be extended by only a factor of 2 or less. In any case, it is conceivable that under cyclic loading, the interpenetrating coils begin to slip past each other so that the total number of chains entangled in the fibrils decreases. Since the size of the coil varies with $\sqrt{M}$,[90] coils of a high-M polymer will intrinsically have a more dense network of entanglements than coils of a low-M polymer. Consequently, after a given number of cycles at a particular ΔK level, the material with the higher M will retain a more effective entanglement network than a polymer with a lower M. As a result, the fibrils within the craze of the higher-M material should be stronger and hence, more resistant to fracture by discrete bursts across the craze's entire area. Above some limiting value of M($\sim 2 \times 10^5$ from experimental data), it is suggested that catastrophic craze breakdown no longer occurs with slow slippage of the coils occurring instead; this results in continuous FCP. This hypothesis is supported by results given in Figure 5.15 which show the discontinuous growth band stability in PVC to decrease strongly in concert with a progressive weakening of the craze fibrils as M decreases. Therefore, when crack growth through a craze is initiated by failure of a few

127
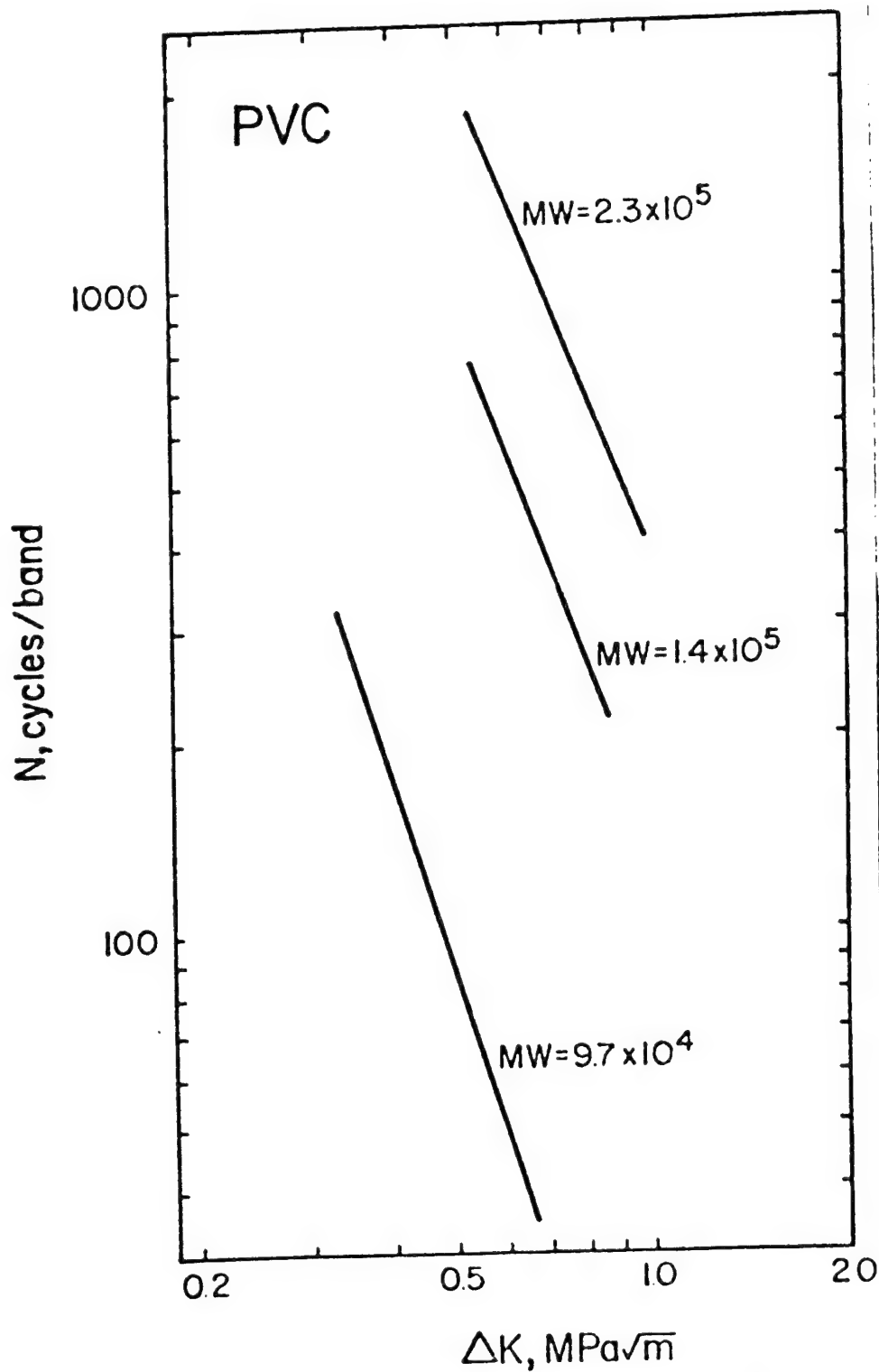
Figure 5.15 Effect of $\overline{M}_w$ on the number of cycles required to [A7,A8]
fracture a DG band in PVC as a function of ΔK.

128

fibrils near the crack tip, the remaining fibrils are too weak to restrain the continued advance of the crack. This condition promotes discontinuous crack growth.

5.2.5 Fatigue Striation Morphology

Fatigue striations of the type formed at higher crack growth rates during one load cycle have been observed in every glassy polymer tested under fatigue loading except PVC. If the striation spacing is compared with the macroscopic crack growth rate and plotted against ΔK for PS,[13] PC,[1] PMMA, PSF, and epoxy (Figure 5.16), good correlation is noted. Fractographs of fatigue striations in common amorphous polymers (Figure 5.17) showed remarkably similar appearance. The striations were very flat with a fine linear structure (oriented parallel to the crack propagation direction). In general, the arrest line between striations was very narrow. Careful observation of either side of the arrest line shows no significant difference in texture as had been noted by Jacoby.[69] If one were to compare these fatigue striations with the DG bands shown in Figure 5.8, the difference in morphology becomes quite evident. In fatigue fracture analysis of polymers where bands are visible, but growth rate data are unavailable, attention should be given to band micromorphology in order not to misinterpret the particular mechanism for band formation.

5.2.6 Fatigue Fracture Surface Micromorphology of Variable M PVC Specimens

Discontinuous growth bands were present on the fracture sur-

129
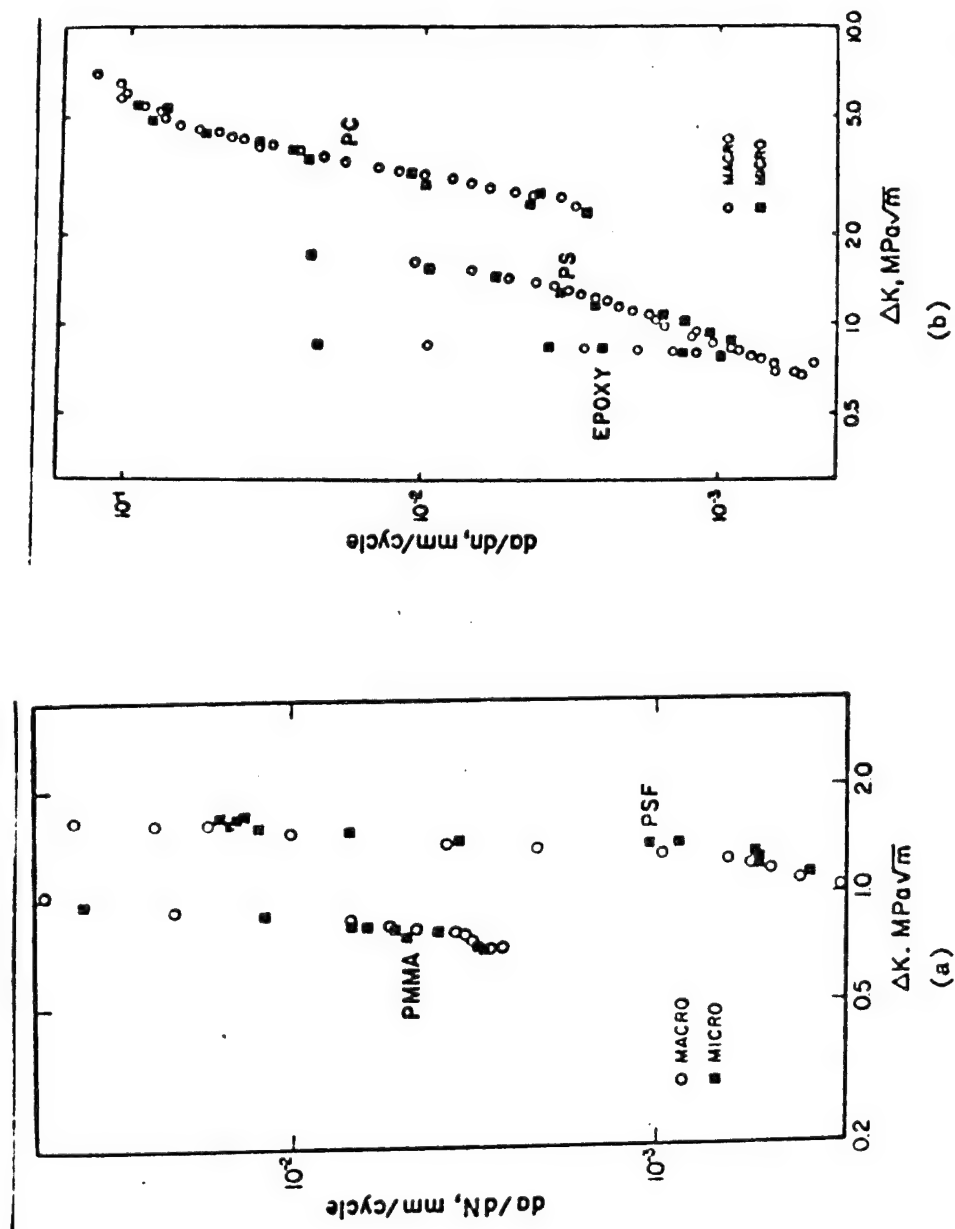
Figure 5.16 Comparison of macroscopic growth rates and striation measurements in (a) PMMA and PSF and (b) Epoxy, PS and PC.

130

(a)

10μm

(b)

40μm
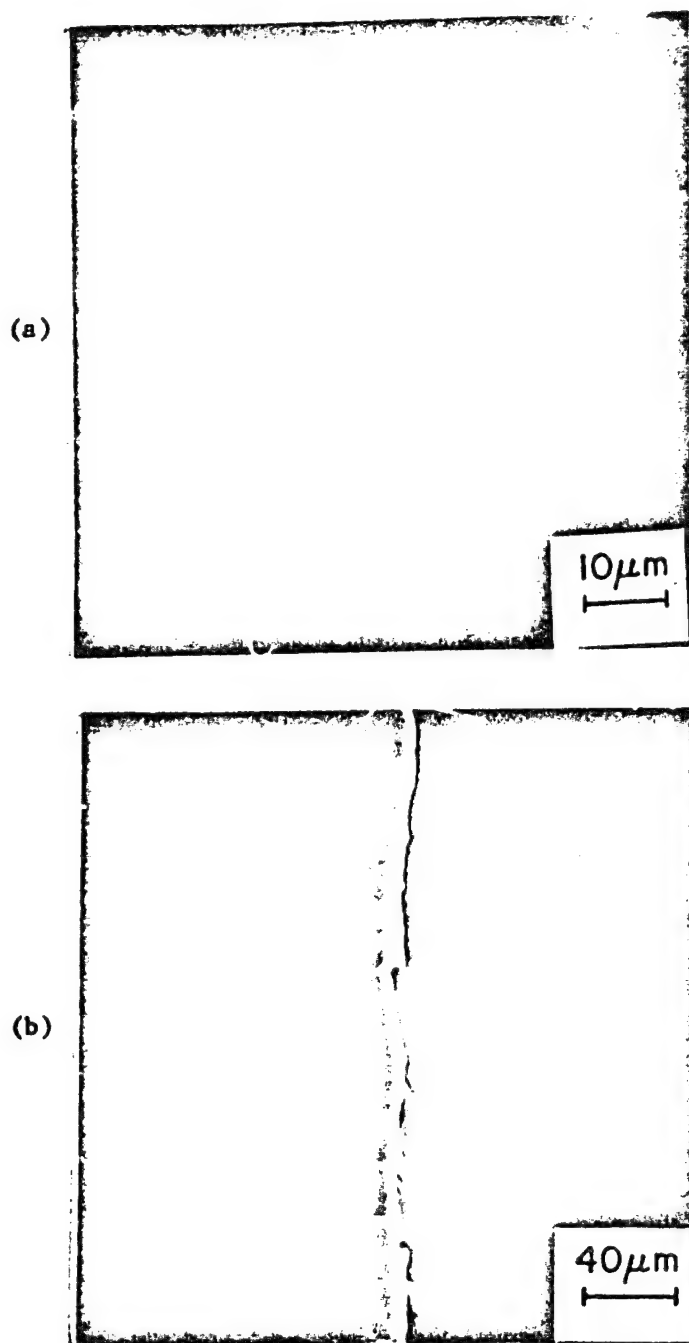
Figure 5.17 Typical striation morphology in (a) PC, (b) PSF,
(c) PS (SEM micrographs), and (d) PMMA (light micro-
graph). Arrow indicates direction of crack growth.[A8]

131

(c)

2 μm

(d)

20μm
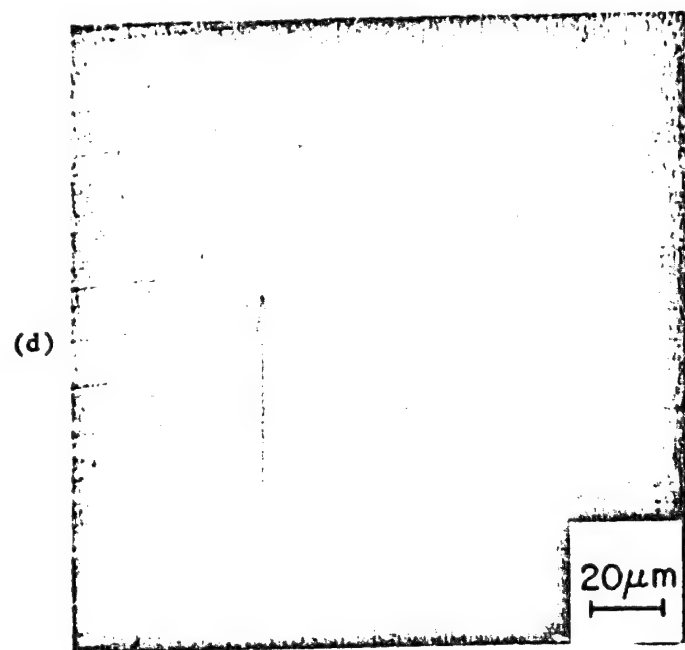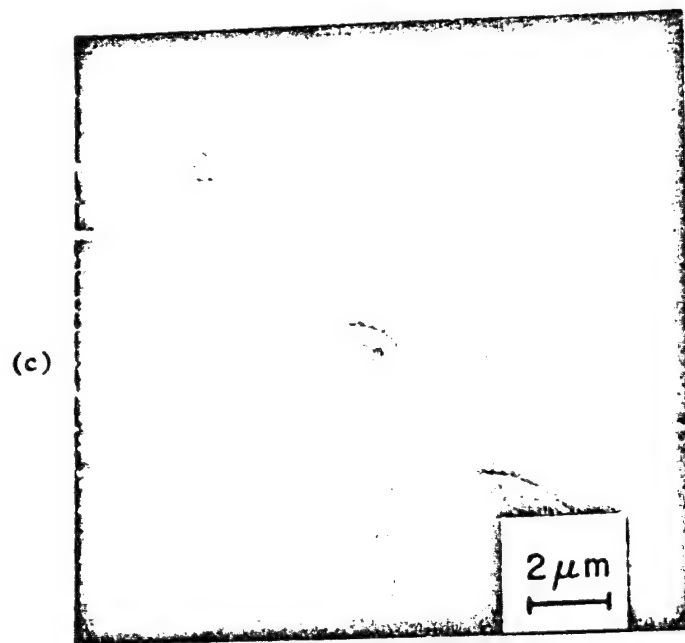
Figure 5.17 Continued

132

faces at low ΔK in all PVC specimens, regardless of M and plasticizer content. A typical fractograph of DGB's in PVC (Figure 5.18) shows a structure similar to Figure 5.8.

Another feature of the fracture surface of PVC is the presence of roughly polygonal particles which seem to constitute a sub-structure within the discontinuous-growth bands shown in Figure 5.18. The average size of these particles is $\sim$ 50 μm, within the range of sizes of the original suspension-polymerized particles used to mold the samples.

At high ΔK levels (1.1 MPa $\sqrt{m}$) at 0% DOP, a different fracture mechanism transition was identified. The DGB's disappear as crack growth no longer proceeds through these grain-like particles but begins to grow around them (Figure 5.19). This transition from trans-particle to inter-particle crack growth was associated with a slight increase in the slope of the FCP curve (seen in Figure 4.6 for $\overline{M}_w$ = 1.4 x 10^5 and 2.3 x 10^5. One may then conclude that the suspension particle boundary region is less resistant to FCP than the material within each particle. It is interesting to note that evidence of these particles was only apparent in the fatigue region of the fracture surface but not in the area of fast fracture. This implies that fatigue cycling provides a much more sensitive indicator of the weak regions within a polymer than does a simple fracture test. In this case incomplete bonding or ineffective chain entanglements at the particle interfaces may be expected to result in relative interfacial weakness, and in probable sites for crack advance.

133
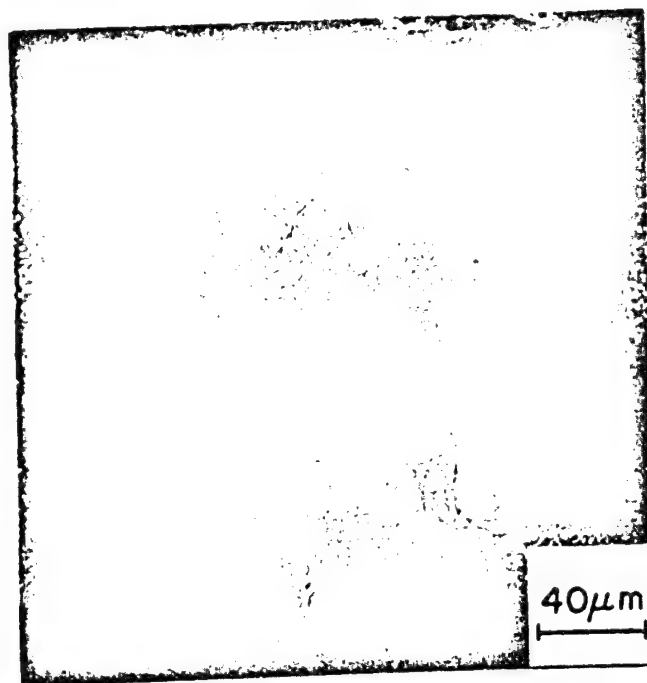
Figure 5.18 SEM micrograph of fracture surface of typical suspension polymerized PVC specimen showing discontinuous growth bands. Note evidence of interfacial failure at boundaries of polygonal shaped primary particles.[A7]

134
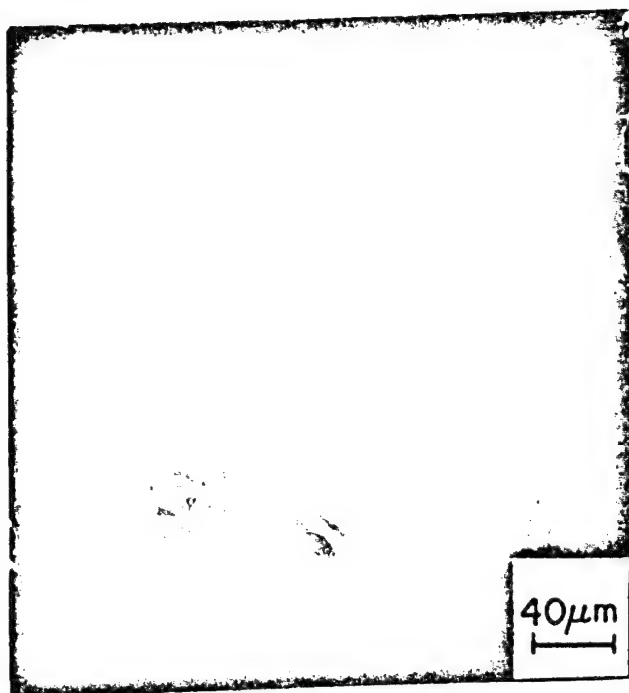
Figure 5.19   Evidence of complete inter-particle crack growth on fracture surface of suspension polymerized PVC specimen.[A7]

5.2.7 Fatigue Fracture Surface Micromorphology of Polyacetal

As mentioned previously, a macroscopic inspection of the fatigue fracture surface of Delrin at 100 Hz and Celcon showed the presence of irregularly shaped discontinuous growth bands. Higher magnification of the fracture surface reveals a complex structure common to both Delrin and Celcon at all frequencies tested. Initial observations show the frequent presence of a radial structure (Figure5.20 which corresponds in overall size to the dimension of a spherulite. This suggests that crack advance is primarily transspherulitic where crack growth proceeds through a spherulite. Evidence of secondary cracking at spherulite boundaries is also present. This mode of fatigue failure is nearly identical to Stage I FCP in polyethylene reported by Andrews and Walker.[48] At low ΔK and da/dN (Stage I), they also found crack growth to proceed primarily by a transspherulitic mechanism. Although total deformation was minimal, secondary cracking along spherulite boundaries was always present.

Higher magnification of the fatigue fracture surface reveals fine striation-like markings, (Figure 5.21) $(2 - 14 \times 10^{-7})$ in width which bear a strong resemblance to fracture details discussed by Crawford and Benham.[5] These markings are believed to be related to two different deformation processes. During transspherulitic crack growth, spherulites are split, revealing their internal structure to be comprised of lamellae. The size of the observed fracture makings agree well with the reported thickness of crystalline lamellae. The second source of linear structure is the transformation

136
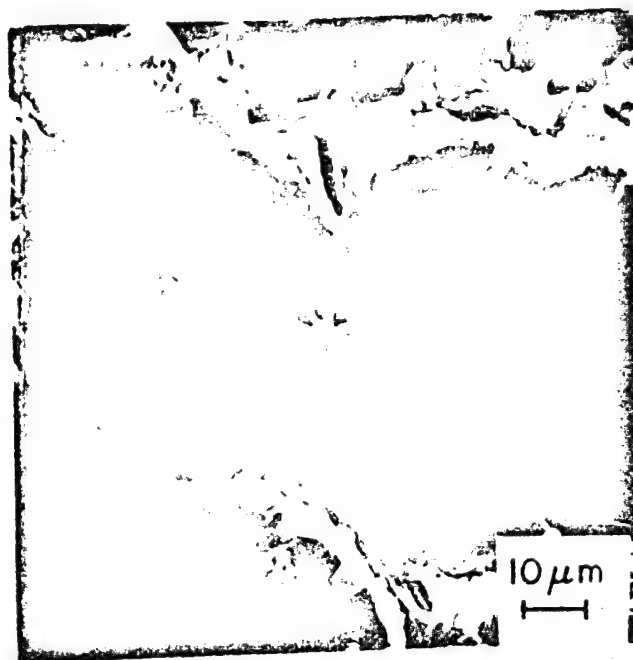
Figure 5.20 SEM micrograph of fracture surface of Delrin showing
internal structure of a spherulite.
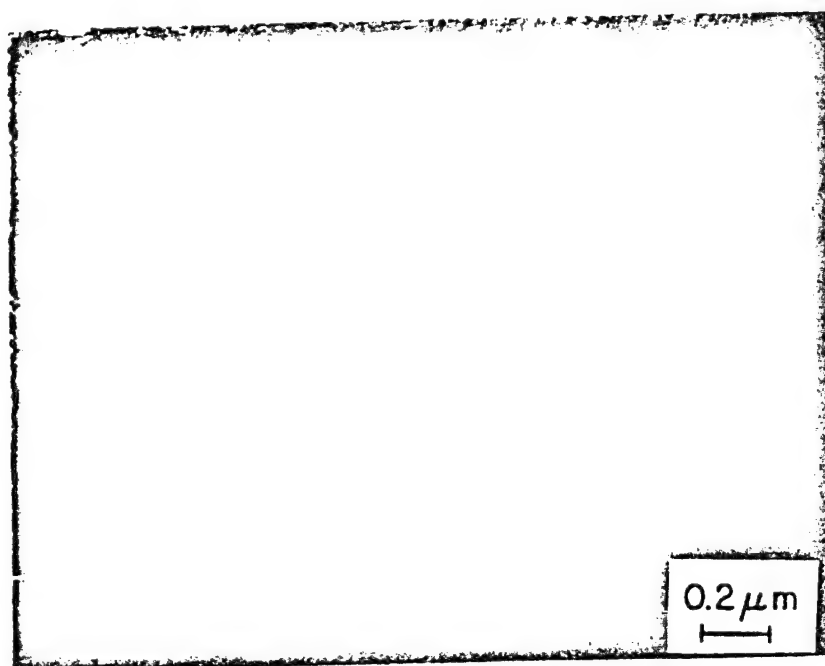
Figure 5.21   Striation-like markings on fatigue fracture surface
of Delrin.   (TEM fractograph)

138

of spherulites into highly oriented filaments as a result of a local cold drawing process. Macroscopic evidence of reorientation is manifested by the whitening of the fracture surface. In some regions, the strain during deformation is sufficient to introduce voids and void clusters, oriented in the direction of fibrillar alignment (Figure 5.22). This craze-like structure has been reported by Olf and Peterlin[90] to be one of the common mechanisms of deformation in crystalline polymers at room temperature and below.

5.3 Conclusions

From observations of discontinuous growth bands of several polymers, one can conclude that discontinuous crack growth is an FCP mechanism common to uncrosslinked glassy polymers and the crystalline polyacetal. Discontinuous crack growth in amorphous polymers occurs by the development and growth of short single crazes ahead of the crack tip. These conditions are met at low ΔK and high frequency. Molecular weights below about 2×10^5 also seem necessary for producing a small number of weaker crazes which encourage discontinuous crack growth.

A somewhat differet growth mechanism is operable in PA where crack advance is primarily transspherulitic in nature involving insignificant crazing. By equating band length to the computed plastic zone dimension, inferred yield strengths were calculated which agreed well with reported values of craze and triaxial yield stresses. At high ΔK levels, continuous crack growth was made
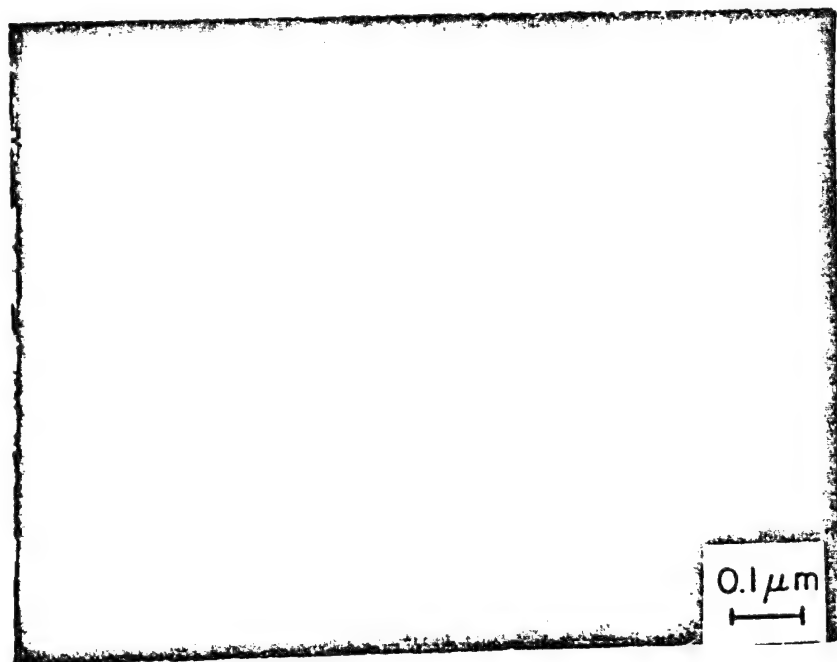
Figure 5.22 TEM micrograph of fracture surface of Delrin showing
voids and void clusters oriented in the direction of
fibrillar alignment.

140

evident by the presence of fatigue striations corresponding to the advance of the crack during each loading cycle.

VI. General Conclusions and Suggested Future Work

6.1 General Conclusions

The β transition appears to dominate many aspects of the fatigue response of polymeric materials. The frequency sensitivity was found to be maximum when the frequency of the β peak occurred in the range of test frequency. This behavior was explained in terms of hysteretic heating at the crack tip which is maximized at the β peak. The resulting crack blunting causes a drop in da/dN which is believed to be responsible for the observed frequency sensitivity in polymers. The β transition also appears to be responsible for the sensitivity of fatigue crack growth rates to both cyclic strain rate and creep crack growth.

Polyacetal was found to be the most FCP resistant polymer. Molecular weight was found to have a large effect on the fracture and FCP properties of PVC. This effect on the fatigue response persisted to high M where little change in static properties was noted. The much enhanced fatigue behavior encountered at high M was related to the increased resistance of the craze preceding the crack to cyclic breakdown on a molecular level.

Plasticizer content was seen to produce a complex effect on FCP in PVC and PMMA. The FCP response of PVC was unaffected by small additions of dioctyl phthalate. However, PMMA, copolymerized with BA, showed fatigue response to be a complex function of BA content believed due to interacting mechanical and thermal processes.

142

Increasing M_c served to decrease toughness and increase crack growth rates in an epoxy resin. The increased molecular constraint encountered at low M_c was believed to restrict large scale plastic deformation; therefore, cyclic loading induces extensive crack tip damage.

Discontinuous crack growth is the dominant mechanism of FCP at low ΔK, $M < 2 \times 10^5$ and high cyclic frequency in uncrosslinked amorphous polymers and crystalline polyacetal. The fracture surface bands formed over many fatigue cycles which are a manifestation of discontinuous crack growth were found to be equal to the crack tip plastic zone size. At high ΔK levels, continuous crack growth was evident by the presence of fatigue striations corresponding to the advance of the crack during each loading cycle.

6.2 Suggestions for Future Work

With the completion of this dissertation, it becomes apparent that certain phenomena require further study and clarification. The resonant condition between test frequency and the β-frequency which induced a maximum in FCP frequency sensitivity was related to a peak in damping. It is conceivable that further fatigue testing in the regime of other damping peaks (e.g. α or γ transitions) may reveal a similar increase in frequency sensitivity. Similarly, further study of the effect of waveform on da/dN is required to fully understand strain rate effects in polymers. In a related manner, attempts should be made to measure the extent of localized crack tip heating.

143

Clearly, crystalline polymers are the most FCP resistant materials currently known. However, further study is required to adequately understand the effects of such important parameters as spherulite size or degree of crystallinity on fatigue crack propagation response. Although much of the work presented involved homopolymers, the commercial importance and desireable properties of copolymers, blends and composites dictates that the FCP response of these materials should also be examined.

Further study of the discontinuous crack growth process is required to fully understand why a craze will resist failure for many cycles but will suddenly fail during one load cycle. The kinetics of craze growth needs to be clarified since it should have a strong bearing on the craze instability process. Using discontinuous crack growth as a tool, the effect of various polymer additives on craze stability may be evaluated.

All data offered in this dissertation were obtained under conditions where the minimum load was near 0. Other published data indicate that an increase in the average or mean stress can dramatically alter the fatigue response. Such behavior should be clarified.

Appendix I. Synthesis of PMMA*

Specimens of a series of PMMA resins having a wide range of M were synthesized by casting between glass plates. The technique for casting directly in sheets (6.3 mm and 0.25 mm thick) consisted of two steps:

   (1) prepolymerization at $40^{o}C$ of the desired initiator-monomer-chain stransfer agent combination (Table IA.1) for from 3 to 48 hr, and

   (2) pouring of the syrup thus obtained into the casting mold, with completion of the polymerization at $40^{o}C$.

Before use, MMA (Rohm & Haas) was washed and vacuum distilled. Molecular weight was controlled by the addition of varying amounts of t-butyl mercaptan (t-BuSH) (K & K Laboratories, used as received). Polymerization times were chosen to yield essentially complete conversion of monomer to polymer; unreacted monomer was removed by drying to constant weight under vacuum at $50 \pm 5^{o}C$. Specimens were then annealed at $105^{o}C$ for 3 to 5 min. to remove shrinkage strains.

Another series of specimens having a range of M was prepared in emulsion at 40 and $60^{o}C$, with 0.3 percent sodium lauryl sulfate as emulsifier, and a monomer/water ratio of 1/4. Data are given in Table 3.2.

Copolymers of MMA with n-BA were synthesized using the procedure described above for PMMA (no t-BuSH added). Specimens having the following mole ratios of n-BA were prepared: 90/10, 85/25, 80/20,

*Performed by Dr. S. L. Kim.

145

75/25, 70/30, 60/40, and 50/50.

TABLE IA.1

Recipe for PMMA Synthesis in Bulk[a]

Code Number	wt% t-BuSH	Prepolymerization time, hr
0	0	3-4
1	0.03	5-6
2	0.06	6-7
3	0.2	12-15
4	0.4	16-20
5	0.8	22-26
6	1.2	28-32
7	1.6	36-40
8	3.2	44-48

[a]All syntheses conducted at $40 \pm 2^{\circ}C$ with 0.05 wt%

a,a'-azobis (isobutyronitrile).

Appendix II. Synthesis of Epoxies*

IIA.1 Materials

The epoxy resins used were all diglycidyl ethers of Bisphenol-A oligomers: Epon series 825, 828, 1001, and 1004 (Shell Chemical Company); and Epirez series 520-C and 522-C (Celanese Coatings Company). Of these prepolymers, Epon 1001 and 1004, and Epirez 520-C and 522-C were solids at room temperature. The curing agent used in most syntheses was methylene dianiline (MDA), obtained in the form of Tonox (Shell Chemical Company) and 99%-pure MDA (Aldrich Chemical Company). In a few cases, the following polyamides were used as curing agents: Versamids 115 and 140 (General Mills Chemicals, Inc.). In the latter case, phenylglycidyl ether (Shell Chemical Company) was used as a reactive diluent. All resins of a given type were taken from a given batch; equivalent weight were used as supplied by the manufacturers.

IIA.2 Preparation and Curing

The various procedures for preparation and curing are summarized below. Compositions are given in following sections:

a. The general procedure for systems using liquid epoxy prepolymers with MDA as the curing agent was similar to that used by Bell.[55] Following prior heating to 100°C, the resin and curing agent were evacuated for 5-15 min. to remove bubbles, mixed, cast, and cured as follows: 45 min. in a circulating oven at 60°C; 30 min. at

*Performed by Dr. S. L. Kim, Ms. Carol Vasoldt, and Mr. Subodh Misra

147

$80^{\circ}C$, and 2.5 hr at $150^{\circ}C$; slow cooling to room temperature. The mold assemblies comprised clamped 130 mm by 130 mm glass plates separated by .51 mm or 6.35 mm ethylene-propylene copolymer or Teflon spacers were heated to $100^{\circ}C$ prior to the casting step. Both Mold Release 225 (Ram Chemical Company) and Epoxy ParFilm (Price Driscoll Co.) were used successfully as mold release agents; sheets of Mylar were also effective. With care, clear, yellowish to brown specimens were obtained from which bubble-free sections could be cut.

The cure cycle used was reported by Bell to give essentially complete curing[55] - a conclusion supported by data presented elsewhere. Somewhat higher temperatures were used by Selby and Miller,[54] but the effect of curing temperature as a variable was not examined in this study.

b. Higher molecular weight epoxies such as Epon 1001 are solids at room temperature and are usually used in conjunction with a solvent. In order to avoid at this time the question of a possible role of solvent in network formation, it was decided to conduct curing in bulk. It was difficult to achieve defect-free specimens in these cases, for at the higher temperatures needed to give the fluidity necessary for handling curing proceeded at an undesirably fast rate. However, thin specimens (0.5 mm thick) were successfully made as follows.

The resin was melted at $125^{\circ}C$ and evacuated. The curing agent was mixed in and samples cast between glass plates without further

148

evacuation. The curing cycle was modified to 100°C for 1.5 hr., and 150°C for 2.5 hr.; dynamic modulus studies indicated complete curing. A similar method was used for Epon 1004. By this technique, it was possible to get bubble-free sections for dynamic modulus studies.

c. For Versamid-cured systems the procedure developed by Manson and Chiu[86,87] was followed. First 6 percent by weight (based on the total mix) of phenyl glycidyl ether was mixed with the epoxy prior to addition of the polyamide in order to reduce viscosity and thus facilitate mixing and removal of bubbles. The epoxy resin was heated to 40°C, and evacuated in a vacuum oven to remove absorbed air and moisture. After the curing agent is heated to 40°C and added to the resin, the total mixture then evacuated for about 5 min. Sheets of samples were formed by use of the mold assemblies described in section 2.a.

IIA.3 Series A (varied stoichiometry)

This series (with MDA as curing agent) was prepared to provide a standard for comparison with other specimens prepared in this study and with the literature. Table IIA.1 gives the compositions, on the basis of equivalent weights (based in turn on specifications supplied by the manufacturer). Theoretical values of M_c, as cal-culated are given in Table IIA.1, along with compositions.

149

TABLE IIA.1

Compositions of Series A Epoxy Resins

Designation	Amine/epoxy Ratio[a]	M_c (theoretical)[b]
A-7	0.7 : 1	1523
A-8	0.8 : 1	526
A-9	0.9 : 1	383
A-10	1.0 : 1	326
A-10A	1.0 : 1	326
A-11	1.1 : 1	370
A-14	1.4 : 1	592
A-16	1.6 : 1	924
A-18	1.8 : 1	1922
A-20	2.0 : 1	∞ (Linear)

[a]All are based on the use of Shell TONOX curing agent, except for the A-10A case, for which 99% MDA was used.

[b]For reasons discussed by Bell[55] actual $\overline{M}_c$ values for specimens A-16 to A-20 may be in error. However, estimation of absolute values will require analysis of the residual amine content. In any case, the error will not affect any trends observed in properties as a function of stoichiometry.

IIA.3 Series B (Blends at equal $\overline{M}_c$)

For this series, various resins were blended to achieve an epoxy equivalent weight of 190 g/eq (equivalent to that of Epon 828, and to a value of $\overline{M}_c$ of 326). Stoichiometric amounts of MDA were used in all cases. Details are given in Table IIA.2, which also includes data on the blending resins themselves.

TABLE IIA.2

Compositions of Series B (Blends) Epoxy Resins

Desig-nation	wt% of						Eq wt	wt%		
	Epon 1004	Epirez 522-C	Epon 1001	Epirez 520-C	Epon 828	Epon 825		n=0	n=1	n=2-8
B-1	-	-	11.4	-	-	88.6	190	89.9	1.8	8.3
B-2	-	-	10.3	-	9.6	80.1	190	88.4	4.1	7.5
B-3	-	10.0	-	-	-	90.0	190	-	-	-
B-4	-	-	-	11.8	-	88.2	190	-	-	-
B-5	-	-	-	-	100	-	190	75	25	-

Appendix III. Characterization of Polymers*

IIIA.1 Characterization of $\bar{M}_v$.

Intrinsic viscosities of PMMA were measured in benzene using a
Cannon-Ubbelohde dilution viscometer; molecular weights were computed
from suitable equations relating intrinsic viscosity $[\eta]$ to $\bar{M}_v$:

$$\text{at } 30^\circ C^{88} \qquad [\eta] = 5.2 \times 10^{-5} \bar{M}_v^{0.76}$$

$$\text{at } 25^\circ C^{89} \qquad [\eta] = 5.5 \times 10^{-5} \bar{M}_v^{0.76}$$

Intrinsic viscosities of MMA-nBA copolymers were determined in
chloroform at $20^\circ C$, and values of $\bar{M}_v$ obtained by the use of constants
developed by Panke[90] for the Mark-Houwink relationship:

$$[\eta] = K M^a$$

where K and a depend on the composition of the copolymer.

Using a similar relationship, values of $\bar{M}_v$ were obtained for
PVC, Noryl, PC and PS. The constants K and a are given in Table
IIIA.1.

Dynamic mechanical properties were determined with a Rheovibron
apparatus at 110 Hz. The glass-transition (T_g) and β-transition tem-
peratures were taken from the major and lower maxima, respectively,
in the loss modulus vs. temperature curves   th the copolymers,
values of the glass transition slope and breadth were also determined.
Values of T_g were determined using a differential scanning calorimet-
er (DSC) at a heating rate of $10^\circ C$/minute.
*Characterization by Dr. S. L. Kim

153

IIIA.2 <u>Characterization</u> <u>of</u> <u>Crosslink</u> <u>Density</u> <u>in</u> <u>Epoxies</u>.

Detailed analysis of the degree of cure and crosslinking of those epoxies studied in this dissertation have been presented elsewhere[95] and will not be discussed here.

Table IIIA.1 $\overline{M}_v$ Constants

Polymer	Solvent	K	a
PS[96]	Toluene	1.7×10^{-4}	0.69
Noryl[97]	Toluene	2.8×10^{-4}	0.68
PVC[98]	THF	1.63×10^{-4}	0.766
PC[99]	Methylene Chloride	1.19×10^{-4}	0.80

Appendix IV. Special References

The following technical articles were coauthored by this writer prior to the completion of this dissertation.

A1. R. W. Hertzberg, J. A. Manson, and M. D. Skibo, Polym. Eng. and Sci., 15(4), (1975) 252.

A2. M. D. Skibo, R. W. Hertzberg and J. A. Manson, J. Mat. Sci., 11, (1976) 479.

A3. J. A. Manson, R. W. Hertzberg, S. L. Kim and M. D. Skibo, Polymer, 16, (1976) 479.

A4. M. D. Skibo, R. W. Hertzberg and J. A. Manson, to be published in the Proceedings of the Fourth International Conference on Fracture, June 1977.

A5. S. L. Kim, M. D. Skibo, J. A. Manson and R. W. Hertzberg, Polymer Preprints, 16(2), (1975) 559.

A6. S. L. Kim, M. D. Skibo, J. A. Manson and R. W. Hertzberg, Polym. Eng. and Sci., 17(3), (1977) 194.

A7. M. D. Skibo, J. A. Manson and R. W. Hertzberg, to be published in J. Macromol. Sci.

A8. M. D. Skibo, R. W. Hertzberg, and J. A. Manson, J. Mat. Sci., 12, (1977) 531.

References

1. J. A. Manson and R. W. Hertzberg, <u>CRC Rev. Mac. Sci.</u> <u>1</u>, (1973) 433.

2. M. N. Riddell, G. P. Koo, and J. L. O'Toole, <u>Polym. Eng. Sci.</u>, <u>6</u>, (1966) 363.

3. G. P. Koo, M. N. Riddell, and J. L. O'Toole, <u>Polym. Eng. Sci.</u>, <u>7</u>, (1967) 182.

4. D. A. Opp, D. W. Skinner, and R. J. Wiktorek, <u>Polym. Eng. Sci.</u>, <u>9</u>, (1969) 121.

5. R. J. Crawford and P. P. Benham, <u>J. Mat. Sci.</u>, <u>9</u>, (1974) 18.

6. R. J. Crawford and P. P. Benham, <u>J. Mech. Eng. Sci.</u>, <u>16</u>(3), (1974) 178.

7. R. J. Crawford and P. P. Benham, <u>J. Mat. Sci.</u>, <u>9</u>, (1974) 1297.

8. K. V. Gotham, <u>Plastics and Polymers</u>, August 1969, 309.

9. I. Constable, J. G. Williams, and D. J. Burns, <u>J. Mech. Eng. Sci.</u>, <u>12</u>(1), (1970) 20.

10. K. V. Gotham and S. Turner, <u>Polym. Eng. Sci.</u>, <u>13</u>(2), (1973) 113.

11. J. D. Ferry, <u>Viscoelastic Properties of Polymers</u>, John Wiley & Sons, New York, 1961.

12. R. W. Hertzberg, J. A. Manson, and W. C. Wu, ASTM STP 536, 391.

13. M. D. Skibo, R. W. Hertzberg, and J. A. Manson, <u>J. Mat. Sci.</u>, <u>11</u>, (1976) 479.

14. P. Paris and F. Erdogan, <u>J. Basic Eng. Trans. ASME</u>, Series D <u>85</u> (1963) 528.

15. N. E. Waters, <u>J. Mat. Sci.</u>, <u>1</u>, (1966) 354.

16. H. F. Borduas, L. E. Culver, and D. J. Burns, <u>J. Strain Analysis</u>, <u>3</u>, (1968) 193.

17. N. H. Watts and D. J. Burns, <u>Polym. Eng. Sci.</u>, <u>7</u>, (1967) 90.

18. B. Mukherjee and D. J. Burns, <u>Polym. Eng. Sci.</u>, <u>11</u>, (1971) 433.

19. S. Arad, J. C. Radon, and L. E. Culver, J. Mech. Eng. Sci., 13, (1971) 75.

20. R. W. Hertzberg and J. A. Manson, J. Mat. Sci., 8, (1973) 1554.

21. S. Arad, J. C. Radon, and L. E. Culver, J. Mech. Eng. Sci., 14(5) (1972) 328.

22. J. C. Radon, J. Appl. Polym. Sci., 17, (1973) 3515.

23. J. P. Elinck, J. C. Bauwens, and G. Homes, Int. J. Frac. Mech., 7, (1971) 227.

24. T. Kurobe and H. Wakashima, 13th Japan Cong. on Mat. Res. - Non - Metallic Materials, (1970) 192.

25. T. Kurobe and H. Wakashima, 15th Japan Cong. on Mat. Res. - Non - Metallic Materials, (1972) 137.

26. G. C. Martin and W. W. Gerberich, J. Mat. Sci., 11, (1976) 231.

27. W. W. Gerberich and G. C. Martin, to be published.

28. S. Arad, J. C. Radon, and L. E. Culver, J. Appl. Polym. Sci., 17, (1973) 1467.

29. E. Foden, D. R. Morrow, and J. A. Sauer, J. Appl. Polym. Sci., 16, (1972) 519.

30. J. A. Sauer, E. Foden, and D. R. Morrow, SPE Tech. Papers, 22, (1976) 107.

31. J. R. Martin and J. F. Johnson, J. Appl. Polym. Sci., 18, (1974) 257.

32. J. R. Martin and J. F. Johnson, J. Appl. Polym. Sci., 18, (1974) 3227.

33. K. Suzuki, S. Yada, N. Mabuchi, K. Seiuchi, and Y. Matsutani, Kobunshi Kagaku, 28, (1971) 920.

34. R. P. Kambour, Polymer Eng. Sci., 8, (1968) 281.

35. D. Hull, J. Mat. Sci., 5, (1970) 357.

36. J. Murray and D. Hull, Polymer, 10, (1969) 451.

37. J. Murray and D. Hull, Polymer Letters, 8, (1970) 159.

38. W. F. Brown, Jr. and J. E. Srawley, ASTM STP 410, (1966).

39. R. Attermo and G. Östberg, Int. J. Frac. Mech., 7, (1971) 122.

40. J. S. Harris and I. M. Ward, J. Mat. Sci., 8, (1973) 1655.

41. Yu. S. Urzhumtsev and R. D. Maksimov, Mekhanika Polimerov, 4(1), (1968) 34.

42. R. D. Maksimov and Yu. S. Urzhumtsev, Mekhanika Polimerov, 4(2), (1968) 246.

43. R. F. Boyer, Polym. Eng. Sci., 8, (1968) 161.

44. N. G. McCrum, B. E. Read and G. Williams, "Anelastic and Dielectric Effects in Polymeric Solids", John Wiley and Sons, New York (1970).

45. E. Butta, S. dePetris and M. Pasquini, Ric. Sci., 38, (1968) 927.

46. J. A. Manson, S. A. Iobst, and R. Acosta, J. Macromol. Sci., B9(2), (1974) 301.

47. J. Heijboer, J. Polym. Sci., C16, (1968) 3755.

48. E. H. Andrews and B. J. Walker, Proc. R. Soc. Lond., A,325, (1971) 57.

49. J. H. Dillon, in Advances in Colloid Science, Vol. III, ed. by H. Marl and E. J. W. Verwey, Interscience, New York, 1950.

50. R. P. Kusy and D. T. Turner, Polymer, 17, (1976) 161.

51. J. R. Martin, J. F. Johnson, and A. R. Cooper, J. Macromol. Sci. Rev. Macromol. Chem., C8(1), (1972) 57.

52. E. H. Merz, L. E. Nielsen, and R. Buchdahl, Ind. Eng. Chem., 43, (1951) 1396.

53. J. P. Berry, J. Polym. Sci., A2, (1964) 4069.

54. K. Selby and L. E. Miller, J. Mat. Sci., 10, (1975) 12.

55. J. P. Bell, J. Appl. Polym. Sci., 14, (1970) 1301.

56. J. O. Outwater and M. C. Murphy, 26th Annual Tech. Conf., Reinforced Plastics / Composite Div., The Soc. of Plas. Ind., Inc. in Section 10A, (1971) 1.

57. S. A. Sutton, Eng. Frac. Mech., 6, (1974) 587.

58. B. Tomkins and W. D. Biggs, J. Mat. Sci., 4, (1969) 544.

59. R. P. Kusy and D. T. Turner, Polymer, 15, (1974) 394.

60. A. N. Gent and G. Thomas, J. Polym. Sci. A2, 10, (1972) 571.

61. R. Kambour, J. Polym. Sci., D-Macromol. Rev., 7, (1973) 1.

62. J. F. Fellers and B. F. Kee, J. Appl. Polym. Sci., 18, (1974) 2355.

63. G. W. Weidmann and W. Doll, Colloid and Polym. Sci., 254, (1976) 205.

64. S. Wellinghoff and E. Baer, J. Macromol. Sci., B11, (1976) 367.

65. H. H. Kausch, Kunstoffe, 65(8), (1976) 1.

66. P. Vincent, Polymer, 1, (1960) 425.

67. P. Vincent, Polymer, 13, (1972) 558.

68. J. A. Sauer, A. D. McMaster, and D. R. Morrow, J. Macromol. Sci., B12(4), (1976) 535.

69. G. H. Jacoby, ASTM STP 453, (1969) 147.

70. G. H. Jacoby and C. Cramer, Off. of Nav. Res., A. F. Mat. Lab., Proj. NR064-470 (1967).

71. N. J. Mills and N. Walker, Polymer, 17, (1976) 335.

72. S. Rabinowitz, A. R. Krause and P. Beardmore, J. Mat. Sci., 8, (1973) 11.

73. V. Havlicek and V. Zilvar, J. Macromol. Sci., B5(2), (1971) 317.

74. A. D. McMaster and D. R. Morrow, Polym. Eng. Sci., 14, (1974) 801.

75. G. P. Marshall, L. E. Culver, and J. G. Williams, Int. J. Frac. 9(3), (1973) 295.

76. B. Rosen, " Fracture Processes in Polymeric Solids", Interscience, New York, (1964).

77. J. Janiszewski, Master's Thesis, Lehigh University, 1978.

78. D. S. Dugdale, _J. Mech. Phys. Solids_, 8, (1960) 100.

79. B. Tomkins and W. D. Biggs, _J. Mat. Sci._, 4, (1969) 532.

80. N. J. Mills, _Eng. Frac. Mech._, 6, (1974) 537.

81. H. F. Brinson, _Proc. Soc. Exp. Stress Anal._, 27 (1970) 93.

82. R. D. R. Gales and N. J. Mills, _Eng. Frac. Mech._, 6 (1974) 93.

83. R. N. Haward, B. M. Murphy, and E. F. T. White, _J. Polym. Sci._, A2, 9, (1971) 801.

84. G. P. Morgan and I. M. Ward, _Polymer_, 18, (1977) 87.

85. Modern Plastics Encyclopedia, 49, Number 10A, (1972-1973) 143.

86. M. Creager and P. C. Paris, _Int. J. Frac. Mech._, 3(4), (1967) 247.

87. S. Rabinowitz and P. Beardmore, _CRC Rev. Mac. Sci._ 1, (1972) 1.

88. R. P. Kambour, General Electric Co. Technical Information Series, No. 72CR0285 (1972).

89. P. J. Flory, "Principles of Polymer Chemistry", Cornell University Press, Ithaca, New York, 1953.

90. H. G. Olf and A. Peterlin, _J. Polym. Sci._, C12, (1974) 2209.

91. J. A. Manson and E. H. Chiu, _J. Polym. Sci._-Symp. No. 41, (1973) 95.

92. J. A. Manson and E. H. Chiu, _Polym. Prepr._, 14, (1973) 469.

93. H. J. Cantow and G. V. Schulz, Z. Physik. Chem. (N. F.), 2, (1954) 117, 365.

94. T. G. Fox, H. F. Mason, and E. S. Cohn, unpublished work; cited in "Polymer Handbook", J. Brandrup and E. H. Immergut ed., p.IV-26, John Wiley and Sons, Inc., 1966.

95. D. Panke, Rohm Spektrum, 13, n.d., 35. (Rohm GmBH Chemische Fabrik, Darmstadt).

96. P. Outer, G. I. Carr, and B. H. Zimm, _J. Chem. Phys._, 18, (1950) 830.

97. J. M. Barrales-Rienda and D. C. Pepper, $\underline{\text{J. Polym. Sci.}}$, B, $\underline{4}$, (1966) 939.

98. H. Batzer and A. Nisch, $\underline{\text{Makromol. Chem.}}$, $\underline{22}$, (1957) 131.

99. G. C. Berry, H. Nomura, and K. G. Mayhan, $\underline{\text{J. Polym. Sci.}}$, A2, $\underline{5}$, (1967) 1.

100. J. A. Manson, S. L. Kim, and L. H. Sperling, Air Force Materials Laboratory, Wright-Patterson Air Force Base, Technical Report AFML-TR-76-124, July 1976.

VITA

Michael D. Skibo was born October 11, 1952 in Bethlehem, Pennsylvania to John R. and Helen Skibo. He attended elementary and secondary schools in the Bethlehem Area School District and was graduated from Liberty High School in June 1969.

In June 1973, Mr. Skibo was graduated with High Honors from Lehigh University with a degree of Bachelor of Science in Metallurgy and Materials Science. During his undergraduate years at Lehigh, he was mentioned on the Dean's List and received the ASM Noah Kahn Award in Metallurgy.

Upon completion of his undergraduate degree, Mr. Skibo continued his education at Lehigh as a Research Assistant working under Drs. R. W. Hertzberg and J. A. Manson. During this period, he was elected to Sigma Xi, received the Raymond T. Anderson Award and published nine technical articles on subjects related to his doctoral dissertation.